Regulation of motility and polarity in *Myxococcus xanthus*

Dissertation
zur Erlangung des Doktorgrades
der Naturwissenschaften
(Dr. rer. nat.)

dem
Fachbereich Biologie
der Philipps-Universität Marburg
vorgelegt von

Daniela Keilberg

aus Zwickau

Marburg an der Lahn, 2013

Die Untersuchungen zur vorliegenden Arbeit wurden von Oktober 2009 bis November 2012 am Max-Planck-Institut für terrestrische Mikrobiologie unter der Leitung von Prof. Dr. MD Lotte Søgaard-Andersen durchgeführt.

Vom Fachbereich Biologie der Philipps-Universität Marburg als Dissertation angenommen am: 23. April 2013

Erstgutachter: Prof. Dr. MD Lotte Søgaard-Andersen

Zweitgutachter: Prof. Dr. Martin Thanbichler

Weitere Mitglieder der Prüfungskommission:

Prof. Dr. Hans-Ulrich Mösch

Prof. Dr. Andrea Maisner

Prof. Dr. Susanne Önel

Tag der mündlichen Prüfung: 13. Mai 2013

Die während der Promotion erzielten Ergebnisse sind zum Teil in folgenden Orginalpublikationen veröffentlicht:

Herzog A., Voss, **Keilberg D.**, Hot E., Søgaard-Andersen L., Garbe C., Kostina E. (2012) A stategy for identifying fluorescence intensity profiles of single rod-shaped cells. Journal of Bioinformatics and Computational Biology Online Ready 1250024

Keilberg D., Wuichet K., Drescher F. & Søgaard-Andersen L. (2012)
A response regulator interfaces between the Frz chemosensory system and the MglA/MglB GTPase/GAP module to regulate polarity in *Myxococcus xanthus*. PLoS Genetics. 9, e1002951.

Miertzschke M., Koerner C., Vetter I.R., **Keilberg D.**, Hot E., Leonardy S., Søgaard-Andersen L. & Wittinghofer A. (2011)
Mechanistic insights into bacterial polarity from structural analysis of the Ras-like G protein MglA and its cognate GAP MglB. EMBO J. 30, 4185-4197.

Keilberg D., Huntley S. & Søgaard-Andersen L. (2012)
Two-component systems involved in regulation of motility and development in *Myxococcus xanthus.* In "Two component systems in bacteria" ed. Gross, R. & Beier, D.. Horizon Scientific press and Caister Academic Press.

Table of contents

Table of contents **4**
Abstract **7**
Zusammenfassung **9**
1 Introduction **11**
1.1* Motility of *M. xanthus **14**
1.2 S-motility **15**
1.3 A-motility **18**
1.3.1 The motor is driven by PMF 19
1.3.2 The A-motility complex 21
1.4 Regulation of reversal frequencies by the Frz chemosensory system **23**
1.5 Regulation of both motility systems by MglA and MglB **24**
1.6 The response regulator RomR **26**
1.6.1 Bioinformatic analysis of RomR 28
1.6.2 RomR regulates motility and reversals 28
1.7 Scope of the study **31**
2 Results **32**
2.1 MglA and MglB form a complex to regulate motility **32**
2.2 The RomR response regulator **38**
2.2.1 RomR is required for A- and S-motility 38
2.2.2 Functions of the single subparts of the RomR output domain 41
2.2.3 Localization of RomR and the subparts of the output domain in the absence of the A-motility complex 44
2.3 RomR regulates motility together with MglA and MglB **51**
2.3.1 RomR coevolved with MglA and MglB 51
2.3.2 RomR directly interacts with MglA and MglB proteins 53
2.3.3 Localizations of RomR, MglA and MgB are interdependent 55
2.3.4 RomR is a polar targeting factor for MglA 59
2.3.5 RomR acts upstream of the MglA/MglB system 62
2.4 Frz chemosensory system **66**
2.4.1 The Frz system acts upstream of RomR 66
2.4.2 Direct interactions between RomR, the MglA/MglB system and the Frz-system 68
2.4.3 RomR phosphorylation assays 70
2.5 RomX and RomY, new factors involved in motility regulation **72**
2.5.1 Five protein network regulating motility: RomR, MglA, MglB, RomX and RomY 72

2.5.2 RomX and RomY are required for motility ... 75
2.5.3 Localization of RomX and RomY ... 77
2.5.4 Interactions between RomX, RomY and the RomR/MglA/MglB network ... 79
3 Discussion ... 82
3.1 RomR regulates both motility systems ... 83
3.2 A-motility machinery is not required for RomR polar targeting ... 84
3.3 RomR is part of a polarity module together with MglA and MglB ... 85
3.4 Frz system signals upstream of the MglA/MglB/RomR system ... 89
3.5 Signaling between Frz system and RomR is rather indirect ... 90
3.6 RomR connects the inversion module with the polarity module ... 91
3.7 RomX and RomY – Two new factors expand the polarity module ... 93
4 Material and Methods ... 96
4.1 Chemicals and equipment ... 96
4.2 Media ... 98
4.3 Strains of *M. xanthus* and *E. coli* ... 99
4.3.1 Cultivation of *M. xanthus* and *E. coli* ... 106
4.3.2 Storage of *M. xanthus* and *E. coli* strains ... 106
4.4 Molecular biological methods ... 107
4.4.1 Primers and plasmids ... 107
4.4.2 Plasmid construction ... 115
4.4.3 Constuction of in frame deletions ... 119
4.4.4 DNA preparation from *E. coli* und *M. xanthus* ... 122
4.4.5 Polymerase chain reaction (PCR) ... 122
4.4.6 Agarose gel electrophoresis ... 125
4.4.7 Restriction and ligation of DNA fragments ... 125
4.4.8 DNA sequencing ... 125
4.4.9 Preparation of chemical- and electrocompetent *E. coli* cells ... 125
4.4.10 Preparation of eletrocompetent *M. xanthus* cells ... 126
4.4.11 Transformation of E. coli cells ... 126
4.4.12 Transformation of *M. xanthus* cells ... 127
4.4.13 Cotransformation for BACTH system ... 127
4.5 Microbiological methods ... 128
4.5.1 BACTH system ... 128
4.5.2 Motility assays ... 128
4.6 Microscopy and determination of reversal frequency ... 129
4.7 Biochemical methods ... 129
4.7.1 Overproduction and purification of proteins ... 129
4.7.2 Concentration determination of proteins ... 130

4.7.3 SDS polyacrylamide gelektrophoresis (SDS-PAGE) 131
4.7.4 Immunoblot analysis 132
4.7.5 Antibody production 132
4.7.6 Pull down experiments 133
4.7.7 Phosphotransfer assays 133
4.8 Bioinformatics methods 134
4.8.1 Sequences and domain analysis 134
References 135
Abbreviations 140
Acknowledgements 141
Curriculum Vitae 142
Erklärung 144

Abstract

M. xanthus cells possess two independent motility systems: the adventurous (A) system and the social (S) system. S-motility depends on the extension and retraction of Type-4-pili, whereas A-motility is mediated via focal adhesion complexes that incorporate a MotAB-like motor. The rod-shaped *M. xanthus* cells can reverse the direction of movement, which is accompanied by a polarity inversion of components of both motility systems. Reversals are induced by the Frz chemosensory system, acting upstream of a small GTPase, MglA and its cognate GTPase activating protein, MglB. MglA and MglB localize to opposite cell poles in a moving cell, defining the leading pole (MglA) and the lagging pole (MglB). MglA and MglB directly interact. In this study we identified residues in MglB that are required for the interaction with MglA. Furthermore, we show that inhibition of the MglA/MglB interaction affects MglA GTPase activity and localization of MglB.

In addition to the MglA/MglB system, the response regulator RomR is required for motility and reversals. RomR localizes in a bipolar asymmetric pattern with a large cluster at the lagging cell pole. Previously RomR was reported to regulate the A-motility system. We show that RomR localization does not depend on A-motility proteins. In contrast, we found that RomR is required for both motility systems, suggesting that it acts upstream of the two motility machineries. Consistent with that, we found that RomR directly interacts with MglA and MglB. Moreover, RomR, MglA and MglB affect the localization of each other in all pair-wise directions suggesting that RomR stimulates motility by promoting correct localization of MglA and MglB in MglA/RomR and MglB/RomR complexes at opposite poles. Furthermore, localization analyses suggest that the two RomR complexes mutually exclude each other from their respective poles. We further showed that RomR interfaces with FrzZ, the output response regulator of the Frz chemosensory system, to regulate reversals. Thus, RomR serves at the interface to connect a classic bacterial signalling module (Frz) to a classic eukaryotic polarity module (MglA/MglB). This modular design is paralleled by

the phylogenetic distribution of the proteins suggesting an evolutionary scheme in which RomR was incorporated into the MglA/MglB module to regulate cell polarity followed by the addition of the Frz system to dynamically regulate cell polarity.

Importantly, RomR possesses a conserved aspartate in its receiver domain, required for activation via phosphorylation. Because we found no evidence for direct phosphotransfer between FrzE and RomR, further phylogenetic studies were carried out. These analyzis revealed two candidate proteins involved in motility, RomX and RomY, which display a co-evolutionary relationship with RomR. We show that both proteins are involved in motility and that RomX behaves similarly to RomR with respect to phenotype and localization. We suggest that RomX and RomY play a role in regulation of motility together with RomR, MglA and MglB and possibly in RomR activation.

Zusammenfassung

M. xanthus Zellen besitzen zwei unabhängige Systeme um sich fortzubewegen: das A-(adventurous)-System, und das S-(social)-System. Zellen, die sich mit dem S-System fortbewegen benötigen Typ-4-Pili, wahrend Zellen, die sich mit dem A-System fortbewegen von Adhesionskomplexen und deren MotAB Motorproteinen angetrieben werden. Weiterhin können *M. xanthus* Zellen die Bewegungsrichtung umkehren, die durch eine Umkehrung der Polarität der beiden Fortbewegungssysteme begleitet wird. Zellumkehrungen werden durch das Frz chemosensorische System ausgelöst, welches oberhalb der kleinen GTPase, MglA und dem zugehörigen GTPase aktivierenden Protein, MglB wirkt. MglA und MglB lokalisieren an gegenüberliegenden Zellpolen während sich eine Zelle fortbewegt, und definieren den vorderen Pol (MglA) und den hinteren Pol (MglB). Die Proteine MglA und MglB interagieren direkt miteinander. In dieser Studie konnten wir ermitteln, welche Aminosäuren von MglB für die MglA/MglB Interaktion erforderlich sind. Darüber hinaus konnten wir zeigen dass die Hemmung der MglA/MglB Interaktion die MglA GTPase-Aktivität und die Lokalisation von MglB beeinflusst.

Ähnlich dem MglA/MglB System ist der Antwortregulator RomR für die Fortbewegung und Zellumkehrungen in *M. xanthus* erforderlich. RomR lokalisiert bipolar asymmetrisch mit einem großen Cluster am hinteren Zellpol. Frühere Studien zu RomR schlugen ein Model vor, in dem RomR ausschließlich das A-System reguliert. Im Gegensatz dazu fanden wir, dass RomR für beide Fortbwegungssysteme erforderlich ist, was darauf hindeutet, dass es stromaufwärts von beiden Fortbwegungssystemen agiert. Weiterhin zeigen wir, dass die RomR Lokalisierung nicht von Proteinen des A-Systems abhängt. Im Einklang damit fanden wir, dass RomR direkt mit MglA und MglB interagiert. Außerdem beeinflussen RomR, MglA und MglB ihre Lokalisierung gegenseiteig, was nahe legt, dass RomR die Fortbwegung stimuliert mittels Förderung der korrekten Lokalisation von MglA und MglB und im speziellen durch MglA/RomR und MglB/RomR Komplexe an entgegengesetzten Polen. Außerdem deuten die Lokalisierungsanalysen darauf hin, dass die beiden RomR Komplexe sich

gegenseitig von den Polen ausschließen. Weiterhin zeigten wir, dass RomR mit FrzZ, dem Response-Regulator der als Ende der Signalkette des Frz chemosensorischen Systems wirkt, interagiert um Zellumkehrungen zu regulieren. Somit dient RomR als Schnittstelle, um eine klassisches bakterielles Signal-Modul (Frz) mit einem klassischen eukaryotischen Polaritätsmodul (MglA/MglB) zu verbinden. Dieser modulare Aufbau wird durch die phylogenetische Verteilung der Proteine unterstützt, und deuted auf folgendes evolutionäres Model hin: RomR wurde dem MglA/MglB Polaritätsmodul zugefügt um die Zellpolarität zu regulieren gefolgt von der Integration des Frz-Systems um die Zellpolarität dynamisch zu regulieren.

Zudem besitzt RomR ein konserviertes Aspartat in seiner Empfänger-Domäne, welches für die Aktivierung durch Phosphorylierung erforderlich ist. Da bisher keine Phosphorylierung von RomR durch FrzE gezeigt werden konnte, wurden weitere phylogenetische Studien durchgeführt, um das erforderliche Protein für die RomR Aktivierung zu finden. Mittels bioinformatischer Analysen wurden zwei neue unbekannte Proteine gefunden, RomX und RomY, mit einer ähnlichen phylogenetischen Verteilung wie RomR. Wir zeigten, dass beide Proteine an der Fortbwegung von *M. xanthus* beteiligt sind und dass RomX sich in Bezug auf Phänotyp und Lokalisierung ähnlich verhält wie RomR. Wir schlagen vor, dass RomX und RomY zusammen mit RomR, MglA und MglB eine Rolle bei der Regulierung der Fortbewegung spielen könnten, und möglicherweise zusätzlich bei der RomR Aktivierung.

1 Introduction

Bacteria exist in a wide variety of environments that undergo fast changes in conditions such as temperature, pH and nutrient content. Therefore, all bacteria need systems that enable them to adjust to the changing conditions. To first recognize alterations in the habitat, bacteria possess proteins containing sensor domains, which are coupled to signal transduction systems. Typically, environmental responses involve a change in gene expression, which in turn alter protein levels for example after sensing stress factors (Morano and Thiele 1999). These types of shifts can also result in dramatic lifestyle changes. For example, in *Bacillus subtilis* lack of nutrients can cause a switch from a vegetative lifestyle to sporulation (Strauch and Hoch 1993).

Myxococcus xanthus is an aerobic Gram-negative δ-proteobacterium living in soil (Shimkets and Woese 1992). As a representative of the myxobacteria, *M. xanthus* possesses a large genome with 9.14 million base pairs and about 7500 genes (Goldman et al. 2006). *M. xanthus* has a complex life cycle consisting of a vegetative phase in the presence of nutrients (Wireman and Dworkin 1977), during which cells can swarm and prey on other bacteria to lyse them (Rosenberg et al. 1977), and a developmental phase in the absence of nutrients, when the cells form fruiting bodies, a multicellular structure filled with spores (Wireman and Dworkin 1977). Development and predatory behavior are dependent on coordinated movements of cells.

M.xanthus cells contain two genetically distinct motility systems, which work synergistically to generate gliding, movement on solid surfaces (Hodgkin and Kaiser 1979).

In contrast to eukaryotic cells, where different organelles and cytoskeleton structures have been studied for a long time, bacterial cells were thought to consist of one unorganized compartment (Hunter 2008). This erroneous conclusion was due to the small size of bacteria, which made it harder to observe subcellular structures. Fluorescent reporters became a powerful tool to track proteins in vivo, giving new insights into the complex spatial regulation of bacteria. Internal separation of protein complexes and

structures facilitate sophisticated behaviors of bacteria including cell division, motility, chemotaxis and differentiation, as well as the formation of multicellular fruiting bodies (Shapiro et al. 2009).

A B

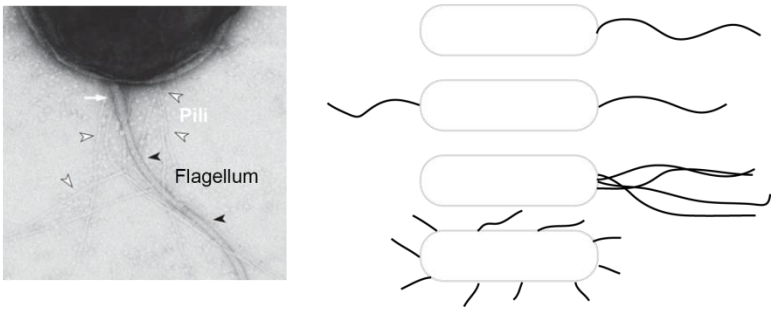

Figure 1: Polar appendices required for motility. (A) Pili and flagellum at the cell pole of *Caulobacter crescentus*, modified after (Kirkpatrick and Viollier 2011) (B) from up to down arrangements of flagella in different bacteria: monotrichous (e.g., *Vibrio cholerae*), amphitrichous (e.g. *Aquaspirillum serpens*), lophotrichous (e.g., *Spirillum volutans*), Peritrichous (e.g., *Escherichia. coli*)

Correct positioning and regulation of extracellular motility structures is required for directed movement (Fig.1). Microscopic analyses of motile bacteria have shown that motility components are often restricted to one cell pole (Kirkpatrick and Viollier 2011), indicating the existence of intracellular information for the positioning of these structures. *E. coli* possesses flagella distributed over the entire cell surface, but polarly localized chemotaxis proteins are involved in their regulation (Maddock and Shapiro 1993).

Polarly localized proteins can be targeted to their correct subcellular localization by a variety of processes such as: (i) interaction with proteins as studied for the chemotaxis system in *E. coli* (Maddock and Shapiro 1993); (ii) interaction with the septum during cell division as found for TipN/F in *C. crescentus* (Huitema et al. 2006; Lam et al. 2006); (iii) interaction with lipid domains in the membrane as for example the interaction between cardiolipin and ProP in *E. coli* (Romantsov et al. 2007) and finally, (iv) recognition of membrane curvature at the cell pole as described for DivIVA in *E. coli* (Lenarcic et al. 2009). Although many mechanisms of polar protein targeting have been described, it still remains an open question for most of the studied proteins how they achieve their localization. Additionally, many polarly localized proteins display a dynamic localization, which can be cell cycle regulated, as for TipN/F

in *C. crescentus* (Lam et al. 2006) or cell cycle independent as for PilB/T in *M. xanthus* (Bulyha et al. 2009).

More extensive studies on the regulation of polarity have been conducted in eukaryotes, often revealing that small GTPases play an important role in regulating dynamic polarity (Wennerberg et al. 2005). For example, directional migration of neutrophils depends on the dynamic localization of three small GTPases. While activated Rac and Cdc42 GTPases at the front edge of the cell stimulate formation of new cellular protrusions via actin polymerization, Rho at the rear end of cells drives retraction of protrusions (Ridley et al. 2003). Similarly, a small Ras-like GTPase is involved in chemotaxis of *Dictyostelium discoideum* activating actin polymerization leading to the formation of protrusions at the front (Kortholt and van Haastert 2008). Interestingly, recent studies suggest that the function of Ras GTPases in polarity is also conserved in prokaryotes (Bulyha et al. 2011). The best characterized small GTPase in prokaryotes, MglA, has been shown to be required for both motility systems in *M. xanthus* (Hartzell and Kaiser 1991a). It was shown that MglA localizes to the leading cell pole and establishes the polarity of other motility proteins (Leonardy et al. 2010, Zhang et al. 2010).

1.1 Motility of *M. xanthus*

M. xanthus cells do not possess flagella, and therefore they are not able to swim in liquid media. However, they harbor type IV pili (T4P) at the leading cell pole and are able to glide on solid surfaces along their long axis. Compared to other bacteria, *M. xanthus* cells move relatively slowly, reaching up to 6 µm per minute, approximately one cell length (Spormann and Kaiser 1995; Jelsbak and Søgaard-Andersen 1999). *M.xanthus* cells use two genetically independent systems to move, the adventurous (A) – system and the social (S) – system (Hodgkin and Kaiser 1979) (Fig.2). The first motility system was named adventurous, because it is required for single cells to move independently of each other. In contrast, the second motility system was termed social motility because it is cell-cell contact dependent. Mutations in both motility machineries completely abolish motility, while mutations in only one of the systems lead to reduced motility as compared to wild type (WT) (Hodgkin and Kaiser 1979). Furthermore, *M. xanthus* cells can change direction typified by reversals every 10-15 minutes on average (Blackhart and Zusman 1985a; Leonardy et al. 2008). A reversal is defined by a 180° switch of direction which causes an inversion of the polarity, causing the old lagging pole become the new leading pole and vice versa (Leonardy et al. 2008). During a reversal, the cell stops and then moves in the opposite direction after reorganizing the motility machineries. In particular, the T4P required for S-motility are disassembled at the old leading pole and reassembled at the new leading cell pole (Sun et al. 2000; Bulyha et al. 2009). Additionally, proteins required for A-motility have been shown to localize dynamically and switch poles during reversals (Mignot et al. 2005; Leonardy et al. 2007).

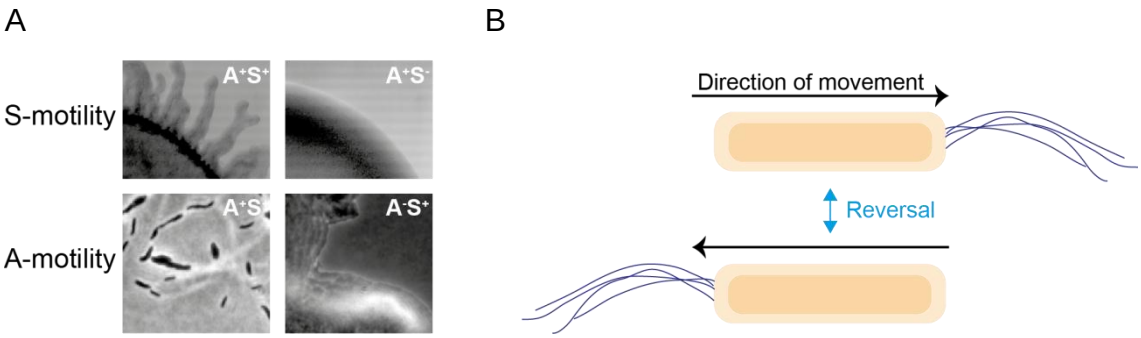

Figure 2: *M. xanthus* motility depends on two motility systems and reversals. (A) Wild type cells (A+S+) form flares under soft agar or on the soft agar surface conditions favorable for S-motility, and move preferentially as single cells on hard agar surfaces favorable for A-motility. Cells with mutations in S-motility (A+S-) show a smooth edge on soft agar, because they are not able to move. Cells with mutations required for A-motility (A-S+) are not able to move as single cells on hard agar surfaces. (B) During reversals cells change the direction of movement. Additionally the polarity of the cells changes, including the disassembly of T4P at the old leading pole as well as the re-assembly of T4P at the new leading cell pole.

Various fractionation and localization studies revealed that both machineries, S-motility and A-motility, span the whole cell envelope (Bulyha et al. 2009; Nan et al. 2010; Luciano et al. 2011). While S-motility depends on a protein complex that forms T4P at the leading cell pole, the exact mechanism of A-motility remains unknown.

1.2 S-motility

Cells using only the S-motility system move in groups. S-motility requires T4P and cell-cell contact (Fig.3). T4P extend from the leading cell pole, attach to the surface or other cells, and then retract, pulling the cell forward (Wu and Kaiser 1995). An extracellular matrix composed of polysaccharides, carbohydrates and proteins is essential for the retraction of T4P in *M. xanthus* (Li et al. 2003). In addition to their involvement in S-motility, T4P have been shown to mediate twitching motility in *Neisseria* and *Pseudomonas* species (Wu and Kaiser 1995). T4P are widespread among diverse species of bacteria and play a role in a wide variety of functions including pathogenesis (Craig and Li 2008), biofilm formation (Mattick 2002), natural transformation (Dubnau 1999) and cell motility (Kaiser 1979).

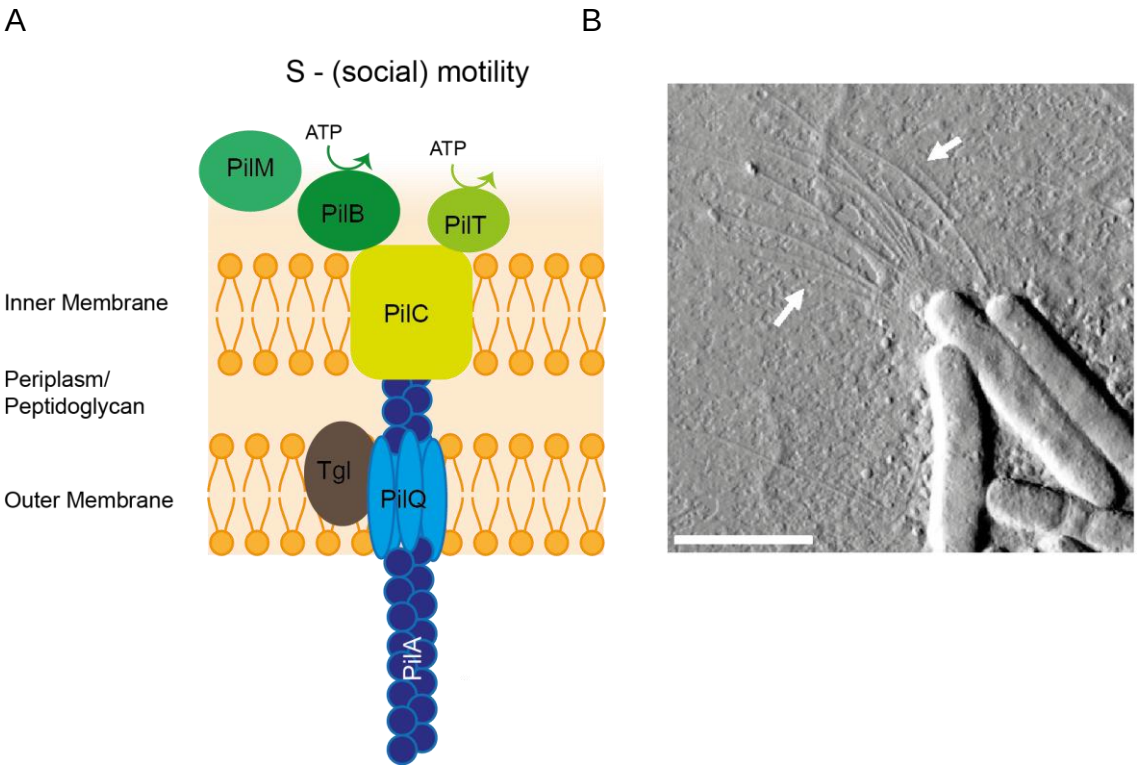

Figure 3: *M. xanthus* S-motility system. (A) Proteins involved in S-motility are displayed with their respective localization within the cell envelope. ATP indicates ATPase activity of the proteins PilB and PilT. Fractionation experiments have been performed for all the proteins included in the model. More detailed descriptions are provided in the text. (B) T4P of *M. xanthus* located at the leading cell pole are indicated by white arrows, modified from (Pelling et al. 2005), scale 2 µm.

Most T4P genes of *M. xanthus* are present in one gene cluster that includes genes for type-IV-pili assembly and for extension and retraction (Wu and Kaiser 1995; Wall and Kaiser 1999). Gene disruptions in this cluster, by transposon mutagenesis screens (Youderian and Hartzell 2006) and in frame deletions (Bulyha et al. 2009) confirmed that these genes are required for S-motility.

M. xanthus cells typically have 5-10 T4P, each of which are long flexible filaments uniformly composed of a pilin, PilA (Skerker and Berg 2001; Maier et al. 2002). To assemble pili, prepilin precursors of PilA are secreted into the periplasm and cleaved by PilD, the PilA peptidase. Then PilA subunits polymerize to form pilus fibers, 5-8 nm thin filaments that are visible by electron microscopy at the pole of the cell (Pelicic 2008) (Fig. 3). The pilus crosses the outer membrane via the PilQ/Tgl secretin complex that acts as a channel to transfer the PilA filament outside of the cell (Nudleman et al. 2006). The pilus

fibers can, after full extension promoted by the PilB ATPase, reach several cell lengths and attach to other cells (Pelicic 2008).

Studies in multiple organisms have identified a set of approximately 10 conserved proteins that, with the aid of additional system-specific accessory components, form the T4P apparatus (Pelicic 2008). To understand the mechanism of disassembly and reassembly of T4P in *M. xanthus* during a cellular reversal, the localizations of the proteins required for T4P function were assessed (Nudleman et al. 2006; Bulyha et al. 2009). Two classes of proteins were described. The first class includes stationary proteins: PilQ in the outer membrane, PilC in the inner membrane and PilM in the cytoplasm, which are localizing symmetrically to both cell poles and do not relocate between the poles during cellular reversal (Nudleman et al. 2006; Bulyha et al. 2009). The second class is composed of dynamic T4P proteins that switch poles during reversals: PilB, an ATPase that stimulates T4P extension and localizes predominantly to the leading pole, (Bulyha et al. 2009), and PilT, an ATPase that stimulates T4P retraction and localizes predominantly to the lagging pole (Jakovljevic et al. 2008; Bulyha et al. 2009).

While the role of the T4P core components has been studied extensively in *M. xanthus* as well as in other organisms, the polarity regulation involved in S-motility remains a mystery. Intriguingly, the stationary components in the inner and outer membrane are located at both cell poles, while the regulatory ATPases are predominantly localized to a single cell pole. Similarly, the pseudo-response regulator FrzS, which has been shown to be reguired for S-motility, is restricted to the leading cell pole (Mignot et al. 2005). Recent studies indicate that MglA and an additional small GTPase, SofG, are required to set up the polarity for S-motility (Bulyha et al, in review).

1.3 A-motility

Cells motile only via the A-system move as single cells independently of T4P. Transposon mutagenesis screens revealed many genes involved in A-motility, and most of them are predicted to be involved in metabolism or have an unknown function (Youderian et al. 2003; Yu and Kaiser 2007). One of the original models of A-motility mechanism proposed that slime secretion generates the force for movement (Yu and Kaiser 2007). However, more recent studies suggested the existence of a molecular motor underlying A-motility. The current model emerged after studying the localization of AglZ, a pseudo-response regulator required for A-motility, which localizes as a large cluster at the leading cell pole and smaller clusters – focal adhesion complexes (FACs) – along the cell body (Mignot et al. 2007). AglZ-YFP clusters remain at fixed positions with respect to the substratum in moving cells, as displayed in Fig.4 (Mignot et al. 2007). While the cell is moving forward, the clusters appeared to be moving from the leading cell pole to the lagging cell pole, and after reaching the lagging cell pole, they disperse. Therefore, FACs were predicted to assemble at the leading cell pole and disassemble at the lagging cell pole (Nan et al. 2011; Sun et al. 2011).

Sun et al. hypothesized that FACs move in the opposite direction of the cell with the same velocity as the cell moves forward to appear at fixed positions.

To investigate if FACs are able to generate movements, beads were attached to the cell surface and tracked over time. Interestingly, Sun et al. observed that beads attached to the cell surface of immobilized cells were moving from the leading to the lagging cell pole, indicating, that force to move forward is generated by the FACs (Sun et al. 2011).

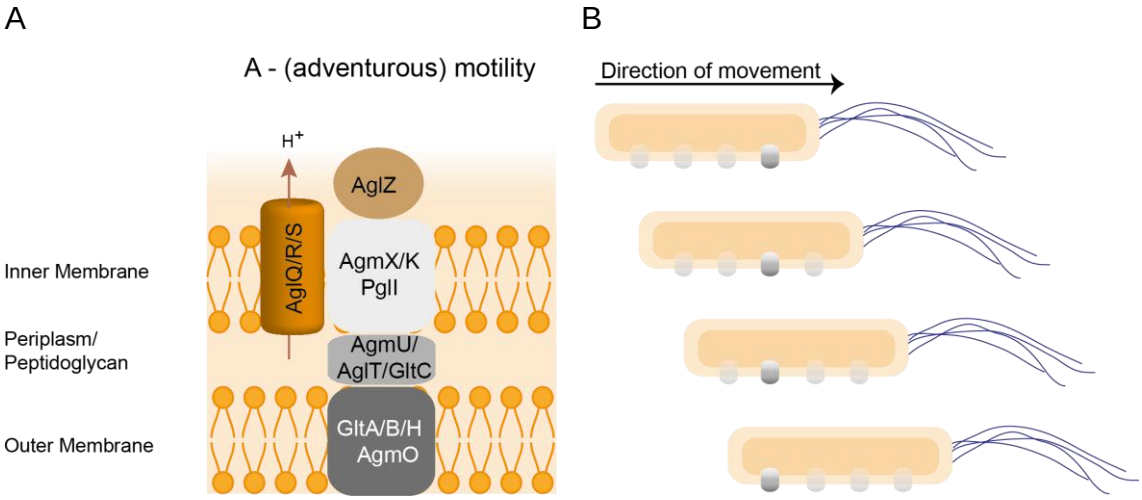

Figure 4: *M.xanthus* A-motility system. (A) Subcellular localization of the A-motility proteins. Proteins involved in A-motility are displayed with their respective localization in the cell envelope. AglQRS form a proton channel. H^+ proton flow is displayed by the orange arrow. While AglQ, AglZ, PglI, AgmU, GltC, GltA, GltB, AgmO and GltH have been analyzed directly in fractionation experiments, the localization of the other proteins included in the model are based on interaction studies, or co-localization experiments. (B) FACs are displayed in grey colors, they are stationary with respect to the substratum, while the cell is moving forward. The FAC colored with full opacity represents one focal adhesion complex, and its stationary localization.

The FAC model of A-motility led to additional studies of the localizations and interactions of known A-motility proteins. Interestingly, AgmU, a protein required for A-motility located in the cytoplasm and periplasm, was shown to co-localize with AglZ (Nan et al. 2010). Further interaction and localization studies led to the suggestion that A-motility proteins including AglZ, AgmU, AglT, AgmK, AgmX, AglW and CglB constitute multi-protein FACs (Nan et al. 2010). The current model suggests that these protein complexes are spanning the cell envelope while simultaneously binding to the substratum and a cytoskeleton component (Mignot et al. 2007). In line with that, a direct interaction between AglZ and the cytoskeleton protein MreB was demonstrated by in vitro studies (Mauriello et al. 2010).

1.3.1 The motor is driven by PMF

To identify the A-motility motor, mutants previously obtained in transposon mutagenesis screens with defects in A-motility gliding were reexamined. While most of the encoded proteins were involved in metabolism and proteins of unknown function, two clusters encoded putative motor proteins

(Youderian et al. 2003). One transposon insertion was found in the *aglX* gene that is part of a gene cluster coding for a Tol-Pal-like system (Nan et al. 2011). Other insertions hit the genes *aglS* and *aglR*, which are found in a gene cluster, that includes a MotA/TolQ/ExbB homolog AglR, as well as two MotB/TolR/ExbD homologs AglQ and AglS (Sun et al. 2011). In-frame deletion mutants of *aglX* and *aglQ* confirmed that both clusters are required for A-motility in *M. xanthus* (Nan et al. 2011; Sun et al. 2011). However, since Tol-Pal systems are mainly involved in general envelope processes such as cell division and transmembrane transport (Gerding et al. 2007), the MotAB homologs encoded in the second cluster were favored to power the FACs. Similarly, the MotAB complex in *E. coli* powers flagella rotation via proton motor force (Blair and Berg 1990). To distinguish between ATP and proton motive force (PMF) as the energy source powering the motor, drugs destroying the PMF were employed (Nan et al. 2011; Sun et al. 2011). CCCP (carbonyl cyanide-m-chlorophenylhydrazone) destroys the PMF and caused the cells to stop moving in a reversible manner. Furthermore, the chemical potential energy and the pH gradient were independently abolished using valincomycin and nigericin, respectively, in order to discriminate between their influences. The use of nigericin led to the complete inhibition of motility and, moreover, inhibited dynamics of A-motility protein clusters in immobilized cells. In contrast, valinomycin did not affect motility, indicating that the pH gradient is essential to power motility.

Furthermore, AglQ co-localizes with AglZ and therefore is suggested to be a part of FACs (Sun et al. 2011). In accordance with that, AglQ clusters have been observed to move from the leading cell pole to the lagging cell pole in immobilized cells. Additionally, all three proteins, AglQ, AglR and AglS, were shown to be required for gliding and interact forming a complex. Genetic inactivation of the H^+-channel by a single amino acid substitution in AglQ blocked gliding as well as dynamics of the FACs (Sun et al. 2011). Thus, the AglQ/AglR/AglS complex appears to be the motor component involved in force generation of the A-motility-system.

1.3.2 The A-motility complex

Previous genetic studies based on transposon mutagenesis screens suggested that multiple A-motility genes are distributed randomly in the *M. xanthus* genome (Youderian et al. 2003, Yu and Kaiser 2007). However, in depth bioinformatic analyses identified a core set of A-motility genes, the ancestral core complex which consists of 7 genes displayed in Fig. 5 (Luciano et al. 2011). These phylogenetic studies were based on the distribution of three motor proteins (M) and identified two gene clusters (G1 and G2) that encode the basal gliding machinery in *M. xanthus* (Luciano et al. 2011). In detail, proteins involved in A-motility (encoded by *agmU*, *aglT*, *pglI* and *gltC*), which share the genomic distribution of the motor proteins, were found to belong to two gene clusters (G1 and G2), coding for additional A-motility proteins, with a smaller genomic distribution (Fig. 5). Luciano et al. proposed that the A-motility machinery emerged from an ancestral conserved core of proteins of unknown function by the recruitment of additional proteins in Myxococcales (Luciano et al. 2011).

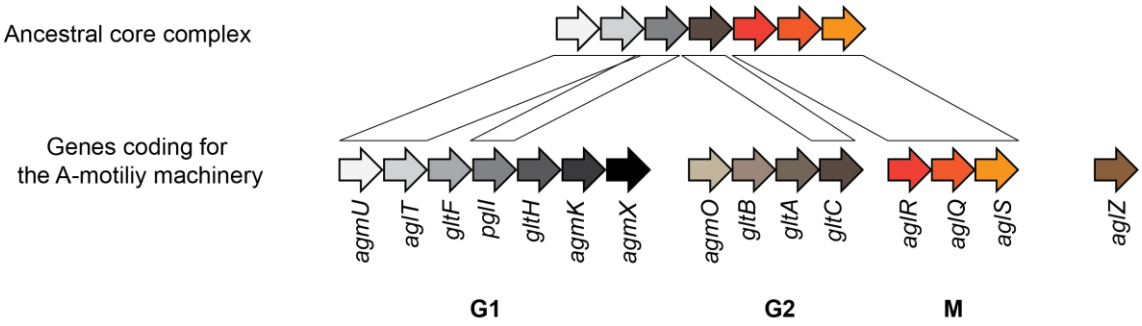

Figure 5: Genetic organization of A-motility genes. Genes as indicated. G1: gene cluster 1, G2: gene cluster 2, M: motor cluster. Details in the text.

In frame deletions of *agmU*, *aglT*, pglI, *agmX* and *agmK* caused defects in A-motility indicating that the whole G1 cluster is required for A-motility (Nan et al. 2010). In contrast not much is known about the four products of the second gene cluster (G2) containing *agmO*, *gltA*, *gltB* and *gltC*. However, two of the four genes (*agmO* and *gltC*) in this motility cluster were hit by a transposon in the previous screens and found to be important for A-motility as well (Youderian et al. 2003; Yu and Kaiser 2007). Therefore, the current model suggests that

the proteins encoded by the two newly identified gene clusters together with the motor proteins build the A-motility machinery. Most of these genes are coding for hypothetical proteins and their precise function remains to be characterized. In addition to the G1 and G2 cluster and the motor proteins, the pseudo-response regulator AglZ is involved in A-motility, co-localizing with AglQ and AgmU but encoded in a different genomic region (Fig. 5). While the ancestral core complex is highly conserved, AglZ is only conserved in *Myxococcales* (Wuichet, personal communication). Interestingly AglZ also directly interacts with FrzCD, part of the Frz chemosensory system, which is required to regulate reversal frequencies in *M. xanthus* (Mauriello et al. 2009). Notably, the Frz system is similarly to AglZ restricted to *Myxococcales* (Keilberg et al. 2012). This suggests that the pseudo-response regulator AglZ was incorporated in the A-motility system by a Myxococcales common ancestor in order to connect the A-motility gliding machinery with the Frz chemosensory system.

Moreover, the conserved core proteins involved in A-motility have additional paralogous gene clusters within the *M. xanthus* genome. However, deletions in the paralogous gene clusters did not cause any effect on motility, indicating, that these genes might have originated from gene duplication and have acquired new functions over time. Intriguingly, one of the paralogous gene clusters has been shown to be required for sporulation in previous studies (Muller et al. 2010). However, while these proteins involved in sporulation are highly similar to the components of the motility machinery on a sequence level, no additional set of motor-proteins paralogous to AglQRS regulating sporulation has been found. Therefore, it was hypothesized that *M. xanthus* only requires one motor to drive both motility and sporulation (Luciano et al. 2011).

1.4 Regulation of reversal frequencies by the Frz chemosensory system

Reversals in *M. xanthus* are induced by the Frz chemosensory system (Blackhart and Zusman 1985).

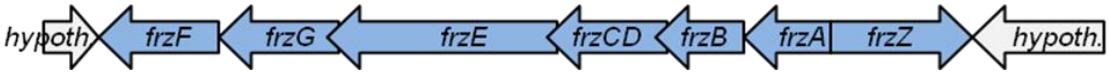

Figure 6: Genetic organization of the *frz* cluster. All known genes required for the Frz-chemosensory system are organized within one gene cluster. With the exception of *frzZ,* all genes are encoded in the same direction often with overlapping start and stop codons, which is indicative of an operon. The *frz* gene cluster (blue) is surrounded by two hypothetical genes (white). Arrows indicate the orientation of the gene

Chemosensory systems are widespread among diverse bacteria and have been shown to regulate both flagellar and T4P-based motility (Wuichet and Zhulin 2010). The *frz* genes comprise a single cluster that is composed of all essential chemosensory components (McBride et al. 1989; Trudeau et al. 1996) (Fig. 6).

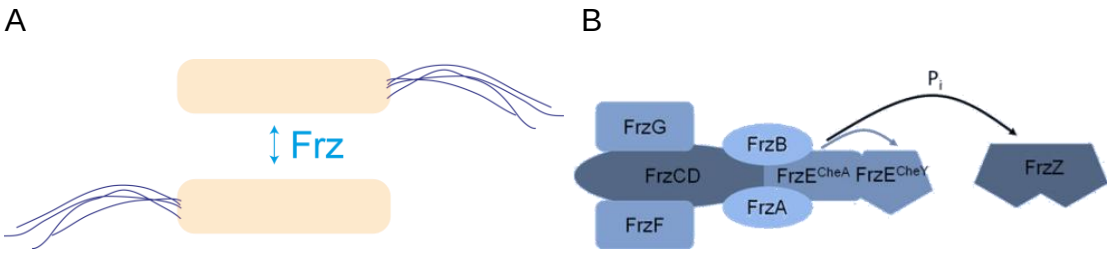

Figure 7: The Frz chemosensory system induces reversals. (A) Frz system induces reversals: switch in direction of movement and relocation of dynamic motility proteins from old leading pole to new leading pole and from old lagging pole to new lagging pole, including dissassemly of T4P at the old leading cell pole and reassembly at the new leading cell pole (B) Model of the frz chemosensory system consisting of the indicated proteins. Phosphotransfer occurs from $FrzE^{CheA}$ to $FrzE^{CheY}$ and the two receiver domains of FrzZ

Specifically, the Frz system consists of the following components (Fig.7): a cytoplasmic Methyl-accepting chemotaxis protein (MCP), FrzCD; two CheW homologs, FrzA and FrzB; FrzE, a CheA histidine kinase with a CheY-like receiver domain; a methyltransferase FrzF, which methylates FrzCD; a methylesterase FrzG, which demethylates FrzCD; and, FrzZ, a response regulator composed of two CheY-like receiver domains. To date, the input signals of the Frz system are not known; however, according to current models signals could be sensed by either FrzCD directly or by FrzF, containing multiple

TPR motifs important for protein-protein interactions (Bustamante et al. 2004; Scott et al. 2008). Upon stimulation, FrzE autophosphorylates a conserved histidine residue of its histidine phosphotransfer (Hpt) domain (Inclan et al. 2007; Inclan et al. 2008). *In vitro* phosphorylation assays have demonstrated direct transfer of the phosphoryl group from the FrzE Hpt domain to both receiver domains of FrzZ (Inclan et al. 2007). The current model suggests that in the absence of FrzE stimulation, the phosphoryl group is transferred to the CheY domain of FrzE, which inhibits FrzE autophosphorylation. In contrast, when FrzE is stimulated, the phosphoryl group is transferred to FrzZ to generate FrzZ~PP, which then stimulates reversals (Leonardy et al. 2008). FrzZ~PP is to date the most downstream component of the Frz chemosensory system. To stimulate reversals, the Frz system needs to interact with other regulatory components. Interestingly, MglA, a small Ras-like GTPase is required for the functioning of both motility systems and reversals and could be the downstream target of the Frz system (Zhang et al. 2010, Leonardy et al. 2010). However, to date no direct interaction between MglA and any component of the Frz system has been detected.

1.5 Regulation of both motility systems by MglA and MglB

Ras-like GTPases are binary nucleotide-dependent molecular switches that cycle between an inactive GDP- and an active GTP-bound form (Vetter and Wittinghofer 2001; Bos et al. 2007). The GTP-bound form interacts with downstream effectors to induce a specific response. Generally, Ras-like GTPases bind nucleotides with high affinities and have low intrinsic GTPase activities. Therefore, cycling between the two nucleotide-bound states depends on two types of regulators: Guanine-nucleotide exchange factors (GEFs), which function as positive regulators by facilitating GDP release and GTP binding, and GTPase activating proteins (GAPs), which function as negative regulators by stimulating the hydrolysis of GTP to GDP.

The Ras-like GTPase MglA in combination with its cognate GAP, MglB, acts to regulate both A- and S-motility in *M. xanthus* (Leonardy et al. 2010; Mauriello et al. 2010; Patryn et al. 2010; Zhang et al. 2010) (Fig. 8). Specifically, MglA

establishes the correct polarity of motility proteins between reversals and induces their relocation during reversals in a nucleotide-dependent manner (Leonardy et al. 2010; Zhang et al. 2010). MglA cycles between an inactive GDP-bound form and an active GTP-bound form. While a cell is moving, the active form, MglA/GTP is localized at the leading pole, the inactive MglA/GDP is localized diffusely, and the GAP protein MglB is localized at the lagging pole (Leonardy et al. 2010). The binding of MglA/GTP and MglB at opposite poles is proposed to be the result of a mutual exclusion mechanism that defines the leading/lagging cell pole polarity axis. In the current model, the Frz chemosensory system induces the relocation of MglA/GTP from the old leading pole to the new leading pole and, as a consequence, MglB relocates from the old lagging pole to the new lagging pole. The relocation of MglA and MglB causes an inversion of the leading/lagging pole polarity axis. In this model, FrzZ~PP is thought to either function as a guanine-nucleotide-exchange factor (GEF) that stimulates the accumulation of MglA/GTP directly, or indirectly by inhibiting GAP activity of MglB. MglA/GTP could establish the correct polarity of motility proteins between reversals and their relocation during reversal by interaction with effector proteins.

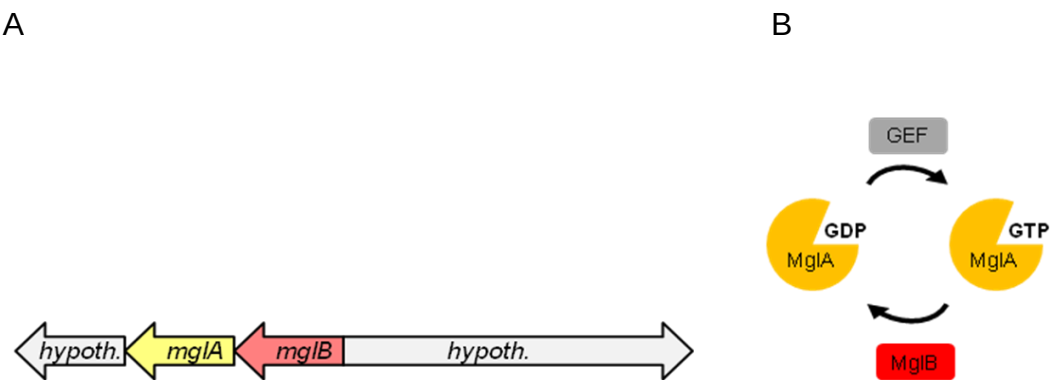

Figure 8: MglB is a GAP of MglA. (A) Genetic organization of *mglA* locus. *mglA* and *mglB* (red and yellow) are encoded within one operon, surrounded by hypothetical (white) genes. Arrows indicate the gene orientation of the gene (B) Model of MglA cycling: MglA cycles between active GTP-bound form and inactive GDP-bound form. MglB is a GAP of MglA, which stimulate the hydrolysis of GTP to GDP.

1.6 The response regulator RomR

Most, if not all, bacteria exist under fluctuating conditions. Therefore, bacteria must be able to sense and respond to environmental changes to optimize their chances of survival. Bacterial species have adopted a variety of survival strategies to respond to changes in their environments. The various strategies played out in response to starvation include adaptive changes in gene expression, the active movement away from nutrient poor conditions, and differentiation resulting in specialized cell types with novel properties. Two component systems are wide spread regulatory systems for signal transduction. They are involved in regulating diverse cell processes such as sporulation, motility, cell division, virulence, metabolism and stress response (Stock et al. 2000). A classic two component system consists of a histidine protein kinase and a response regulator (Fig. 9).

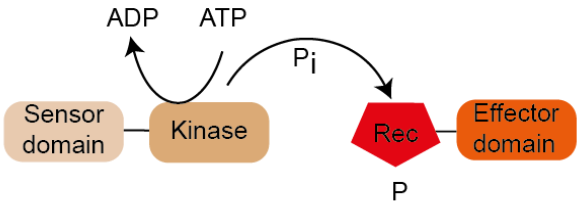

Figure 9: Classic two component system. Schematics show structure and phosphotransfer reactions in a simple two-component system. Details in the text.

The histidine kinase has a modular architecture with a variable N-terminal sensor or input domain and a C-terminal kinase domain. The variable sensor domain of the kinase receives an intercellular or intracellular signal. Additionally, this part of the kinase may contain one or more transmembrane helices that anchor the kinase in the cytoplasmic membrane. In response to the relevant signal, the sensor domain signals to the kinase module to autophosphorylate a conserved histidine residue using ATP as a phosphoryl donor. Subsequently, this phosphoryl group is transferred to a conserved aspartate residue in the receiver domain of the cognate response regulator. Response regulators also have a modular structure typically composed of an N-terminal receiver domain and a C-terminal output domain. The phosphorylation

state of the response regulator controls the output response. Typically, phosphorylation activates the output domain. The output domain can regulate a variety of responses including changes in gene expression via DNA-binding, changes in enzymatic activity, and protein-protein interactions (Jenal and Galperin 2009; Galperin 2010).

Comparative genomics approaches have documented that most bacterial genomes encode proteins of two component systems: a recent survey by Wuichet et al. showed that 864 out of 899 completely sequenced bacterial genomes encode such proteins (Wuichet et al. 2010). Generally, the number of two-component proteins encoded by a genome positively correlates with genome size and the total number of encoded proteins (Galperin 2005; Ulrich et al. 2005). Often the sensor histidine kinase and the response regulator are coupled genetically which means they are next to each other in an operon, but many orphan kinases and response regulators have also been identified (Rodrigue et al. 2000). Analysis of the *M. xanthus* genome identified 272 genes encoding proteins for two component systems, 132 of which are orphan genes (Shi et al. 2008). As a result, there is no straightforward approach to identify the cognate partners for the orphan genes. Often, bioinformatics and phenotype analysis are combined, under the assumption that a kinase and a cognate response regulator acting in the same signaling pathway co-evolve or are required for the same function, respectively.

Figure 10: Genetic organization of *romR* response regulator. *romR* is encoded downstream of *romA* and upstream of *valS*. (details in the text) Arrows indicate the gene orientation.

The open reading frame *MXAN_4461* encodes the orphan response regulator RomR (Fig.10). The deletion of this open reading frame causes a strong motility defect (Leonardy et al. 2007). The flanking gene upstream encodes a hypothetical protein (RomA) with two CheW domains that was shown to be involved in development (Leonardy et al. 2007), and the gene downstream encodes for a protein homologous to Val-tRNA synthetase.

1.6.1 Bioinformatic analysis of RomR

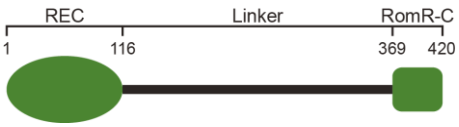

Figure 11: Domain architecture of the response regulator RomR. RomR has two conserved domains: an N-terminal receiver domain typical of response regulators and a conserved C-terminal domain, which are linked by a proline rich region. Numbers correspond to the RomR amino acid sequence from *M. xanthus*.

Sequence analysis shows that the RomR protein possesses a conserved N-terminal receiver domain (residues 1–115) and a C-terminal output domain (residues 116–420) that can be subdivided into a Pro-rich region (residues 116–368) and a conserved Glu-rich tail (residues 369–420) (Fig. 11). The receiver domain includes a conserved aspartate residue, which is predicted to be phosphorylated (Leonardy et al. 2007). However, no cognate kinase or phosphotransfer protein, which would fulfill this function, has been identified. Given that RomR is encoded downstream of a CheW-like protein, it is possible that the kinase phosphorylating RomR is not a classic histidine-protein kinase, but rather a CheA-like histidine kinase that is part of a complex chemosensory system. Surprisingly, while RomR has been found to be required for motility in *M. xanthus*, an in-frame deletion of *romA*, which encodes the CheW-like protein upstream of *romR*, did not show any defect in motility (Keilberg, Diploma thesis 2009). Therefore, a direct connection between RomR and this CheW-like protein remains unclear. Moreover, no kinase required for the phosphotransfer reaction to RomR has been identified. Therefore, it remains an interesting question, how the RomR response regulator is activated, and how it is incorporated into the signaling pathways of motility in *M. xanthus*.

1.6.2 RomR regulates motility and reversals

To investigate the function of RomR, Leonardy et al. constructed mutants lacking RomR or expressing RomR with glutamate or asparagine substitutions of the conserved aspartate in the receiver domain (Leonardy et al. 2007). While the lack of RomR completely abolishes A-motility, substitutions in the conserved

aspartate only affect the reversal frequencies. Cells expressing the protein RomR^{D53E}, a phospho-mimic mutant, hyper-reverse. Consistently, cells expressing the protein RomR^{D53N}, a non-phosphorylatable mutant, only rarely reverse (Leonardy et al. 2007). In conclusion, RomR is sufficient for motility independently of its activation state. Moreover, RomR phosphorylation is predicted to be required for its activation leading to induction of reversals in *M. xanthus*. To further characterize the protein, RomR-GFP localization was investigated in vivo. Fully functional RomR-GFP localizes asymmetrically in a cell with a large cluster at the lagging cell pole and a small cluster at the leading cell pole (Fig.12). During a reversal the large cluster switches from the old lagging pole to the new lagging pole (Leonardy et al. 2007). Remarkably, at the same time, a marker protein for the S-motility system, FrzS relocates from the old leading pole to the new leading pole (Leonardy et al. 2007). Thus, RomR localization switches during a reversal simultaneously with the S-motility protein FrzS indicating that components of both A- and S-motility machineries switch poles in synchrony.

A B C

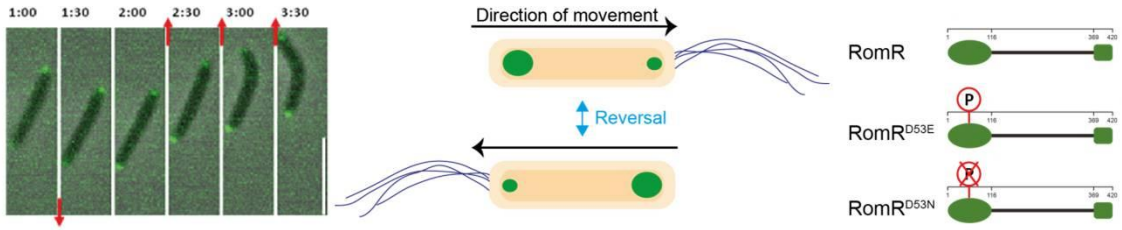

Figure 12: RomR is required for A-motility and reversals. (A) RomR localization is dynamic. Depicted are overlays of fluorescence and phase-contrast images recorded at the indicated time points in minutes. Arrows indicate the direction of movement. From 1:30 to 2:00, the cell did not move. From 2:00 to 2:30, the cell reversed. (B) Asymmetric localization of RomR in a moving cell, direction of movement as indicated (C) Model of RomR substitutions which have been shown to cause a hyper-reversing phenotype (RomR^{D53E}) and a hypo-reversing phenotype (RomR^{D53N}), respectively.

In a previous study it was shown that the output domain of RomR is sufficient for both the asymmetric localization of RomR and for the stimulation of motility (Leonardy et al. 2007). However, cells expressing the output domain only, were not able to reverse, and the dynamic relocation of the protein was abolished (Leonardy et al. 2007). Therefore, the receiver domain, and more specifically the phosphorylation of the conserved aspartate within the receiver

domain, is required for RomR dynamics and cell reversals (Leonardy et al. 2007). Since cells that are not able to activate RomR by phosphorylation are not able to reverse, RomR was hypothesized to be a regulator of reversals. To understand how RomR regulates reversals, epistasis analysis using FrzE and RomR have been performed. Intriguingly, substitutions in RomR regulating the reversal frequency can bypass the lack of FrzE, demonstrating that RomR acts downstream of FrzE (Leonardy et al. 2007). Based on these studies, the authors proposed a model, in which the Frz system coordinates reversals upstream of MglA and MglB. Moreover, RomR was placed downstream of MglA and predicted to regulate motility and reversals for the A-motility system specifically (Fig.13).

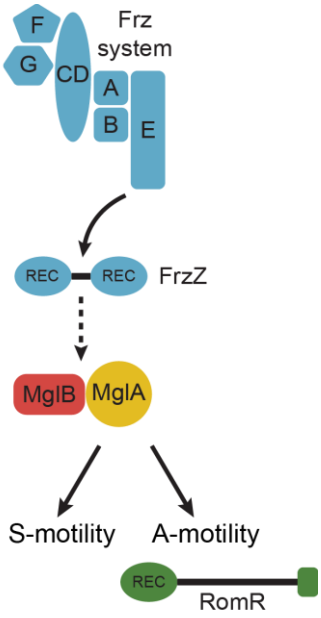

Figure 13: RomR acts downstream of the Frz system and MglA/MglB. Details in the text.

1.7 Scope of the study

RomR was proposed to regulate motility and reversals in the A-motility system based on the strong A-motility defect observed for a *ΔromR* mutant (Leonardy et al. 2007). Furthermore, RomR was shown to localize dynamically with a large cluster at the lagging cell pole and a small cluster at the leading cell pole.

In this study, I investigated how RomR is targeted to the cell poles and how it regulates motility and reversals. I suggested that the RomR response regulator is part of a signaling cascade, which requires a kinase or phosphotransferase for its activation. Furthermore, I hypothesized that one or more proteins may interact with RomR for function and localization. To further characterize RomR function, I perfomed interaction studies to identify interaction partners and analyzed the dependency of RomR localization on other motility proteins. First, in-frame deletions of representative A-motility genes were generated followed by RomR localization analysis. Interestingly, bioinformatics analysis indicated a co-evolutionary relationship between RomR, and a subset family of MglA and MglB. Therefore, interaction studies, epistasis analysis and localization studies were performed to investigate the relationship between RomR, MglA and MglB.

Phosphorylation of RomR was hypothesized to be essential for its activation. Therefore I performed interaction and phosphotransfer studies between RomR and FrzE, the kinase of the Frz chemosensory system that regulates reversals upstream of RomR. Furthermore, new interaction partners were identified by bioinformatics and supported by experimental characterization including in-frame deletion mutants, localization and interaction analyses.

2 Results

2.1 MglA and MglB form a complex to regulate motility

To date, MglA (motility gliding protein A) is one of the best characterized proteins in *M. xanthus*, due to its major role in the regulation of motility. Early studies of MglA characterized its function in motility about 20 years ago (Hartzell and Kaiser 1991). Later, MglA was found in transposon mutagenesis screens that were carried out in order to identify genes important for both A- and S-motility (Youderian et al. 2003; Youderian and Hartzell 2006). Later studies revealed the importance of MglA in regulating polarity and cellular reversals, which include the switch of polarity of proteins in both motility systems (Leonardy et al. 2010; Zhang et al. 2010). Furthermore, MglA is required indirectly for correct fruiting body formation, because the abolishment of motility prevents aggregation (Kim and Kaiser 1990). Initial characterization of *mglA* revealed it was located in an operon with *mglB* (Hartzell and Kaiser 1991). While the involvement of MglA in A- and S- motility was established over two decades ago, the function of MglB remained unknown (Hartzell and Kaiser 1991). Whereas a mutation in *mglA* completely abolishes A- and S- motility, an *mglB* mutant only shows reduced motility for both systems. MglA was characterized as a small GTPase; therefore, it was possible to lock MglA in a GTP-bound conformation by substitutions in its active site such as G21V or Q82A, leading to the same phenotype as observed for an *mglB* mutant (Leonardy et al. 2010; Zhang et al. 2010; Miertzschke et al. 2011). Detailed analysis revealed that the reduction of motility was due to hyper-reversals in Δ*mglB*, *mglA*^{G21V} and *mglA*^{Q82A} mutants. However, Δ*mglB* and *mglA*^{G21V} as well as *mglA*^{Q82A} cells displayed velocities similar to WT. Recent studies demonstrated that MglB acts as the GTPase activating protein of MglA, and that MglA-GTP, the active form of MglA, is required for A-motility, S-motility and reversals (Leonardy et al. 2010, Zhang et al. 2010). High concentrations of MglA-GTP in the cell, which can be obtained by locking MglA in the GTP-bound form or by indirectly inhibiting GTPase hydrolysis via deleting *mglB*, cause a hyper-reversing phenotype. To analyze the interaction between MglA and MglB

in more detail, we aimed to crystallize the two proteins together in complex (Fig.14). Homologs of MglA and MglB in *Thermus thermophilus* were co-crystallized because *M. xanthus* MglA and MglB could not be obtained in soluble form (Miertzschke et al. 2011). The MglA and MglB proteins encoded in the *T. thermophilus* genome show 62/81% and 28/52% identity/similarity to MglA and MglB of *M. xanthus*, respectively. To test the functionality of MglA and MglB of *T. thermophilus,* the two proteins were expressed in a *M. xanthus ΔmglAΔmglB* strain and provided at least partial complementation, indicating that the *T. thermophilus* proteins can function in *M. xanthus* motility (Miertzschke et al. 2011).

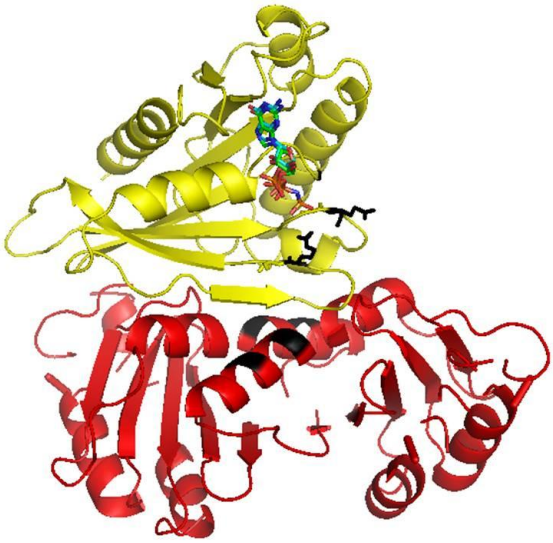

Figure 14: MglA and MglB form a complex. Structure of MglA (yellow) bound to an MglB dimer (red) of *Thermus thermophilus*. Complex displays a 1: 2 (MglA: MglB) stoichiometry.

We obtained crystals of MglB, MglA, and the MglA/MglB complex. Moreover, the complex was also crystallized in the transition state for GTP hydrolysis of MglA. For successful crystallization of the MglA/MglB complex, alanine substitutions were introduced in the α-helix mediating polymerization of MglB dimers, which were identified when crystalizing MglB alone.

The crystals of the MglA/MglB complex revealed an MglA monomer and an MglB dimer, an unusual stoichiometry for GTPase/GAP complexes, which are typically found in a 1:1 ratio. To support this finding, titration experiments were performed, verifying the 1:2 ratio of MglA/MglB.

Importantly, the mechanism of GTPase activation by MglB is unique. Known GAPs typically activate GTP hydrolysis by providing a conserved arginine residue that is required for the completion of the active site in the GTPase; however, MglB does not contain any residue that is positioned in the active site during complex formation (Fig.15). Instead, the conformation of MglA changes slightly upon binding MglB, which results in the correct positioning of active site residues such as Q82 and R53. Importantly, MglA undergoes striking conformational changes upon GTP binding, involving a screw-type forward movement of the central β-strand, which have never been described in other small Ras-like GTPases.

From the MglA/MglB complex structure it was possible to predict the residues in MglA and MglB that play major roles in GTP binding, GTP hydrolysis, and MglA/MglB interaction. Detailed characterization of these residues was carried out *in vitro* beginning with alanine substitutions in the *T. thermophilus* proteins followed by interaction and GTPase hydrolysis analyses. These experiments confirmed that the MglB residues A68 and A72 are required for binding to MglA via a hydrophobic interface (Fig. 15).

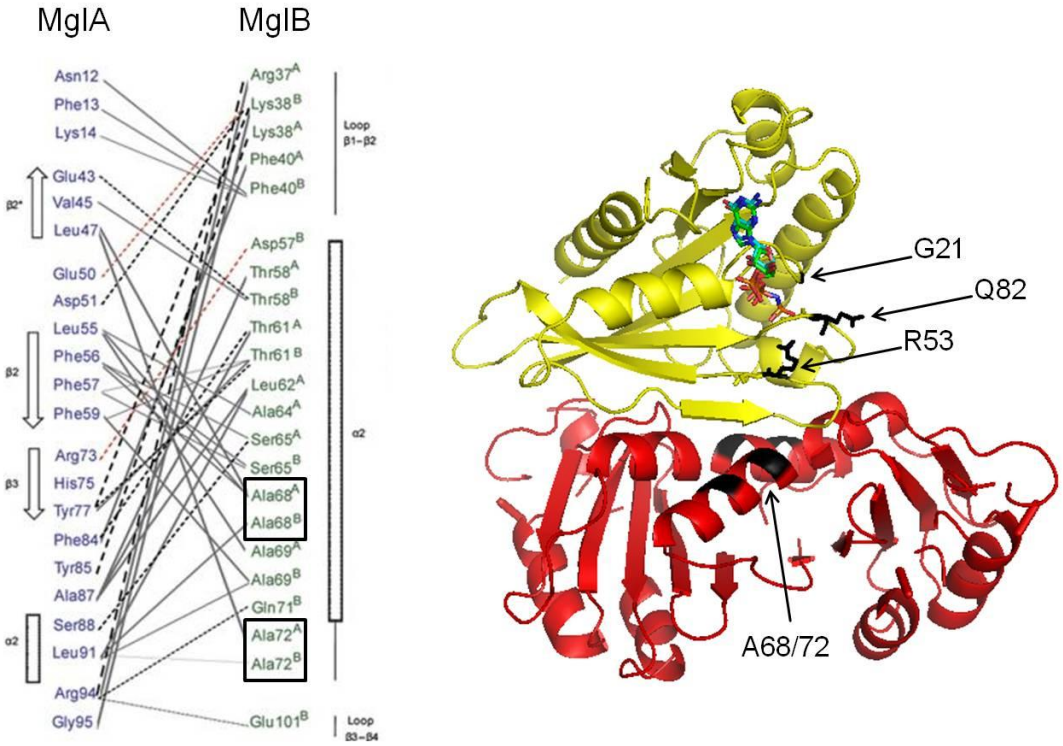

Figure 15: MglA and MglB interface. (left) residues in MglA and MglB involved creating a hydrophobic interface. Black boxes mark important residues. Details in the text. (right) Structure of MglA (yellow) bound to MglB dimer (red) of *Thermus thermophilus*. Important residues marked in black.

Furthermore, it was shown that the substitutions that abolish MglA/MglB binding also eliminate the activation of MglA GTP hydrolysis by MglB. In contrast, the substitutions in MglB that prevent its oligomerization (E14/R15/R124/E127/R131), which were required to obtain the MglA/MglB complex, did not interfere with MglA interaction or GTP hydrolysis (Miertzschke et al. 2011).

Next, we aimed to assess the function of the above-mentioned residues *in vivo*. While MglA from *M. xanthus* and *T.thermophilus* show high degree of identity on the amino acid level (62 %), their MglBs are less conserved (28% identity). However, secondary structure analysis supports that the MglB structure is highly conserved between the two organisms, thus allowing for the identification of corresponding amino acids required for MglA/MglB interaction in *M. xanthus*. To investigate whether *M. xanthus* MglA and MglB employ the same mechanism as described for *T. thermophilus*, the homologous substitutions were introduced into the *M. xanthus* proteins *in vivo*. Therefore, two forms of *M. xanthus* MglB were expressed. In the first form, the residues A64/G68, homologous to A68/A72 in *T. thermophilus*, were substituted by arginines. In the second form, the residues T13/K14/K120/D123/K127 that correspond to E14/R15/R124/E127/R131 in *T. thermophilus* were substituted with alanines, and are referred to as A5 (five alanine substitutions). Next, the effects on function and localization of the substituted MglB proteins were analyzed. First, reversal frequencies were measured. Since a Δ*mglB* mutant as well as an *mglA* mutant locked in the GTP-bound form cause hyper-reversals, we hypothesized that MglB substitutions affecting MglA interaction, and in turn GTP hydrolysis, would also show alterations in reversal frequencies compared to WT. Second, we analyzed if the substitutions led to altered localization of the proteins (Table 1).

Table 1: Characterization of MglB substitutions *in vivo*

genotype	reversal period	unipolar	bipolar	dynamics of localization
mglB⁺A⁺	15.7 ± 4.6			
ΔmglB	6.7 ± 0.8			
mglB^{A5}	17.4 ± 3.1			
mglB$^{A64/G68R}$	6.4 ± 0.5			
ΔmglB/mglB-yfp	8.2 ± 1.0	80	20	dynamic
ΔmglB/mglB^{A5}-yfp	7.8 ± 0.6	67	33	dynamic
ΔmglB/mglB$^{A64/G68R}$-yfp	6.9 ± 0.3	32	68	stationary
ΔmglBA/mglB-yfp	non-motile	40	60	NA
ΔmglBA/mglB^{A5}-yfp	non-motile	37	63	NA
ΔmglBA/mglB$^{A64/G68R}$-yfp	non-motile	48	52	NA

Reversal periods in minutes with standard deviation were calculated observing 100 cells for each strain for 15 minutes. Unipolar and Bipolar localization is presented as percentage of 100 cells. To distinguish between dynamic and stationary localization, cells were tracked in time lapse movies.

The reversal periods of cells with substitutions in MglB important for the MglA/MglB interface (MglB$^{A64/G68R}$) or the polymerization of MglB dimers (MglB^{A5}) are displayed in Table 1. While WT cells reversed on average every 15.7 minutes, a Δ*mglB* mutant reversed on average every 6.7 minutes. These results are in agreement with previous studies, which reported a hyper-reversing phenotype for an *mglB* mutant (Leonardy et al. 2010; Zhang et al. 2010). Substitutions that interfere with the polymerization of MglB dimers *in vitro*, did not cause any observed effect *in vivo*. The respective mutants reversed on average every 17.4 minutes, similarly to WT. In contrast, substitutions that affected the MgA/MglB interaction *in vitro* also had an effect *in vivo*, leading to a hyper-reversing phenotype similar as in the Δ*mglB* mutant. Thus, critical residues identified based on the crystal structure in MglA and MglB from *T.thermophilus* also play crucial roles in *M. xanthus in vivo*. Therefore, we hypothesize that MglB$^{A64/G68R}$ cannot interact with MglA *in vivo*, resulting in high accumulations of MglA-GTP in the cells. To test the effects on localization of the proteins, corresponding YFP-fusions of the different MglB proteins were constructed, and their localizations were analyzed in presence and absence of MglA (Table 1/Fig 16).

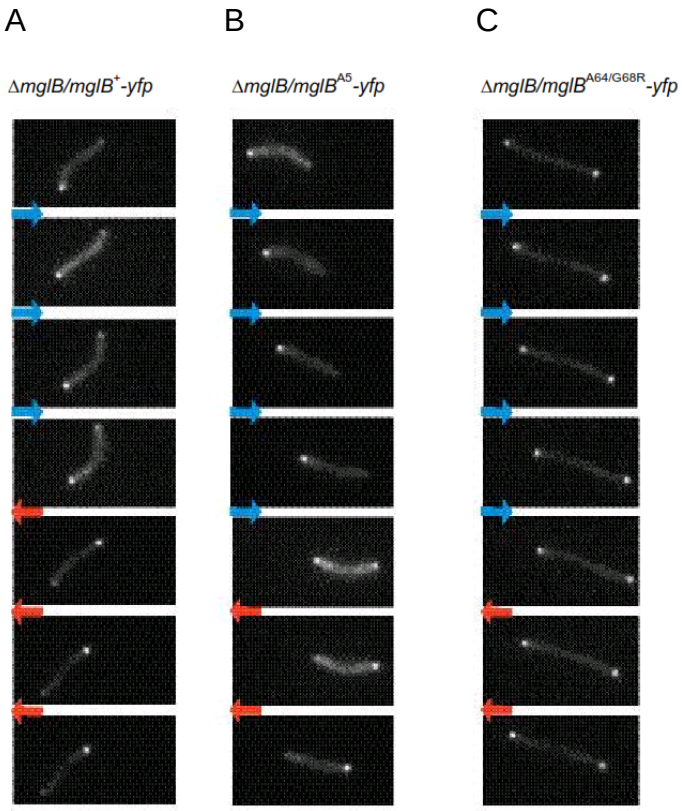

Figure 16: MglB GAP activity is essential for its correct localization. Time-lapse recordings of cells expressing three different MglB-YFP constructs are displayed. A: WT protein, B: substitutions preventing polymerization of MglB dimers (MglB^{A5}) and C: substitutions required for MglA/MglB interaction (MglB$^{A64/G68R}$). Strains of the indicated genotypes were transferred from exponentially growing cultures to a thin agar-pad on a microscope slide, and imaged by time-lapse fluorescence microscopy. Red and blue arrows indicate direction of movement.

While the localization of MglB-YFP in the Δ*mglB* mutant showed a dynamic unipolar localization at the lagging cell pole as reported (Fig. 16A) (Leonardy et al. 2010), this protein was not able to fully complement the hyper-reversing phenotype, leading to a reversal periods of 8.2 minutes on average (Table 1). Nevertheless, the fusion protein was used as a control for examining MglB^{A5}-YFP and MglB$^{A64/G68R}$-YFP localization because it showed a dynamic polar localization. As expected, these fusions did not restore reversal periods to the WT levels; however, each displayed distinct localization patterns. MglB^{A5}-YFP localized similar to MglB-YFP in unipolar clusters, which switched the pole during a reversal (Fig. 16B), whereas MglB$^{A64/G68R}$-YFP localized in a bipolar manner (Fig. 16C). Localizations of MglB-YFP, MglB^{A5}-YFP and MglB$^{A64/G68R}$-YFP were also analyzed in the absence of MglA, revealing a predominantly bipolar, non-dynamic localization of all three (Table 1).

In summary, we observed that MglB-YFP showed a predominantly unipolar dynamic localization, but becomes more bipolar when lacking the MglA/MglB interaction, either due to the substitutions at the MglA/MglB interface or to the absence of MglA. Therefore, we conclude that the MglA/MglB interaction is essential for a correct MglB localization, which in turn is necessary to establish the cell polarity axis with MglA-GTP at the leading cell pole and MglB at the lagging cell pole.

The *in vitro* and *in vivo* analyses from Miertzschke et al. provided valuable new insights into the diversity of small GTPase mechanisms. While this study verified that MglB is the GAP of MglA, a guanine nucleotide-exchange factor (GEF) that would convert MglA from the inactive GDP bound form to the active GTP bound form has yet to be identified. Additional interesting questions remain, including which proteins directly interact with the MglA/MglB system to regulate motility, and what is the direct output of MglA? It is known that activated GTPases interact with effector proteins. Current data suggest that MglA in the GTP-bound form interacts with proteins from the A-motility machinery and the S-motility machinery. However, MglA may play additional roles since it is needed to coordinate the polarity of the proteins in addition to activating both machineries. To understand how motility in *M. xanthus* is regulated, finding direct interaction partners of MglA and MglB is fundamental.

2.2 The RomR response regulator

2.2.1 RomR is required for A- and S-motility

While detailed studies have shown that MglA together with its cognate GAP MglB are involved in regulating both motility systems and reversals, another regulatory protein, the response regulator RomR (required for motility reponse), became of interest due to its similar range of functions in motility. It had been reported that RomR is required for motility and reversals (Leonardy et al. 2007), and from that work RomR was speculated to be involved in regulating reversals in the A-motility system, acting as a master regulator of A-motility. However, the exact cellular function of the protein remained unknown. Thus, we

aimed to carry out in depth studies to characterize the function of RomR. First, we reexamined the *romR* phenotypes with respect to A- and S-motility.

Therefore, motility assays were performed with a Δ*romR* mutant by spotting 5 µl of concentrated cell suspensions (OD = 7) on plates with a low agar concentration (0.5 %) where cells have been reported to mostly move by T4P (S-motility), and on plates with a high agar concentration (1.5 %) where cells move predominantly with the A-motility machinery (Hodgkin and Kaiser 1979). After the spots dried, the plates were incubated overnight at 32°C and then the colony morphology as well as the increase in the colony size was recorded. Specifically, the expansion of the colony diameter was measured, by calculating the difference between colony size immediately after spotting and after 24h incubation. Additionally, a qualitative analysis of motility has been performed. While WT cells moving by S-motility typically form flares composed of many cells on soft agar, cells moving via A-motility on hard agar can be visualized independently under high magnification (Fig. 17).

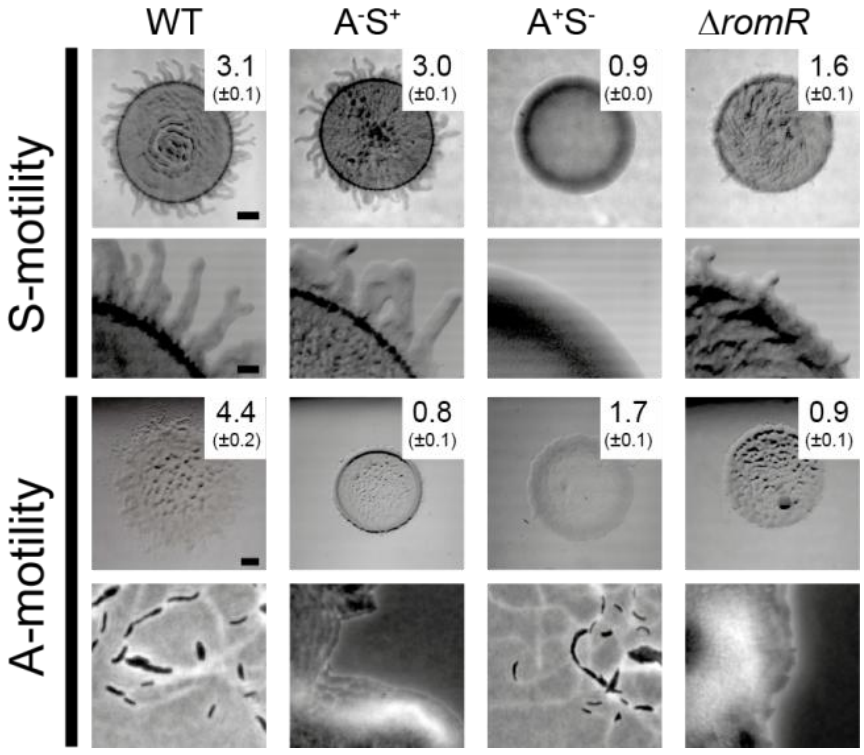

Figure 17: RomR is important for A- and S-motility. The indicated strains were incubated at 32°C for 24 h on 0.5% agar/0.5% CTT medium to score S-motility and 1.5% agar/0.5% CTT medium to score A-motility. The numbers indicate the increase in colony diameter in mm and standard deviation after 24 h.

Three additional strains were used as controls in the motility assays characterizing the phenotype of Δ*romR*: WT strain DK1622, A^-S^+ strain DK1217,

carrying a deletion in *aglB* gene *(a-motility gliding protein B)*, and finally A^+S^- strain DK1300 carrying a deletion in *sglG* gene *(s-motility gliding protein G)*. WT cells, which are able to move by both systems, formed flares at the edge of the colony on soft agar leading to a colony expansion of over 3 mm after 24h (Fig. 17). Additionally, WT cells were able to spread on hard agar, which favors A-motility, leading to an increase of the colony size of over 4 mm, primarily caused by single cell movement (Fig. 17). The control strain containing a defect in A-motility (A^-S^+), was still able to form flares on soft agar leading to a similar expansion as WT (3.0 mm), but no single cell movement, and thus no significant spreading on hard agar (0.8 mm) was detected (Fig. 17). In parallel, the control strain containing an S-motility defect (A^+S^-) could not form flares on soft agar (0.9 mm), but was still able to spread by single cell movement (1.7 mm) (Fig. 17). The Δ*romR* colony displayed much shorter S-motility flares (1.6 mm), about half the size compared to WT, and was impaired in A-motility as reported in the previous study (Leonardy et al. 2007), leading to the formation of a smaller colony on hard agar plates (0.9 mm) as compared to WT and the A^+S^- strain (Fig. 17). Additionally, no single cells at the edge of the Δ*romR* colony were observed. Thus, a Δ*romR* strain shows an abolishment of A-motilty and a previously unrecognized strong defect in S-motility. These results gave a first indication that RomR might be a master regulator of A- and S-motility motility, rather than an A-motility regulator alone as originally reported (Leonardy et al. 2007).

It has been previously published that RomR protein exhibits an asymmetric bipolar localization with the larger cluster located at the lagging cell pole, which then switches to the new lagging pole during a reversal (Leonardy et al. 2007). To further investigate the function of RomR, we analyzed how RomR is targeted to the cell pole. While polar localization often depends on interacting proteins, polar targeting can also be due to the recognition of the membrane curvature or lipid interaction (Romantsov et al. 2007, Lenarcic et al. 2009). Our first approach for identifying RomR polar targeting determinants focused on intrinsic RomR motifs. RomR consists of a receiver domain and an output domain. Previous studies showed that the receiver domain of RomR is required for the dynamic localization of RomR during reversals, while the output domain is required for the correct asymmetric bipolar localization and its activity

in motility (Leonardy et al. 2007). Moreover, Leonardy et al. suggested that the conserved aspartate in the receiver domain is required for RomR phosphorylation and activation. RomR activation in turn results in the induction of reversals. A substitution of the aspartate to an asparagine, as well as the deletion of the whole receiver domain caused an inhibition of reversals. Interestingly, the output domain was found to be able to fulfill all RomR functions except for the induction of reversals, indicating that the output domain is sufficient for motility and localization (Leonardy et al. 2007). The RomR output domain is 304 amino acids but lacks any characterized domains. These interesting features of both the RomR receiver and output domains led us to independently characterize them further in parallel.

2.2.2 Functions of the single subparts of the RomR output domain

To confirm the localization and activity of full-length RomR vs the output domain alone, RomR$^{116\text{-}420}$ (Fig. 18A), we compared two fusion constructs, *romR-gfp* and *romR$^{116\text{-}420}$-gfp*, which were expressed from the constitutively active *pilA* promotor in a Δ*romR* strain. The ability to complement the motility defect caused by a *romR* deletion as well as protein cellular localization was determined (Fig. 18C). Western blot analyses demonstrated that RomR-GFP and RomR$^{116\text{-}420}$-GFP are expressed at similar protein levels as RomR in WT. (Fig. 18B). In line with previous analyses carried out in a *romR* insertion mutant, we verified that both RomR-GFP and RomR$^{116\text{-}420}$-GFP localize in an asymmetric bipolar pattern (Leonardy et al. 2007). Moreover, RomR-GFP was able to fully restore A- and S-motility to WT levels displaying flares, which led to a colony increase of 3 mm (WT: 3.1 mm) on soft agar as well as single cell movements leading to a colony increase of 4.5 mm (WT: 4.4 mm) (Fig. 18C). The GFP fusion of the output domain (RomR$^{116\text{-}420}$-GFP) could only partially restore A- and S-motility as displayed by shorter flares (2.3 mm) and a smaller increase in colony size on hard agar (1.6 mm) when compared to a strain expressing full-length RomR-GFP. Consistent with the observation that the output domain cannot restore reversals, the smaller colony size can be explained by the hypo-reversing phenotype (Leonardy et al. 2007). However, it

is important to note that cells expressing only the output domain are able to move with both motility systems, despite their inability to reverse, and show the same protein localization as observed for the full-length protein. Consequently, it is plausible that the output domain could incorporate two motifs, one important for RomR localization and one important for RomR function in motility. To analyze which parts of the output domain could function independently, detailed bioinformatic analyses were performed, which revealed that the output domain consists of two distinct parts, a proline-rich linker region extending from amino acid 116 to 368 and a glutamate-rich C-terminal domain extending from amino acid 369 to 420 (Fig. 18A).

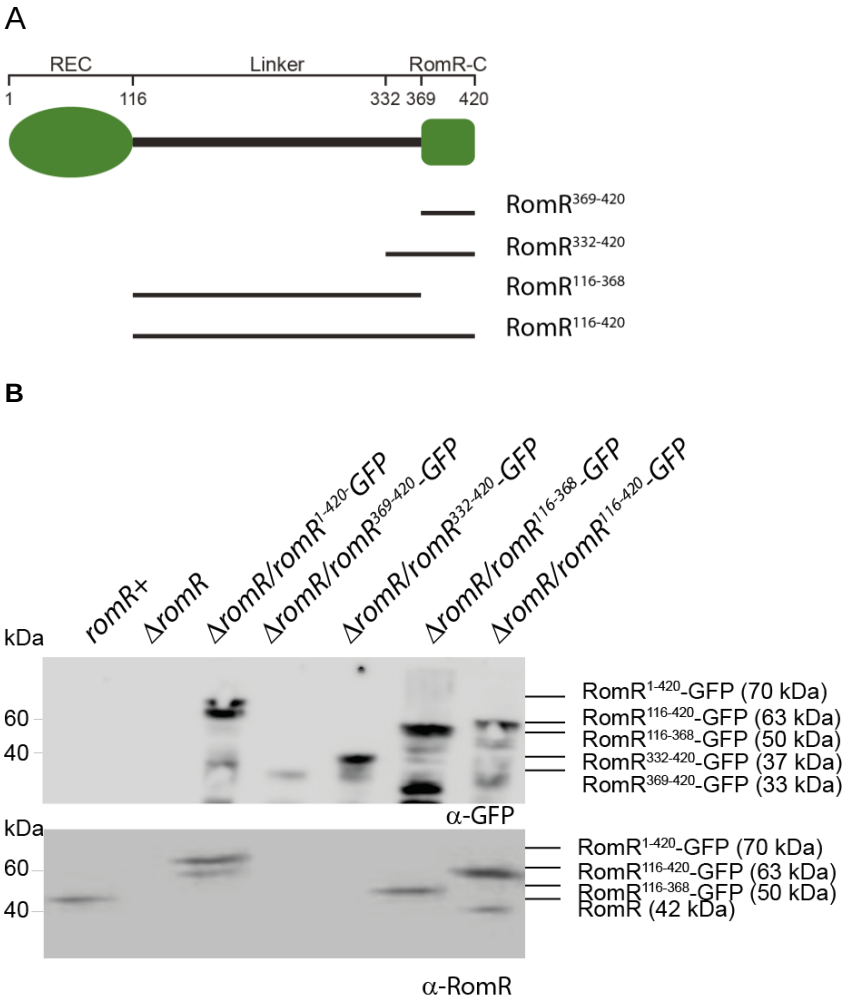

C

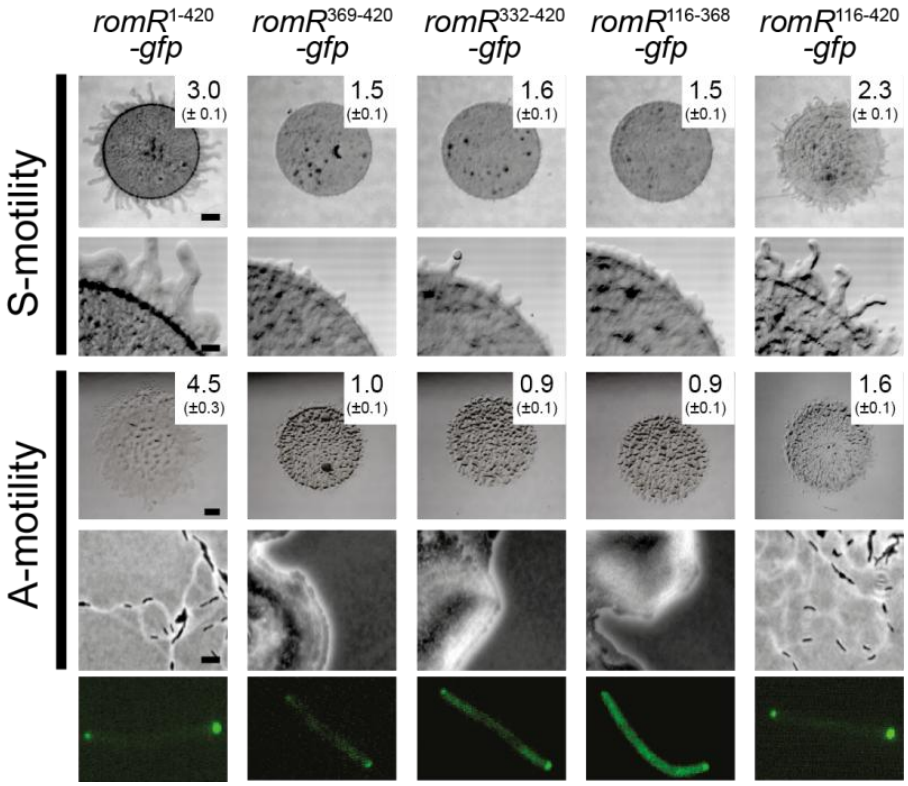

Figure 18: RomR-C and the linker region are independent pole-targeting determinants and both are required for motility. (A) black lines indicate a RomR part which has been fused to GFP to construct the strains in B. Numbers correspond to the RomR amino acid sequence from *M. xanthus*. Details in the text. (B) Immunoblots of RomR-GFP proteins. Cells were grown in liquid culture, harvested, and total protein (1 mg per lane) was separated by SDS–PAGE and analyzed by immunoblotting using α-GFP (top panel) and α-RomR (bottom panel). RomR and RomR-GFP are indicated. The migration of molecular size markers is indicated on the left. (C) Motility assay as described previously. For the experiments in the bottom row, Δ*romR* cells expressing the indicated GFP fusions were transferred from liquid cultures to an agar-pad on a slide and imaged by fluorescence microscopy.

To analyze the function of the single parts of the output domain, GFP fusions were constructed and analyzed in a Δ*romR* background. Additionally, western blots were performed to determine protein levels of these constructs, which revealed that the GFP fusion to the C-terminal region (RomR$^{369-420}$ –GFP) was expressed at five-fold lower level than the WT protein or GFP fusions to the full length RomR (RomR$^{1-420}$-GFP) or linker region (RomR$^{116-368}$-GFP) (Fig. 18AB). Due to the low expression levels of RomR$^{369-420}$-GFP, an extended construct containing a small part of the linker region was generated (RomR$^{332-420}$-GFP). Importantly, the RomR$^{332-420}$-GFP protein was expressed at WT levels (Fig. 18AB). When cell motility was examined, strains expressing only truncated parts of the output domain were not able to move by A- or S-motility, leading to

similar colony morphology as observed for a Δ*romR* mutant (Fig. 18C). However, all three constructs, expressing one subpart of the output domain, RomR$^{116-368}$ –GFP, RomR$^{369-420}$ –GFP or RomR$^{332-420}$-GFP were able to localize to the cell poles. Moreover, these polar clusters localized in an asymmetric bipolar manner, similar to the pattern observed for the output domain and full length RomR. Thus, we conclude that the linker region, RomR$^{116-368}$, as well as the C-terminal region, analyzed using RomR$^{369-420}$ –GFP and RomR$^{332-420}$-GFP contain motifs that independently target RomR to the cell pole. Those observations led us to the hypothesis that RomR interacts with at least two partner proteins required for polar targeting. Furthermore, it implies that the interaction with only one of these proteins at the pole is not sufficient for function, leading to defects in motility. To extend our understanding of how RomR regulates motility, we expanded our study on finding trans-acting polar targeting factors of RomR.

2.2.3 Localization of RomR and the subparts of the output domain in the absence of the A-motility complex

Even though RomR was shown to be involved in the regulation of A- and S-motility, it remained unclear how RomR functions, how it achieves its polar localization and which proteins RomR interacts with at the cell pole. While S-motility was reduced in a Δ*romR* mutant, A-motility was completely abolished. Therefore, we first focused on A-motility proteins as putative interaction partners. Detailed bioinformatic analyses revealed that the A-motility machinery likely consists of at least 14 proteins (Luciano et al. 2011).

However, only few A-motility proteins have been studied in detail, specifically AglZ, AglQ and AgmU. Notably, all three proteins, AglZ, AglQ and AgmU formed clusters interpreted as FACs (Nan et al. 2010; Sun et al. 2011). Consistent with this observation, AglQ and AgmU proteins co-localize with AglZ, further supporting that the A-motility proteins form FACs. Interestingly, none of the analyzed A-motility proteins localized specifically to the cell poles, while RomR was found exclusively at the poles.

Thus, we focused on investigating RomR connection to the A-motility proteins. At first, we aimed to determine whether other A-motility proteins are

important for RomR polar localization. For this, a transposon mutagenesis screen was carried out in order to identify new factors involved in A-motility, particularly proteins required for RomR localization (Keilberg, Diploma thesis 2009). In our screen we focused on the mutants that completely lacked A-motility, but remained able to move by S-motility. Interestingly, in this screen we identified mutants carrying insertions in eight different genes, all of which were encoded in the G1 and G2 clusters (1.3.2.). Specifically, mutations were found in genes coding for AgmK, AgmX, AglT, and AgmU, of the G1 cluster, as well as for GltA, GltB and GltC of the G2 cluster. To further characterize the function of these genes, RomR-GFP localization was determined in the mutants. While the asymmetry of RomR-GFP was affected for some of the mutants, none of the investigated A-motility proteins were required for polar RomR-GFP localization (Keilberg, Diploma thesis 2009). Specifically, bipolar symmetric RomR-GFP localization was found in mutants lacking AgmX and AgmK, but remained bipolar asymmetric in the absence of AgmU and AglT or only changed to slightly more symmetric for GltA, GltB and GltC (Keilberg, 2009). Therefore, we hypothesized, that asymmetric RomR localization depends on other A-motility proteins. To analyze this in more detail, we included previously characterized A-motility proteins that have been predicted to form a complex to regulate A-motility in our analysis. To score the effects on RomR function in detail, we analyzed the localization of RomR in the in-frame deletion mutants lacking the following proteins of the A-motility machinery: AglZ, in the cytoplasm; AgmX and AgmK, in the inner membrane; AgmU, AglT and GltC, in the periplasm; GltA, GltB and AgmO, in the outer membrane, and AglQ as a representative for the motor in the inner membrane. First, in frame deletions mutants of *agmX, agmK, agmU, aglT, agmO, gltA, gltB* and *gltC* were constructed, and their A-motility was scored (Fig. 19). The in frame deletion mutants of *aglZ* and *aglQ* were generated in previous studies (Leonardy et al. 2007; Sun et al. 2011).

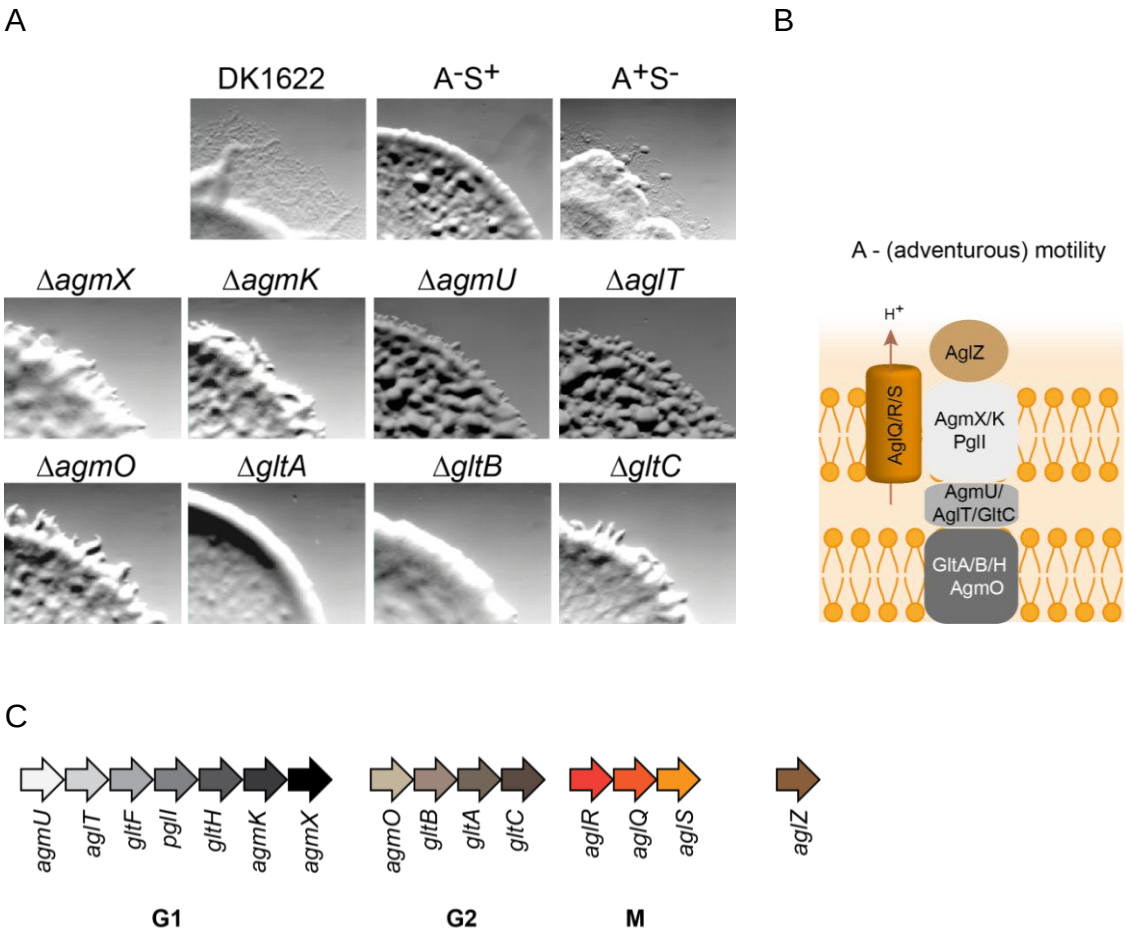

Figure 19: In frame deletions of genes required for A-motiliy. (A) Motility phenotypes on 1.5% hard agar plates scoring for A-motility. DK1622: WT, A-S+: strain with defect for A-motility; A+S-: strain with defect for S-motility. In frame deletions of *agmX*, *agmK*, *agmU*, *aglT*, *agmO*, *gltA*, *gltB* and *gltC* show defects in A-motility (B) Model for A-motliity complex. Explained in detail in the text. (C) Gene clusters involved in A-motility.

To exclude polar effects of the deletions, each mutant was complemented with a copy of the deleted gene expressed under the *pilA* promoter at the Mx8 attachment site. In this study, the following complementation strains were created: *ΔagmO/pilA-agmO*, *ΔgltA/pilA-gltA, ΔgltB/pilA-gltB, ΔgltC/pilA-gltC.* All four complementation strains exhibited WT levels of A- and S-motility (B. Jakobczak personal communication), fully complementing the A-motility defect. The remaining deletion mutants have been complemented previously, verifying functions of AglZ and AglQ in A-motility (Yang et al. 2004; Nan et al. 2010; Sun et al. 2011).

To analyze the localization of RomR in the absence of A-motility proteins, double deletions lacking one of the A-motility components and *romR* at the native site were generated. Next, RomR-GFP was introduced into the double

deletion mutants. Subsequently, we analyzed the localization of RomR in all the mutants, to verify a symmetric localization in the A-motility mutants as seen in the transposon mutagenesis screen. While RomR-GFP in the Δ*romR* strain served as a control for the asymmetric bipolar localization, which was reported to be the WT localization of RomR, the Δ*aglZ*Δ*romR* double deletion served as a control for symmetric RomR-GFP localization, which has been analyzed previously (Leonardy, PhD thesis 2009, Keilberg, 2009). As expected, we were able to observe a more symmetric localization specifically for mutants lacking AglZ, AgmK and AgmX. However, the remaining A-motility mutants also displayed a greater percentage of RomR symmetric localization when compared to the control (Fig. 20).

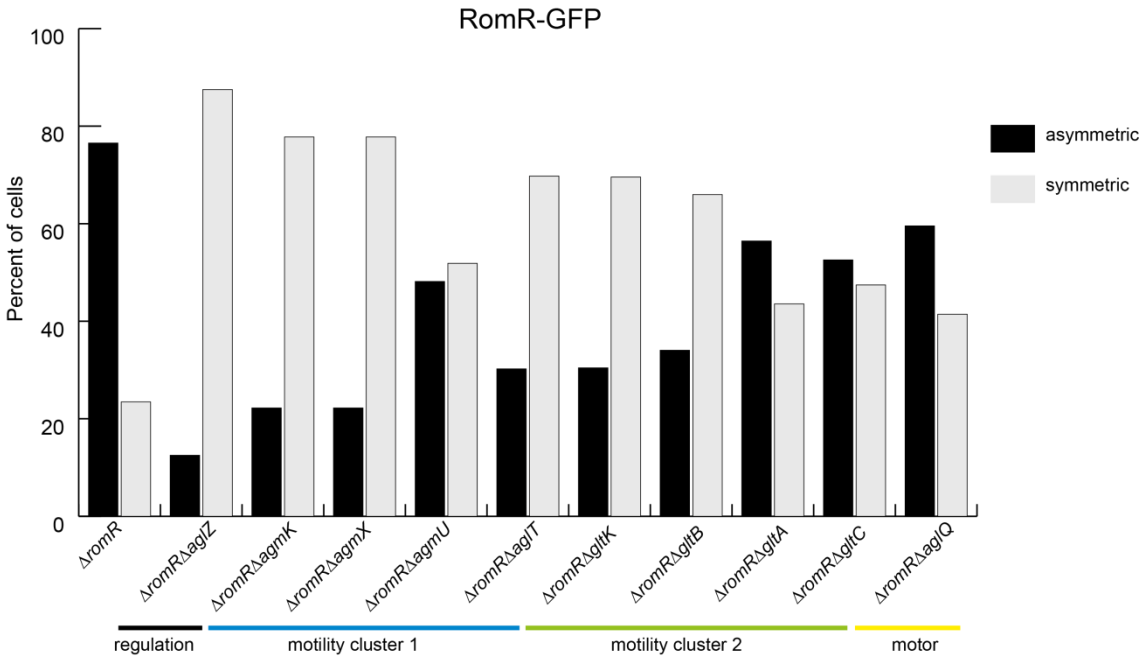

Figure 20: Effects on localization of the RomR. Diagram shows percentage of cells with asymmetric (black bars) and symmetric (grey bars) localization of RomR fused to GFP. For each strain (genotype as indicated below the histogram) n=100 cells were analyzed. Quantification of GFP signals is explained in Material and Methods.

It is important to note that in contrast to the control strain *ΔromR/romR-gfp*, all the mutants containing an additional deletion in the A-motility system were not able to move or reverse under the conditions tested. The lack of A-motility could contribute to the more symmetric localization of RomR in absence of A-motility factors. Therefore, it remains open, whether the change from asymmetric RomR localization to symmetric RomR localization in A-motility mutants is a direct

effect or an indirect effect. In the simplest model, the dynamics of the RomR protein would be affected because the cells are not able to move. For a dynamic localization of RomR, activation via phosphorylation in the receiver domain is needed. Even if the cells are not able to move due to the lack of essential parts of the A-motility machinery, RomR might still receive signals to induce reversals from its potential cognate kinase. Therefore, the RomR dynamics might become erratic, leading to a more symmetric localization.

Previously we found that the RomR sequence appears to incorporate two independent motifs for polar localization within the output domain. To analyze the effects on RomR localization in detail, additional fusion proteins of the output domain, RomR$^{116-420}$-GFP, as well as the linker region, RomR$^{116-368}$, and the C-terminal region, RomR$^{332-420}$ were expressed in the double mutants, as described for full length RomR. The output domain, RomR$^{116-420}$, had been shown to localize asymmetrically, similar to the full length protein (Leonardy et al. 2007). In contrast to the full length protein, the output domain is not able to display any dynamics, for which the receiver domain and its activation is required. To analyze if the RomR protein shifts to a more symmetric localization in the absence of A-motility without the input from an upstream kinase, we tested the localization of RomR$^{116-420}$-GFP protein in the double deletion mutants (Fig. 21).

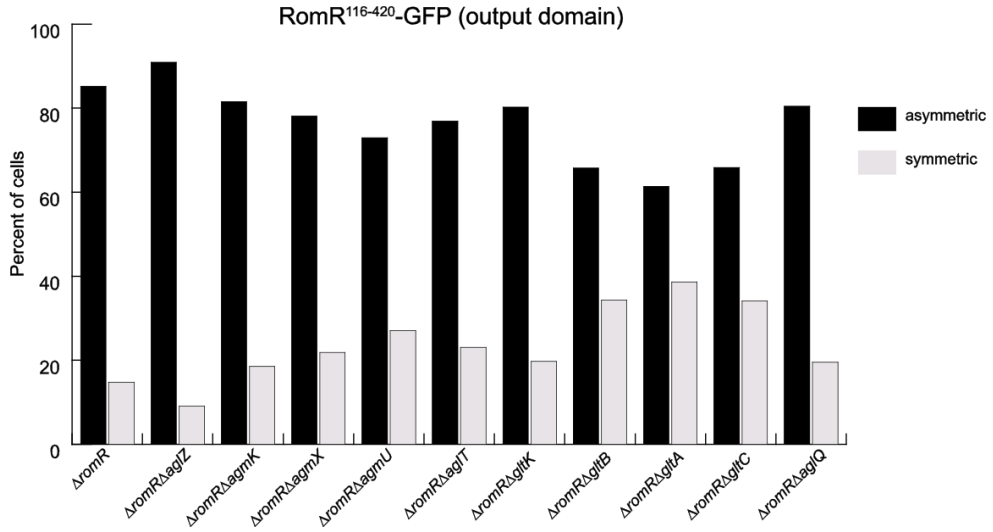

Figure 21: Effects on localization of the RomR output domain. Diagram shows percentage of cells with asymmetric and symmetric localization of the RomR output domain fused to GFP. For each strain (genotype as indicated on the X-axes) n=100 cells were analyzed. Details to quantification of GFP signals are explained in Material and Methods.

Similar to the full length protein, the localization patterns observed for RomR$^{116-420}$-GFP were either asymmetric bipolar or symmetric bipolar. As stated earlier, in the Δ*romR* mutant the output domain localizes mainly asymmetric bipolar, which was observed in 85% of the cells. In all double deletion mutants analyzed, the majority of the cells displayed an asymmetric bipolar localization of the output domain indicating that the A-motility machinery does not directly affect RomR localization (Fig. 21), but rather interferes with the dynamics of RomR. Therefore, the receiver domain, RomR$^{1-115}$, seems to be required for the switch from an asymmetric bipolar localization to a symmetric bipolar localization of RomR in the absence of A-motility.

As demonstrated in 1.6.1 the output domain can be split into two parts, which localize to the cell pole independent of each other. Therefore, we hypothesized, that each of the two motifs targeting RomR to the pole is able to interact with polar factors independently. Thus, we suggested that the RomR output domain would still be able to localize at the cell pole, while the localization of the single subparts of the output domain could depend on one of the A-motility proteins. To address this, we localized the linker region, RomR$^{116-368}$-GFP, and the C-terminal region, RomR$^{332-420}$-GFP, in the double deletion mutants (Fig. 22 A/B).

A

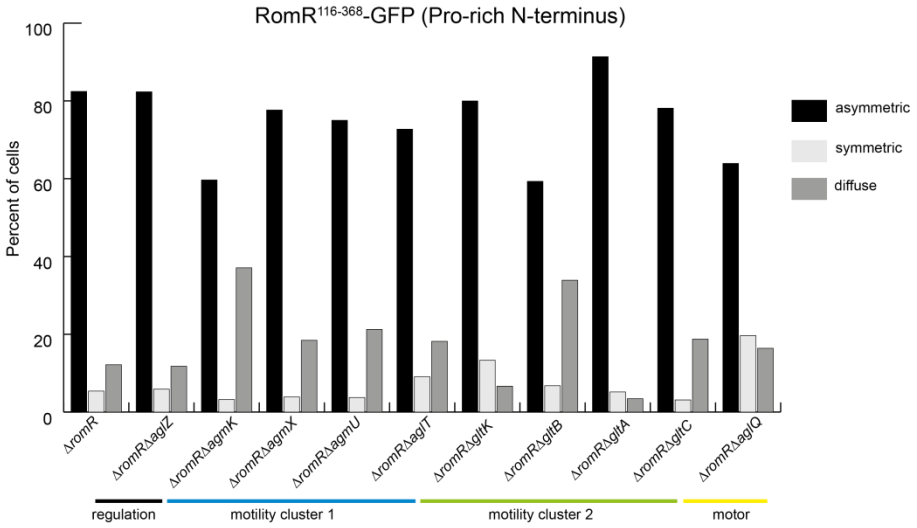

B

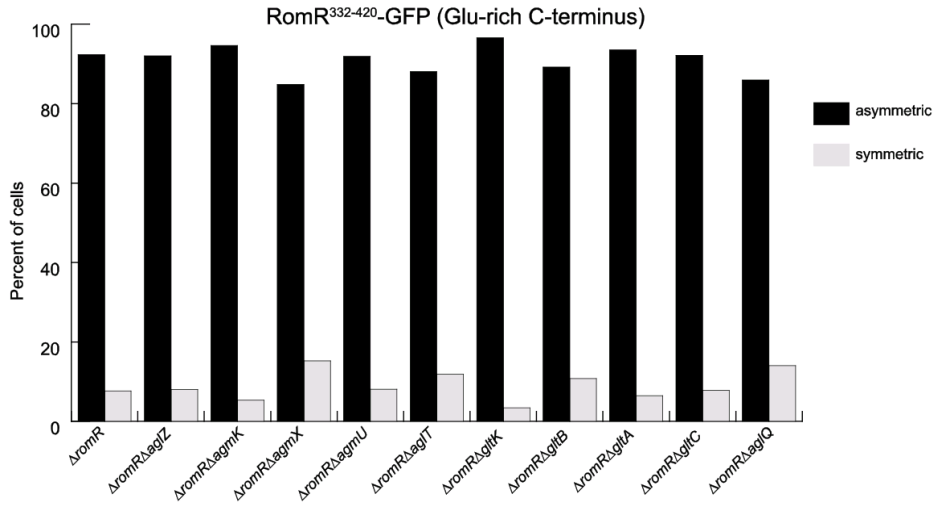

Figure 22: Effects on localization of the subparts of the RomR output domain. Diagram shows percentage of cells with asymmetric and symmetric and diffuse localization of (A) RomR Pro-rich region and (B) RomR Glu-rich C-terminus fused to GFP. For each strain (genotype as indicated on the X-axes) n=100 cells were analyzed. Details to quantification of GFP signals are explained in Material and Methods.

Contradictory to our hypothesis, the localizations of RomR$^{116-368}$–GFP and RomR$^{332-420}$-GFP observed in the double deletions (Fig. 22) were comparable to the localizations seen for the control strain only lacking *romR*. Thus, we conclude, that the A-motility machinery is not required to target RomR to the cell pole.

In summary, we confirmed that AglZ and AglQ and furthermore eight proteins encoded by the G1 and G2 cluster are required for A-motility. While AglZ, a pseudoresponse regulator, and AglQ, a motor protein, have been analyzed in

detail (Yang et al. 2004; Sun et al. 2011), including their localization in FACs, the two other motility clusters are still subject to the ongoing research ((Nan et al. 2010; Luciano et al. 2011) Jakobczak, Keilberg et al. unpublished). Future research will be directed to solve the question how the A-motility machinery works. Intriguingly, RomR localization studies indicate, that the A-motility machinery is not required to localize RomR. In contrast, AglZ, which has been shown to act as a regulator upstream of the A-motility machinery, does depend on the main components of the A-motility machinery, to form focal adhesion complexes (Nan et al. 2010). Taken together, our data strongly suggest that RomR is not a part of the A-motility machinery, and rather acts upstream as a regulatory protein. Consistently, RomR-GFP shows a different localization compared to the localized A-motility proteins described so far, such as AglZ, AgmU and AglQ. Additionally, a Δ*romR* mutant shows defects in both A- and S-motility. Consequently, we examined the additional motility factors involved in the regulation of A-motility, S-motility and reversals.

2.3 RomR regulates motility together with MglA and MglB

2.3.1 RomR coevolved with MglA and MglB

In this study we showed that RomR localization is independent of all A-motility machinery components tested. Therefore, we suggested that RomR might not be part of the A-motility system. Moreover, in contrast to other A-motility proteins, RomR has been shown to be required for both the A- and S-motility system. Thus, we employed a new approach to characterize the RomR function and to define its position in a genetic pathway regulating motility. For this, we first extracted RomR-containing genomes from the database of sequenced to date bacterial genomes, and then analyzed the co-occurrence of RomR in those genomes with the following motility factors: MglA and MglB, which regulate both motility systems; FrzE representing the Frz system, which regulates reversals; as well as representative proteins of the S- and A-motility motility systems, such as PilT required for T4P function and GltF required for the A-motility machinery. In addition, the distribution of the RomR receiver and

output domain, represented by the conserved C-terminal domain, were analyzed independently, because they were shown to carry out independent functions.

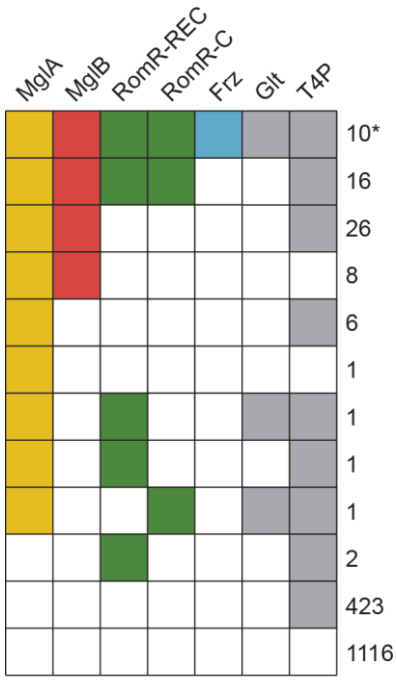

Figure 23: Genomic distributions of RomR and Frz overlap with those of MglA and MglB. Each column indicates the presence or absence of MglA, MglB, RomR-REC (receiver), RomR-C (output), Frz, the gliding motility machinery (Glt), or T4P as a colored or white box, respectively. Numbers on the right indicate the number of genomes with a given pattern of co-occurrence. *indicates the *M. fulvus* genome that contains an incomplete RomR, a complete MglA/MglB system, and Frz system.

Notably, only a small subset of RomR-containing genomes harbored proteins representing the A-motility machinery (12 genomes, Fig. 23, in grey), while RomR was more widespread (31 genomes, Fig. 23, in green), consistent with the hypothesis that RomR might not be part of the A-motility machinery but rather conducts a broader function. Furthermore, all 31 genomes containing RomR were found to have conserved T4P proteins, supporting the hypothesis that RomR also plays a role in T4P-mediated S-motility. Additionally, each genome containing a full-length RomR, defined by a RomR-like receiver domain, and a RomR-like C-terminal region, also contained a conserved MglA/MglB system (Fig 23, yellow/red). In contrast, five genomes, containing truncated RomR homologs, lacking either the receiver domain or the C-terminal domain lacked MglB homologs. These findings indicated a close correlation between RomR and the MglA/MglB system. Therefore, we hypothesized that

the three proteins share a common function in the regulation of both motility systems. Importantly, the Frz system, which is essential for the regulation of reversals, was conserved only in the subgroup of RomR-containing genomes, similar to the distribution of proteins involved in A-motility.

In summary, the Frz system together with the A-motility machinery is present in a subset of the RomR-containing genomes, while RomR is present in a subset of the genomes containing MglA, MglB and T4P. Therefore, we predicted that RomR might have a function beyond regulating the A-motility system. Importantly, RomR was shown to function in motility and reversals, just as the MglA/MglB system. To further investigate, whether RomR is able to interact with MglA or MglB, we performed biochemical assays.

2.3.2 RomR directly interacts with MglA and MglB proteins

To test whether RomR can directly interact with MglA or MglB, pull-down assays and direct interaction studies with purified proteins were performed (Fig. 24). First, pull-down experiments were carried out in which purified proteins were bound to an affinity column and incubated with WT extracts of the *M. xanthus* strain DK1622. When purified proteins were eluted from the column, interacting proteins from the WT extract were coeluted and verified by immunoblot analyses using specific antibodies.

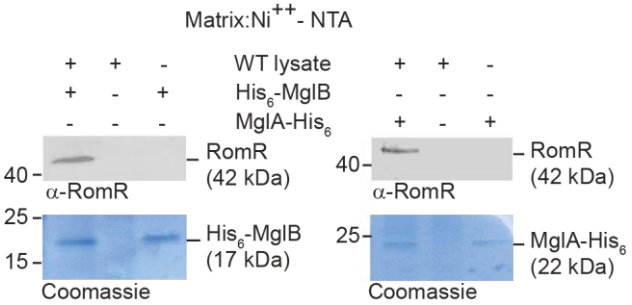

Figure 24: MglB and MglA pull down RomR from WT extracts. WT *M. xanthus* cell extract was applied to a Ni^{++}-NTA-agarose column with or without bound His_6-MglB (left panel) and with MglA-His_6 (right panel). Eluted proteins were separated by SDS-PAGE and visualized in immunoblots with α-RomR (top panels) or by Coomassie Brilliant Blue R-250 staining (bottom panels). Positions of His_6-MglB, MglA-His_6 and RomR including their calculated molecular masses are indicated. Migration of molecular weight markers in kDa is indicated on the left.

Pull-down experiments using purified His_6-MglB (Fig. 24, left) and MglA-His_6 (Fig. 24, right) as bait proteins and WT lysates of *M. xanthus* strain DK1622 were performed to analyze interactions with RomR. Importantly, RomR was pulled down from WT lysate when incubated with purified His_6-MglB or MglA-His_6 bound to Ni-NTA beads (Fig. 24). In contrast, when WT lysates were incubated with empty beads, RomR was not detected in the elution, indicating a specific interaction between RomR and MglB as well as between RomR and MglA. Furthermore, purified proteins that were not incubated with WT lysates did not display any band in the elution fraction, corresponding to the size of RomR. Thus, RomR was pulled down by MglB and MglA specifically. However, additional proteins present in WT lysates could have acted as connector proteins between RomR and MglB or RomR and MglA. To further characterize the interactions, direct interaction studies were performed, using purified RomR, MglA and MglB proteins (Fig.25).

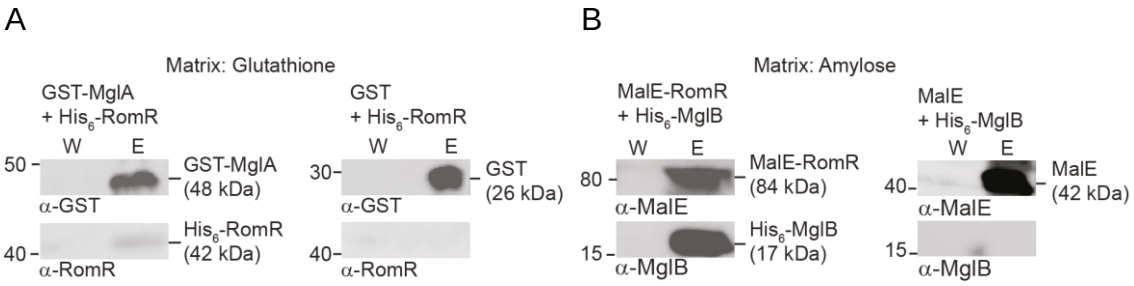

Figure 25: RomR interacts directly with MglB and MglA. Shown are proteins from the last wash fraction before elution (W) and from the elution (E). Calculated molecular masses are indicated. Migration of molecular weight markers in kDa is indicated on the left. (A) Eluted proteins visualized in immunoblots with α-GST (top panels) and α-RomR (bottom panels). (B) Eluted proteins were visualized in immunoblots with α-MalE (upper panels) and α-MglB (lower panels

To test the direct interaction between RomR and MglA, GST-MglA was used as the bait protein and His_6-RomR as the prey protein (Fig 25A). After GST-MglA had been incubated together with His_6-RomR for four hours on a glutathione column, the columns were washed to eliminate unbound proteins. Finally, for elution, the columns were incubated with elution buffer containing 10 mM glutathione. To examine which of the proteins were eluted, the last washing step and the elution fraction were analyzed using α-GST antibodies and α-RomR antibodies. Importantly, both proteins, GST-MglA and His_6-RomR were

eluted together from the glutathione column after the washing steps, while in the control experiment, carried out with the GST protein and His_6-RomR, only GST was eluted, and RomR had been washed away. In a similar experiment, MalE-RomR was incubated with His_6-MglB on an amylose column, to analyze direct interaction between RomR and MglB (Fig. 25). For elution, the columns were treated with elution buffer containing 10 mM maltose. Notably, MalE-RomR and His_6-MglB coeluted, as detected by immunoblots using α-MalE antibodies and α-MglB antibodies. In contrast, in the control experiment, where His_6-MglB was incubated with the MalE protein, only MalE was eluted while His_6-MglB was washed away (Fig 25B). These results show that RomR directly interacts with MglA and MglB independently.

Previous experiments demonstrated that MglA and MglB regulate both motility systems, and therefore act upstream of components specific for S-motility and A-motility. Direct interactions between RomR and the MglA/MglB system indicate that RomR acts within the same pathway. In line with that, it has been observed that RomR is required for both motility systems. However, it also raised new interesting questions. How does RomR interact with the MglA/MglB system? Does RomR act upstream or downstream of MglA and MglB? Furthermore, MglA was shown to act as a small GTPase that requires the GAP MglB to induce GTPase activity (Leonardy et al. 2010; Zhang et al. 2010). Therefore, RomR could also be involved in regulating the nucleotide-bound state of MglA. Additionally, it has been shown that the interaction between MglA and MglB, as well as the GTPase activity of MglA are essential for correct protein localizations (Miertzschke et al. 2011). Therefore, to investigate how the three proteins RomR, MglA and MglB affect each other, we analyzed the localization of all three proteins in presence and absence of each other.

2.3.3 Localizations of RomR, MglA and MgB are interdependent

MglA and MglB have been reported to localize to the leading cell pole and the lagging cell pole respectively, which was proposed to set up the cell polarity (Leonardy et al. 2010; Zhang et al. 2010). Additionally, RomR was

shown to display a similar localization pattern as MglB, with a large cluster at the lagging cell pole (Leonardy et al. 2007). However, this localization was defined as asymmetric bipolar, because small clusters have been observed at the leading cell pole additionally. All three proteins have been shown to dynamically switch the pole during a reversal (Leonardy et al. 2007; Leonardy et al. 2010; Zhang et al. 2010)

To analyze the localization dependencies of RomR, MglA and MglB, we first verified the localizations previously described for the WT proteins. For this, RomR-GFP and YFP-MglA, which had been shown to fully complement defects in motility and reversals, were localized (Leonardy et al. 2007; Leonardy et al. 2010). In contrast, the previously constructed MglB-YFP fusion did not fully complement the hyperreversing phenotype of the *mglB* deletion mutant as described in 2.1 (Mietzschke et al. 2011). Therefore, we created an MglB-mCherry fusion, which was expressed to WT levels and fully complemented the phenotype based on reversal periods (Fig. 26). Similar to WT, a strain expressing MglB-mCherry from its native site reversed on average every 16.3 minutes (Fig. 26B).

A

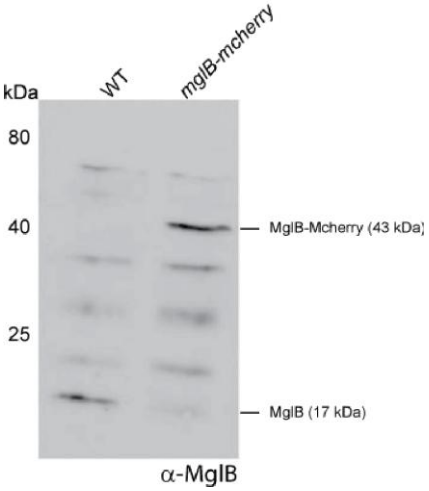

B

genotype	reversal period
mglB^{+}	15.5 ± 4.5
Δ*mglB*	6.7 ± 0.8
mglB-mCherry	16.3 ± 3.5

Figure 26: MglB-mCherry is expressed to WT levels and active. (A) Immunoblot shows similar protein levels for WT MglB and MglB-mCherry. Cells were grown in liquid culture, harvested, and total protein (1 mg per lane) was separated by SDS–PAGE and analyzed by immunoblotting using α-MglB. MglB-mCherry was expressed under the native promoter and integrated at the endogenous site (B). MglB-mcherry is active. Table shows reversal periods of the WT strain compared to the strain expressing *mglB-mCherry* at the endogenous site.

In line with previous observations, YFP-MglA localized in a mainly unipolar pattern, which was shown to be the leading cell pole, while MglB-mCherry and RomR-GFP showed a mainly asymmetric bipolar localization, displaying one bigger and one smaller cluster. It was previously reported that MglB localizes unipolar (Leonardy et al. 2010; Zhang et al. 2010), but instead we found an asymmetric bipolar localization, similar to the localization described for RomR-GFP. To quantify the observed localization patterns, for each strain n=200 cells were analyzed. Moreover, observed localization patterns were binned into three categories for each protein. After confirming MglA, MglB and RomR localizations in the WT background, we aimed to analyze their localizations in deletion backgrounds (Fig. 27).

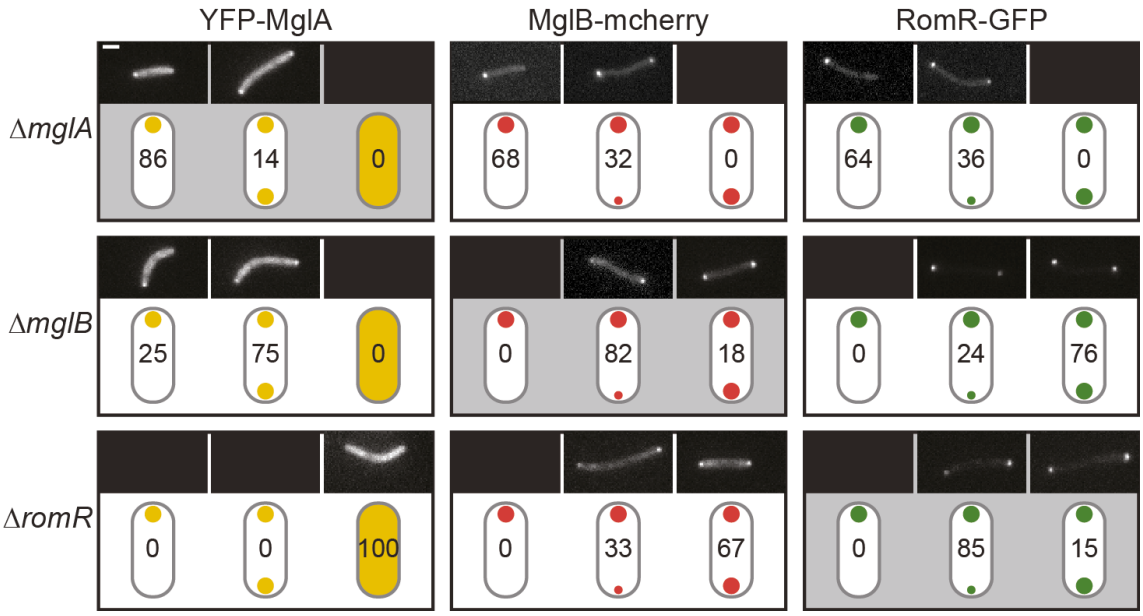

Figure 27: Localization of MglA, MglB, and RomR is mutually dependent. Localization of YFP-MglA, MglB-mCherry and RomR-GFP. Cells were transferred from liquid cultures to a thin agar pad on a microscope slide and imaged by fluorescence microscopy. Representative images of cells are shown for each pattern. Numbers represent percentage of cells with that pattern. n=200. Scale bar: 2 µm. Details on the quantification of fluorescent signals are explained in Material and Methods.

In the absence of MglB, YFP-MglA localization switched from mostly unipolar to mostly bipolar (Fig. 27). This change in the localization has been reported previously (Leonardy et al. 2010), and was hypothesized to be due to the lack of the GTPase activity at the lagging cell pole in the absence of MglB. Current data supports a model in which MglA can only form clusters if present in

the active GTP-bound state, while it is diffuse in the inactive GDP-bound state (Leonardy et al. 2010). Therefore, it has been proposed that the lack of MglB at the lagging cell pole, and therefore the decrease in GTPase activity converting MglA-GTP into MglA-GDP at the lagging cell pole, would lead to the accumulation of MglA-GTP and thus to the formation of MglA clusters at both poles. Interestingly, in a Δ*romR* mutant, YFP-MglA was completely diffuse throughout the cell without any cluster formation. This observation indicates that RomR is essential for MglA localization and cluster formation. However, different mechanisms could explain this phenotype. RomR might target MglA to the pole or RomR might affect the nucleotide-bound state of MglA, leading to the accumulation of MglA-GDP in the absence of RomR.

In the absence of MglA, MglB-mCherry becomes more unipolar. This is in contrast to observations of MglB localization based on MglB-YFP described in 2.1. We suggest that the differences might be caused by MglB-YFP not being fully active.

Moreover, MglB-mCherry becomes more bipolar in the absence of RomR (Fig. 27). Similarly, RomR-GFP becomes more unipolar in the absence of MglA and more bipolar in the absence of MglB (Fig. 27). It is not clear why MglB, as well as RomR, localize unipolar in the absence of MglA. However, similar observations have been made for FrzS (Zhang et al. 2012), a regulator protein of S-motility, indicating that MglA is absolutely required for correct protein localization of motility proteins.

Importantly, also MglB and RomR require each other for correct asymmetric localization, and localize symmetrically in the absence of each other. Thus, all three proteins are mutually dependent for their correct localizations.

Interestingly, RomR and MglB were shown to interact directly and to localize mainly at the lagging cell pole indicating that the MglB/RomR complexes are required to define the lagging cell pole. To investigate whether RomR-GFP and MglB-mCherry co-localize, the fusion proteins were expressed in the same strain, in presence and absence of MglA (Fig. 28). As expected, MglB-mCherry and RomR-GFP colocalize in strains representing the WT situation. Interestingly, they also colocalize in the absence of MglA, albeit in a predominantly unipolar pattern. This finding further supports a connection

between RomR and MglB that is independent of MglA, as observed in direct interaction studies.

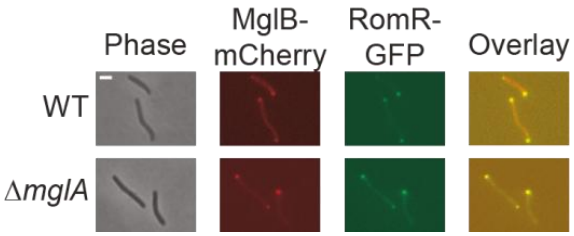

Figure 28: MglB and RomR colocalize. Cells expressing MglB-mCherry and RomR-GFP were transferred from liquid cultures to a thin agar pad on a microscope slide and imaged by fluorescence microscopy. Right column, overlay of RomR-GFP and MglB-mCherry. Scale bar: 2 µm.

Localization experiments performed in this study indicate that RomR interaction with MglA and MglB is required for the correct localization of MglA and MglB. Importantly, MglA and MglB are also required for correct RomR localization. Therefore, we proposed that RomR is part of a genetic circuit regulating motility together with the MglA/MglB system. Furthermore, the lack of RomR led to a complete diffuse localization of MglA, indicating that RomR interacts with MglA, either to directly localize MglA or to convert MglA into its GTP-bound form. Thus, we conclude that RomR function is directly connected to the function of MglA. Further investigation is required to distinguish between these two possible functions of RomR in relation to MglA.

2.3.4 RomR is a polar targeting factor for MglA

In the absence of RomR, MglA displays a diffuse localization. Similarly, and inactive form of MglA (MglA$^{T26/27N}$) also localizes diffusely (Leonardy et al. 2010). Two models to explain MglA localization in the absence of RomR were suggested based on our previous findings: (1) MglA becomes diffuse in a Δ*romR* mutant; because it is converted into its inactive GDP-bound form or (2) MglA requires RomR to be targeted to the cell pole and form a cluster. To distinguish between the two scenarios, we performed assays with MglA mutants that carry a substitution in active site residues that are required for GTP hydrolysis. We hypothesized that if MglA was locked into the GTP-bound form,

each effect observed on MglA localization in a Δ*romR* mutant would be a direct localization effect and not due to the conversion of MglA to its GDP-bound form. Thus, we analyzed the localization of YFP-MglA^{Q82A}, which is locked in the active GTP-bound form, in the presence and absence of RomR. Consistent with previous observations, YFP-MglA^{Q82A} localized bipolar symmetric at both poles in WT cells (Fig. 29A), and displayed an additional oscillating cluster within the cell (Miertzschke et al. 2011). Interestingly, in the absence of RomR, only the cluster oscillating between the cell poles remained, while the two polar clusters were not detectable (Fig. 29A). The same pattern was observed for YFP-MglA^{Q82A} in the absence of both RomR and MglB (Fig. 29A). These observations support that RomR is directly involved in targeting MglA-GTP to the pole rather than affecting GAP or GEF actvity. However, it does not exclude the possibility that RomR may also act on the nucleotide-bound state of MglA.

It has been shown that MglA-GTP activates motility and reversals (Leonardy et al. 2010; Zhang et al. 2010). Similarly, RomR is required for motility, and its activation is required to stimulate reversals (Leonardy et al. 2007). Therefore, if RomR affects the nucleotide-bound state of MglA, the RomR-MglA interaction would likely lead to an increase of MglA-GTP in the cell. However, this increase could be achieved directly or indirectly. In the first scenario, RomR could act as a GEF required to activate MglA by exchanging GDP with GTP. In the second scenario, RomR could inhibit the GAP activity of MglB indirectly, preventing the conversion of MglA-GTP to MglA-GDP. To distinguish between these two scenarios, YFP-MglA was localized in a double mutant lacking RomR and MglB (Fig. 29B). While YFP-MglA localized diffuse in a Δ*romR* mutant, it showed a mostly bipolar localization in a Δ*mglB* mutant. We hypothesized, that if RomR acts on MglA through MglB, a double mutant lacking RomR and MglB would restore the MglA cluster localization, as observed in the *mglB* deletion mutant.

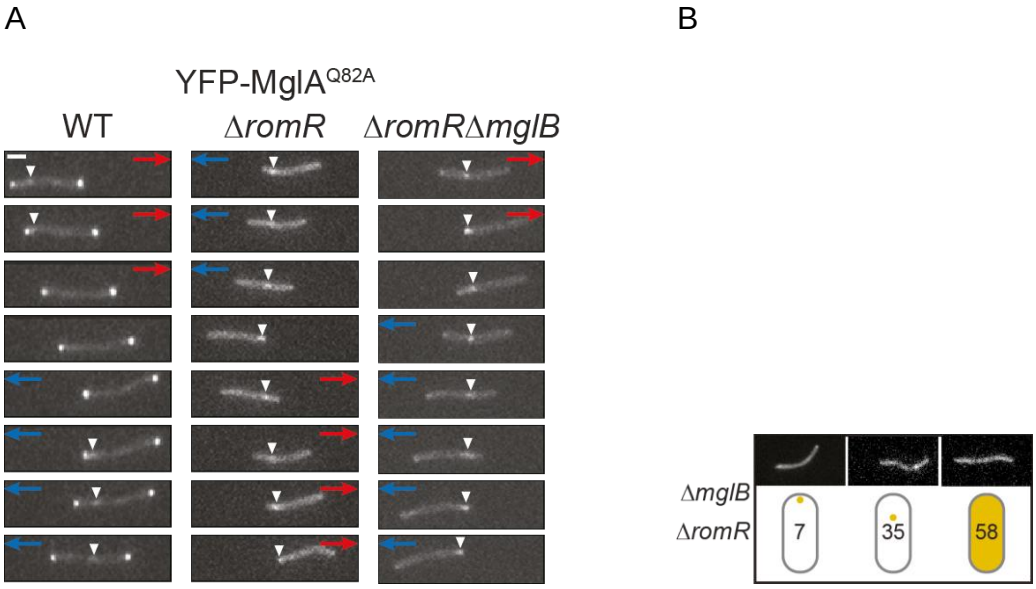

Figure 29: RomR is polar targeting factor of MglA. (A) Time-lapse microscopy of YFP-MglA^{Q82A}representing MglA-GTP. Cells of the indicated genotypes and producing YFP-MglA^{Q82A} were imaged at 30s intervals. Red and blue arrows indicate opposite directions of movement. White arrowheads indicate the oscillating cluster formed by YFP-MglA^{Q82A}. Scale bar: 2 µm (B) YFP-MglA localization in a strain not expressing MglB or RomR.

Interestingly, YFP-MglA is mainly diffuse in the absence of both RomR and MglB (Fig. 29B), similar to the localization of a mutant lacking RomR only (Fig 27). However, in contrast to a *ΔromR* mutant, 35% of the cells displayed YFP-MglA clusters in a *ΔromRΔmglB* mutant. Cluster formation in the absence of both RomR and MglB indicates that MglA is partially in its active GTP bound form in these mutants. The crucial difference between these mutants and a *ΔromR* mutant is the lack of GAP activity in the *ΔromRΔmglB* mutant. Therefore, we suggest that RomR could have an additional function in increasing MglA-GTP levels within the cell indirectly through acting on MglB.

However, if the inhibition of MglB activity by RomR would lead to an accumulation of MglA-GTP, YFP-MglA cluster formation would be expected to be similar as observed in an *mglB* deletion mutant showing polar clusters, which is not the case. Therefore, we suggest that RomR mostly acts on MglA to target MglA to the cell pole. However, since direct interactions with both proteins have been detected, a final conclusion can only be made after detailed biochemical experiments that directly examine the GTP hydrolysis and GDP-GTP exchange of MglA as they relate to other factors.

2.3.5 RomR acts upstream of the MglA/MglB system

RomR was found to be essential for the regulation of reversal frequencies and both motility systems. Furthermore, in this study RomR was shown to directly interact with MglA and MglB. Additionally, we showed that RomR, MglA and MglB depend on each other for correct localization. To map the position of RomR in the circuit controlling motility and reversals, we performed epistasis analyses and used motililty assays and reversal frequencies as readouts (Fig. 30). To investigate the position of RomR in motility, A- and S-motility was evaluated quantitatively by the increase of colony size and qualitatively by the observation of flares (S-motility) and single cells (A-motility) on 0.5% and 1.5% agar surfaces, respectively. The WT strain and the *romR* deletion strain were analyzed as well as the mutants carrying a single deletion in *mglA*, *mglB* and the strain expressing MglA^{Q82A}, which locks MglA in GTP-bound form (Fig. 30). Furthermore, double mutants carrying an additional deletion in *romR* were analyzed. Finally, the single mutants and the double mutants were compared to each other under on the hypothesis that the factor acting more downstream in the signaling cascade would dominate the phenotype. The double mutants were expected not to show additive phenotypes because we predicted that RomR, MglA and MglB act within the same pathway.

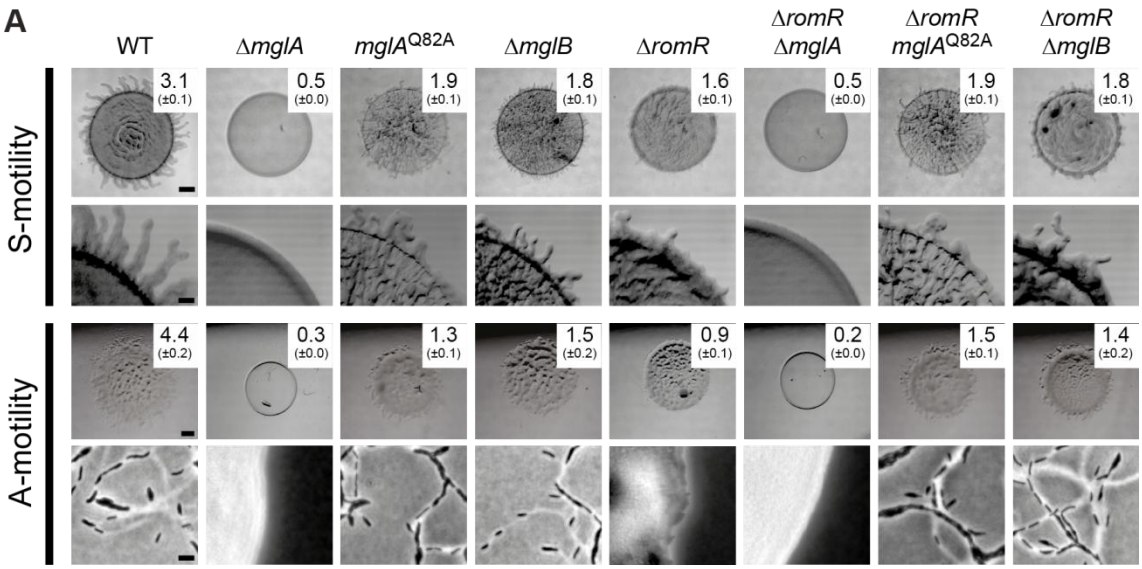

Figure 30: RomR acts upstream of MglA and MglB in motility. Motility phenotypes of strains of the indicated genotypes. Note that hyperreversing mutants expand less than WT colonies due to the abnormal reversal frequency and not due to defects in A- and S-motility. The indicated strains were incubated at 32°C for 24 h on 0.5% agar/0.5% CTT medium and 1.5% agar/0.5% CTT medium to score S- and A-motility, respectively. Scale bars, 1 mm, 200 mm, 1 mm, and 5 mm from top to bottom row.

As expected, colonies of the WT strain displayed long flares on agar favoring S-motility (3.1 mm) and showed spreading on agar favoring A-motility (4.4 mm) with single cells under high magnification (Fig. 30). In contrast, the Δ*mglA* mutant was non-motile on both agar surfaces, leading to a minimal increase of the colony size of 0.5 mm on S-motility agar and 0.3 mm on A-motility agar, which can be explained by cell division (Fig. 30). In addition no flares, characteristic for S-motility and no single cells, characteristic for A-motility were observed for the Δ*mglA* mutant. In comparison, the *mglA*^{Q82A} mutant as well as the Δ*mglB* mutant showed reduced A- and S-motility, indicated by the reduced increase of the colony size below 2 mm for S- and A-motility agar (Fig. 30). However, both mutants were able to move by S-motility, indicated by small flares, and displayed movements by A-motility with single cells. Previous studies showed that the reduced colony size of the Δ*mglB* mutant and the *mglA*^{Q82A} mutant, with MglA locked in the GTP-bound form, results from the hyperreversing phenotype (Leonardy et al. 2010; Zhang et al. 2010). The Δ*romR* mutant showed reduced S-motility and no A-motility as described before (Fig. 30). Next, double deletion mutants were analyzed for motility and compared to the single deletion mutants. A double deletion mutant of *romR* and

mglA phenocopied the Δ*mglA* mutant (Fig. 30). Furthermore, the double mutant of *romR* and *mglA*^{Q82A} phenocopied the *mglA*^{Q82A} single mutant, restoring motility in the absence of RomR, indicating the MglA-GTP acts downstream of RomR (Fig. 30). Similar results were obtained with the double deletion mutant of *romR* and *mglB*, which displayed the same phenotype as the Δ*mglB* mutant (Fig. 30). Strikingly, motility was restored in this mutant, and therefore single cells were observed under high magnification. Therefore, mutants accumulating MglA-GTP caused by either the *mglA*^{Q82A} mutation or the *mglB* deletion were able to restore motility in the absence of RomR. Thus, we proposed that MglA and MglB act downstream of RomR. To verify this hypothesis, reversal frequencies were analyzed. In addition to comparing the previously described mutants, we also analyzed them in relation to two different forms of RomR, which have opposite effects on reversal frequency (Fig. 31). While RomR^{D53N}, mimicking the unphosphorylated form of RomR, was shown to lead to a hyporeversing phenotype, RomR^{D53E}, mimicking the phosphorylated form, was shown to induce reversals (Leonardy et al. 2007).

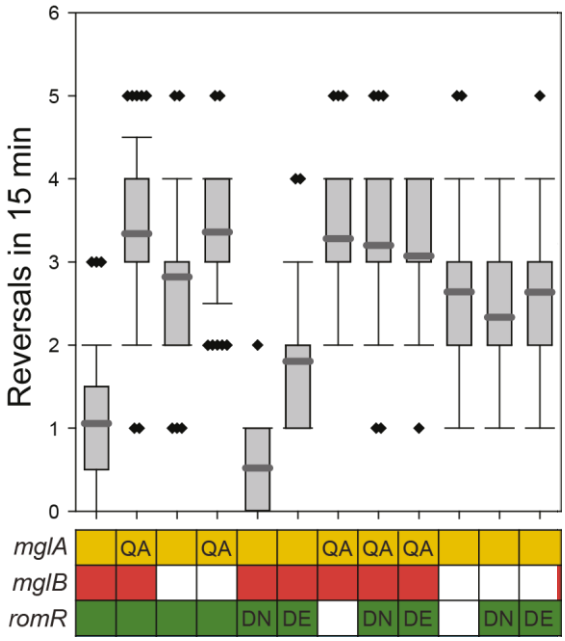

Figure 31: RomR acts upstream of MglA and MglB in reversals. Box plot of reversal frequencies measured in the strains of the indicated genotypes. The boxes below indicate alleles present: Colored, WT; white, in-frame deletion; QA: MglA^{Q82A}, DN: RomR^{D53N} and DE: RomR^{D53E} n=50. Cells were transferred from a liquid culture to a thin agar pad, covered with a coverslip and followed by time-lapse microscopy in which cells were imaged at 30-s intervals for 15 min. For each strain, 50 cells were followed. In the box plot, the Y-axis is the number of reversals per 15 min, boxes enclose the 25th and 75th percentile with the dark grey line represents the mean, whiskers represent the 10th and 90th percentile, and diamonds outliers.

First, WT and single deletion mutants were analyzed counting reversals per 15 minutes for 50 cells of each strain (Fig. 31). Similar to the results reported previously, the WT cells reversed on average every 15 minutes, while the *mglA*^{Q82A} and the *mglB* mutant hyperreversed, reversing approximately three times within 15 minutes (Miertzschke et al. 2011). In a double deletion of *mglA*^{Q82A} and *mglB*, we observed slightly higher reversal frequencies characteristic for the *mglA*^{Q82A} single mutant, supporting the model that MglA-GTP acts downstream of the MglA/MglB system. We verified the importance of RomR substitutions in regulating reversal frequency, confirming that a RomR^{D53N} substitution led to a hyporeversing phenotype, while a RomR^{D53E} mutation led to a hyperreversing phenotype (Fig. 31). When the different mutations were combined, an *mglA*^{Q82A} substitution rescued the motility defect of the *ΔromR* mutant as observed in the motility assays, and was found to exhibit a hyperreversing phenotype similar to the phenotype of the *mglA*^{Q82A} single mutant (Fig. 31). Similarly, both *romR*^{D53N} and *romR*^{D53E} when combined with *mglA*^{Q82A} led to the hyperreversals, characteristic for *mglA*^{Q82A}, indicating that MglA-GTP acts downstream of RomR. In line with that, hypperreversing phenotypes, at levels of the Δ*mglB* mutant, were observed for all combinations with the *mglB* deletion together with the *romR* mutations. Therefore, we hypothesized that MglA and MglB act downstream of RomR to regulate motility and reversals.

Importantly, the epistasis analyses have demonstrated that the phenotype caused by the *romR* deletion can be bypassed by either locking MglA in the GTP- bound form or by deleting *mglB*. These data indicate that the MglA/MglB sytstem acts downstream of RomR. They furthermore verify that RomR is not part of the A-motility machinery, but instead acts as a regulator of both motility systems. However, the mechanism underlying this regulation remains unclear. To investigate this question further, it is important to identify the input of RomR. It was shown that RomR is a response regulator, which is predicted to be activated by phosphorylation based on key substitutions in the receiver domain. Therefore, it would be interesting to find the cognate kinase or phosphotransfer protein acting upstream of RomR to regulate motility.

The Frz chemosensory system seemed to be one potential candidate to activate RomR for two reasons. First, the Frz system regulates reversals for

both motility systems, similarly to RomR (Blackhart and Zusman 1985b; Leonardy et al. 2007). Second, the Frz system has been shown to signal by a phosphotransfer reaction of FrzE to FrzZ as required for the activation of RomR (Inclan et al. 2007).

2.4 Frz chemosensory system

2.4.1 The Frz system acts upstream of RomR

Previous studies of FrzE, FrzZ, MglA and MglB reported that the Frz-system acts upstream of the MglA/MglB system, inducing reversals (Leonardy et al. 2010; Zhang et al. 2010). While MglA-GTP is required for reversals and motility, MglA in the inactive GDP-bound form fails to induce reversals and motility. Current models suggest that the Frz system can induce reversals by directly or indirectly increasing the level of MglA-GTP by either acting on MglA or MglB or both. Our data suggested that RomR acts upstream of MglA and MglB. Therefore, it remained unclear whether the Frz system acts between RomR and MglA/MglB or upstream of RomR. Interestingly, the previous study on RomR demonstrated that RomR locked in its activated state by a D53E substitution can bypass an insertion in *frzE* (Leonardy et al. 2007). However, FrzE was demonstrated not to be the output of the Frz system but rather led to the activation of FrzZ by a phosphotransfer reaction (Inclan et al. 2007).

To investigate the position of RomR in relation to the Frz system, epistasis analyses were carried out using motility assays and reversal frequencies as described previously. For this, mutants lacking FrzZ - the representative output of the Frz system were constructed.

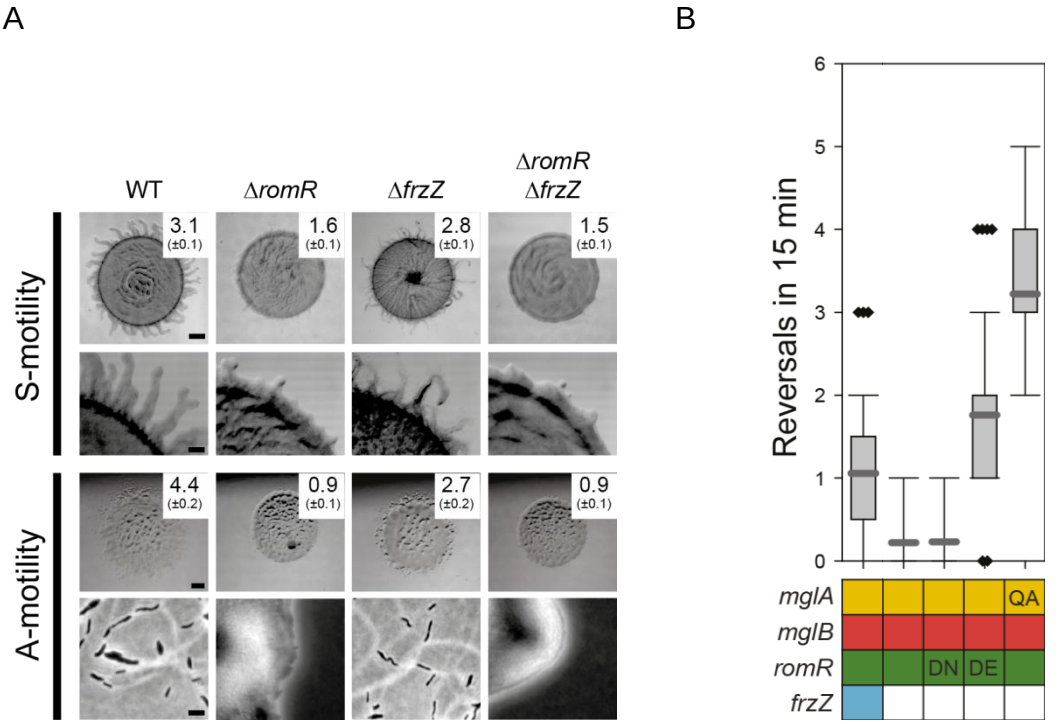

Figure 32: RomR acts downstream of FrzZ in motility and reversals. (A) Motility phenotypes of strains of the indicated genotypes. Note that hypo-reversing mutants expand less than WT colonies due to the abnormal reversal frequency and not due to defects in A- and S-motility. The indicated strains were incubated at 32°C for 24 h on 0.5% agar/0.5% CTT medium and 1.5% agar/0.5% CTT medium to score S- and A-motility, respectively. Scale bars, 1 mm, 200 mm, 1 mm, and 5 mm from top to bottom row. (B) Box plot of reversal frequencies measured in the strains of the indicated genotypes. The boxes below indicate alleles present: Colored, WT; white, in-frame deletion; QA: MglA^{Q82A}, DN: RomR^{D53N} and DE: RomR^{D53E} n=50. Cells were transferred from a liquid culture to a thin agar pad, covered with a coverslip and followed by time-lapse microscopy in which cells were imaged at 30-s intervals for 15 min. For each strain, 50 cells were followed. In the box plot, the Y-axis is the number of reversals per 15 min, boxes enclose the 25th and 75th percentile with the dark grey line represents the mean, whiskers represent the 10th and 90th percentile, and diamonds outliers

Compared to WT (Fig. 32A), the Δ*frzZ* mutant displayed slightly smaller colonies on S-motility agar (2.8 mm instead of 3.1 mm) and A-motility agar (2.7 mm instead of 4.4. mm), although flares were still formed and single cell movements were observed (Fig. 32A). The reduced colony size of the Δ*frzZ* mutant could be explained by defects in cellular reversals, as mutants in the Frz system have been reported to hyporeverse (Blackhart and Zusman 1985b). In line with that, the Δ*frzZ* strain only rarely reversed when calculating reversals per 15 minutes (Fig. 32B). The Δ*romR* strain behaved as described above, displaying less S-motility and no A-motility. In comparison, a double deletion mutant of *frzZ* and *romR* mimicked the phenotype of a Δ*romR* single mutant, with a strong defect in both motility systems and an absence of single cell

movement (Fig. 32A). This indicates that RomR acts downstream of the Frz-system. To further verify these results, reversal frequencies of strains lacking FrzZ and containing RomR with substitutions in D53 were analyzed, (Fig. 32B). We hypothesized that if RomR would act downstream of the Frz system, activated RomR ($RomR^{D53E}$) should bypass a deletion of *frzZ*. Interestingly, while a combination of the *frzZ* deletion with $romR^{D53N}$ could not restore reversals, the combination with $romR^{D53E}$ could bypass the *frzZ* deletion and restore reversals to a level observed before for $romR^{D53E}$ (Fig. 31 and 32B). Therefore, we concluded that RomR acts downstream of the Frz system. To verify the previous observations that MglA acts downstream of the Frz system, we combined the *frzZ* deletion with the $mglA^{Q82A}$ allele, and verified that MglA-GTP can bypass the *frzZ* deletion by restoring reversals and giving rise to the hyperreversing phenotype, characteristic for mutants with MglA locked in the GTP-bound form (Fig. 32B).

In summary, we found that the Frz system acts upstream of RomR, while the MglA/MglB system acts downstream of RomR. However, from this data it was not possible to conclude whether RomR can be directly activated by the Frz system.

2.4.2 Direct interactions between RomR, the MglA/MglB system and the Frz system

Epistasis analyses carried out with FrzZ, RomR, MglA and MglB indicated that RomR acts in a pathway regulating motility and reversals between the Frz system and the MglA/MglB system. In contrast, previous models suggested a direct interaction between the Frz system and MglB or MglA. To investigate direct interactions between these proteins, FrzE as the kinase of the Frz system, FrzZ as the output of the Frz system, as well as MglA and MglB and RomR were analyzed using the bacterial two hybrid system (BACTH). One of the advantages of the BACTH system approach compared to interaction studies using purified proteins is that proteins are expressed in an *in vivo* system, specifically in the *E. coli* strain BTH101. Therefore, the proteins are expected to be in native-like conditions, which could increase the chance of fully

functional proteins and interactions. However, similar to other protein-protein interaction assays, the BACTH assay has limited sensitivity in its ability to detect very weak or transient interactions.

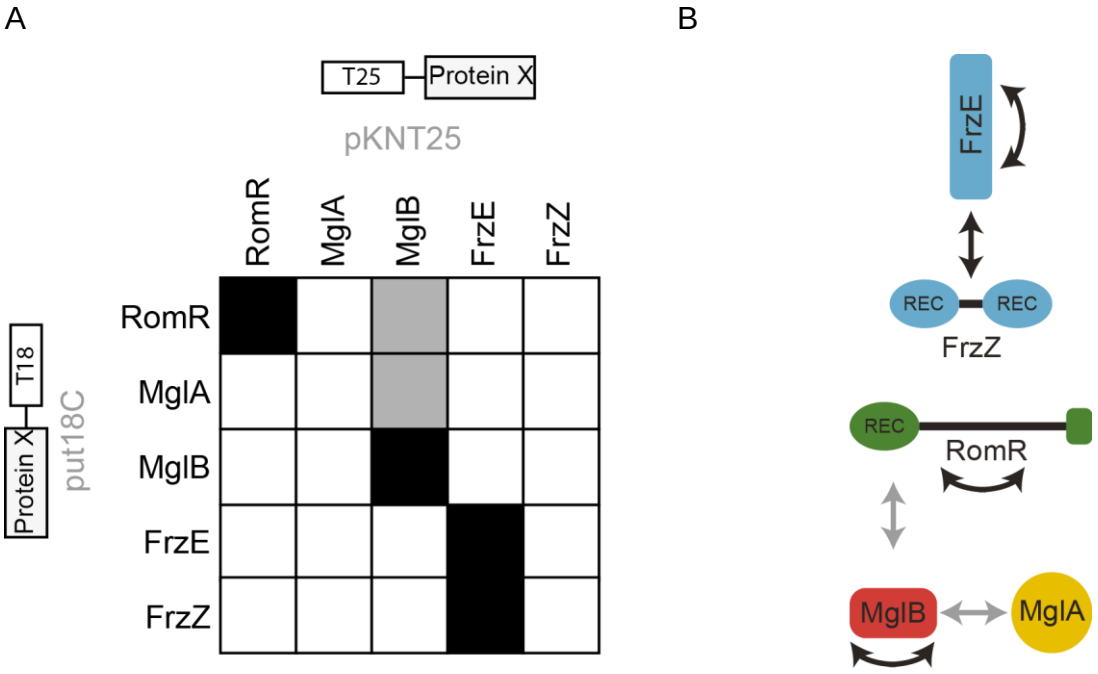

Figure 33: Interactions between RomR, MglA and MglB and the Frz sytem proteins FrzZ and FrzE. (A) Bacterial two hybrid assay performed as decribed (Euromedex), Black boxes represent strong interactions, identified by deep blue colonies, while grey boxes represent weak interactions, identified by slightly blue clonies. White boxes represent no interaction, identified by white colonies. (B) Model for interactions which could be confirmed by BACTH analysis (black arrows indicate strong interactions, grey arrows indicate weak interactions)

To analyze direct interactions, two plasmids expressing each protein of interest were co-transformed into *E. coli* strain BTH101. *In vivo* protein-protein interactions can restore the activity of the *Bordetella pertussis* adenylate cyclase in the *E. coli* reporter strains. Active adenylate cyclase (Cya) results in the expression of the *lacZ* gene, which can be detected by blue colonies on the plates containing X-Gal (5-bromo-4-chloro-indolyl-β-D-galactopyranoside). The plasmids pKT25-zip and pUT18C-zip serve as positive controls for complementation provided by the manufacturer. These plasmids express the T25-zip and T18-zip fusion proteins that strongly interact via dimerization of the leucine zipper motif appended to the T25 and T18 fragments. When pKT25-zip and pUT18C-zip were co-transformed into BTH101, they restored a characteristic Cya+ phenotype, resulting in the deep blue colonies. Additionally,

a negative control was performed, using empty plasmids, resulting in white colonies. As shown in figure 33, strong interactions were detected for the proteins that were expected to dimerize, RomR, MglB and FrzE (Fig. 33 black). Dimerization is common for response regulators (RomR) and kinases (FrzE). Also the dimerization of MglB is supported by crystallography and stoichiometry studies of the MglA/MglB complex (Miertzschke et al. 2011). In particular, it was reported that MglB forms dimers when interacting with MglA. Furthermore, MglB dimers are able to oligomerize. Additionally, a strong interaction was detected between FrzE and FrzZ (Fig. 33 black). This interaction had been shown previously by phosphotransfer assays, showing that FrzE can phosphorylate FrzZ *in vitro* (Inclan et al. 2007). Additionally, weak interactions were detected between MglA and MglB, and RomR and MglB (Fig. 33 grey), both of which were detected by *in vitro* studies described in Chapter 2.3.2. In summary, the BACTH assay confirmed many of the interactions supported by previous analyses; however, this approach failed to detect hypothesized interactions directly linking the Frz system and RomR. Furthermore, some previously characterized interactions could not be detected and verified using the BACTH method. For example, we were not able to confirm the interaction between RomR and MglA with this method, while this interaction was detected using purified proteins in vitro. This could indicate that some of the interactions are very transient within the cell or need additional interaction partners. However, we do not have any evidence that the Frz system directly interacts with RomR, MglA or MglB. While we cannot rule out a direct interaction, it is also possible that accessory or intermediate proteins are required, which have yet to be identified.

2.4.3 RomR phosphorylation assays

Our model suggests that RomR acts downstream of the Frz system; however, it remained an open question whether any of the Frz proteins directly act on RomR. A kinase that can phosphorylate RomR has not been identified. The output of the Frz system is FrzZ, which is activated by phosphorylation, leading to the induction of cellular reversals (Inclan et al. 2007). In contrast,

mutations in FrzE, a CheA-CheY hybrid kinase, that inhibit phosphotransferor to FrzZ, a response regulator, lead to a hyporeversing phenotype (Inclan et al. 2007; Inclan et al. 2008). Similarly, mutations that inhibit phosphorylation of the RomR receiver domain result in a hyporeversing phenotype, whereas phosphomimic mutations result in hyperreversals (Leonardy et al. 2007). Therefore, we hypothesized that FrzE could phosphorylate RomR in addition to FrzZ in order to activate reversals. To test this hypothesis, we performed phosphotransfer assays. Previous studies showed that FrzZ could only be phosphorylated by FrzE, if FrzE lacked its C-terminal CheY domain (Inclan et al. 2007). Additionally, FrzCD, the methyl-accepting-protein, and FrzA, a CheW-like protein, have been reported to be essential for the *in vitro* phosphotransfer between FrzE and FrzZ (Inclan et al. 2007).

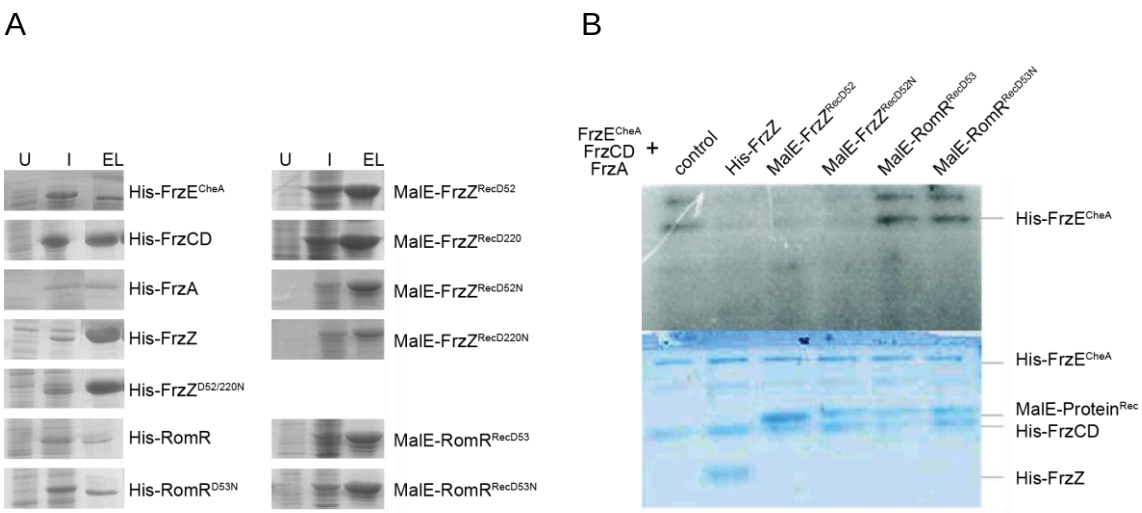

Figure 34: Phosphotransfer of FrzE to FrzZ and RomR. (A) Protein purifications used in phosphotransfer reactions. Proteins were separated by SDS-PAGE and visualized by Coomassie Brilliant Blue R-250 staining. U: uninduced, I: induced (after IPTG Induction), EL: Elution of protein (Protein purified with either Ni^{++}-column for His-tagged proteins and amylose column for MalE- tagged proteins) (B) For each reaction, His-$FrzE^{CheA}$, His-FrzCD and His-FrzA were used, to autophosphorylate FrzE. proteins added to the reaction are indicated above the autoradiograph [upper panel]: Autoradiograph of the identical gel as the SDS gel in the lower panel, Autolabeling by FrzE and transfer to FrzZ, and both receiver domains of FrzZ. [lower panel] Proteins were separated by SDS-PAGE and visualized by Coomassie Brilliant Blue R-250 staining. Positions of His_6-$FrzE^{CheA}$, MalE-$Protein^{Rec}$ (MalE-$FrzZ^{RecD52}$, MalE-$FrzZ^{RecD220}$, MalE-$RomR^{RecD53}$ and MalE-$RomR^{RecD53N}$), His_6-FrzCD and His_6-FrzZ are indicated.

To test phosphorylation of RomR *in vitro*, the same conditions as described for FrzZ phosphorylation were applied to ensure FrzE activity. Therefore, the

proteins His_6-$FrzE^{CheA}$, His_6-FrzCD, and His_6-FrzA were purified as described by Inclan et al. (Inclan et al. 2007) (Fig 34A). FrzZ was employed as a positive control because it was shown that both FrzZ receiver domains can be phosphorylated by FrzE. $RomR^{D53N}$ was used as a negative control, as it has a substitution in the conserved aspartate that prevents the phosphotransfer reaction. The experiment was performed with receiver domains alone and full length proteins testing His_6-FrzZ, His_6-$FrzZ^{RecD52/220N}$, MalE-$FrzZ^{RecD52}$, MalE-$FrzZ^{RecD52N}$, MalE-$FrzZ^{RecD220}$, MalE-$FrzZ^{RecD220N}$, His_6-RomR, His_6-$RomR^{D53N}$, MalE-$RomR^{Rec}$, and MalE-$RomR^{RecD53N}$. Each protein was purified and tested for phosphotransfer reaction using autophosphorylated His-$FrzE^{CheA}$ (Fig. 34B) as the phosphate donor. While the phosphotransfer of FrzE to the full length FrzZ and to the single receiver domains of FrzZ could be confirmed, no phosphotransfer to the RomR receiver domain was detected (Fig. 34B) under the same conditions. Similar results were observed using full length RomR (data not shown).

Importantly, under all tested conditions no phosphotransfer between FrzE and RomR could be detected. In line with the BACTH assay results, there is no evidence for the direct interactions between the Frz system and RomR. However, conditions required for the putative FrzE-RomR interaction may be different from those required for FrzE-FrzZ interaction. In total, the data thus far suggests that FrzE might not act as the RomR kinase despite the evidence that the Frz system acts upstream of RomR and regulates reversals. Therefore, we proposed that the Frz system induces reversals by indirectly activating RomR, and that direct activators and interaction partners of RomR remain undiscovered.

2.5 RomX and RomY, new factors involved in motility regulation

2.5.1 Five protein network regulating motility: RomR, MglA, MglB, RomX and RomY

Consistent with studies of other response regulators, RomR was proposed to be activated by phosphorylation of a conserved aspartate, D53 in

M. xanthus (Leonardy et al. 2007). Interestingly, cells expressing RomR^{D53N} reversed less often, similar to cells lacking components of the Frz-chemosensory system. Since we did not detect direct phosphotransfer from FrzE to RomR, it remained an open question how RomR is phosphorylated. A previous analysis of 1611 genomes identified RomR homologs in 31 taxonomically diverse genomes. To identify putative new interaction partners, such as a kinase or a phosphotransfer protein, we further mined the 1611 genome set for proteins that have a similar phylogenetic distribution as RomR (Fig. 35).

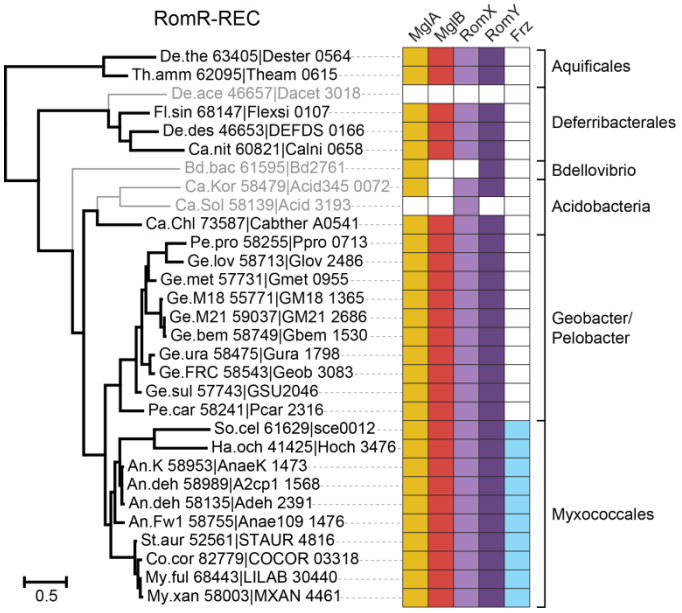

Figure 35: RomX and RomY have the same genomic distribution as RomR. The tree is built from a multiple alignment built of RomR receiver domains. Branches in grey indicate RomR sequences that have lost the conserved C-terminal domain. Each column shows the presence or absence of MglA, MglB, RomX, RomY, and Frz (defined by the presence of FrzE) as a colored or white box, respectively.

In the analyses we identified two proteins predicted to co-evolve with RomR based on distribution and phylogenetic analyses, RomX and RomY (Kristin Wuichet, personal communication). Notably, RomX (RomR-interacting protein X) and RomY (RomR-interacting protein Y) were conserved in 28 out of 30 genomes containing RomR. Furthermore, RomX was conserved in two genomes that encode RomR, but lack MglB or MglA, which suggests a strong link between RomR and RomX. In contrast, RomY was only conserved in the genomes that encode RomR together with MglA, indicating a possible connection between RomY and MglA. To find out if RomX and RomY are part of

the RomR/MglA/MglB system that regulates polarity and motility, in-frame deletions in *romX* and *romY* were constructed, motility phenotypes were characterized, and localization studies were carried out.

First, the two genes and their genomic context were analyzed. Both genes code for hypothetical proteins that have no known function and lack any characterized domains matching models in Pfam (Punta et al. 2012). The genomic contexts of *romX* and *romY* (Fig. 36) do not suggest a function in motility based on the predicted function of neighboring genes. In particular, *romX* is encoded next to *dnaJ* gene, encoding for a chaperone widespread in many genomes, and therefore does not share the genomic distribution of RomX and RomR (Fig. 36). Similarly, downstream gene *rluA* encodes for a pseudouridine synthase, which is also widespread as compared to RomX and RomR (personal communication, K. Wuichet).

Figure 36: Genetic organization of RomX and RomY. Arrows indicate the orientation of the gene; colored genes are the genes of interest. Details in the text.

Interestingly, a previous transposon mutagenesis screen revealed that the *rluA* gene is involved in A-motility and was therefore named *agmF* (Youderian et al. 2003). Since RomX shares the genomic distribution with RomR and the *agmF* mutation has never been complemented, we hypothesize that the insertion in *agmF* might interfere with the correct expression of RomX.

RomY is flanked by *ftsE* coding for a putative cell division ABC transporter and *carF*, coding for a carotinoid synthesis regulator (Fig. 36). Importantly, proteins encoded by the flanking genes do not share the RomR-like genomic distributions of RomX and RomY, suggesting that they do compose a conserved system (personal communication, K. Wuichet).

Based on the bioinformatics analyses, we hypothesized that RomX and RomY are two new regulators of motility. Although they have never been identified in any mutagenesis screens for genes involved in A-motility, S-motility or reversals, we hypothesize that the small size of *romX*, with only 264 bp and *romY* with 651 bp decreases their chances for identification via such methods.

Therefore, bioinformatics analyses serve as a novel and valuable tool to identify small factors that might act as accessory proteins.

While *romX* and *romY* are both encoded in gene clusters potentially involved in cell division, the phylogenetic analysis supports that RomX and RomY co-evolve with RomR, unlike their neighboring genes, and thus, we predicted that these two genes are involved in regulation of motility.

2.5.2 RomX and RomY are required for motility

RomX and RomY are predicted to co-evolve with RomR and the MglA/MglB system, supporting that all five proteins are part of a conserved interaction network. To explore this hypothesis, in-frame deletion mutants of *romX* and *romY* were constructed and their phenotypes were analyzed by A- and S-motility assays (Fig. 37). To further exclude polar effects, complementation strains have been constructed, expressing a copy of the deleted gene from the *pilA* promotor.

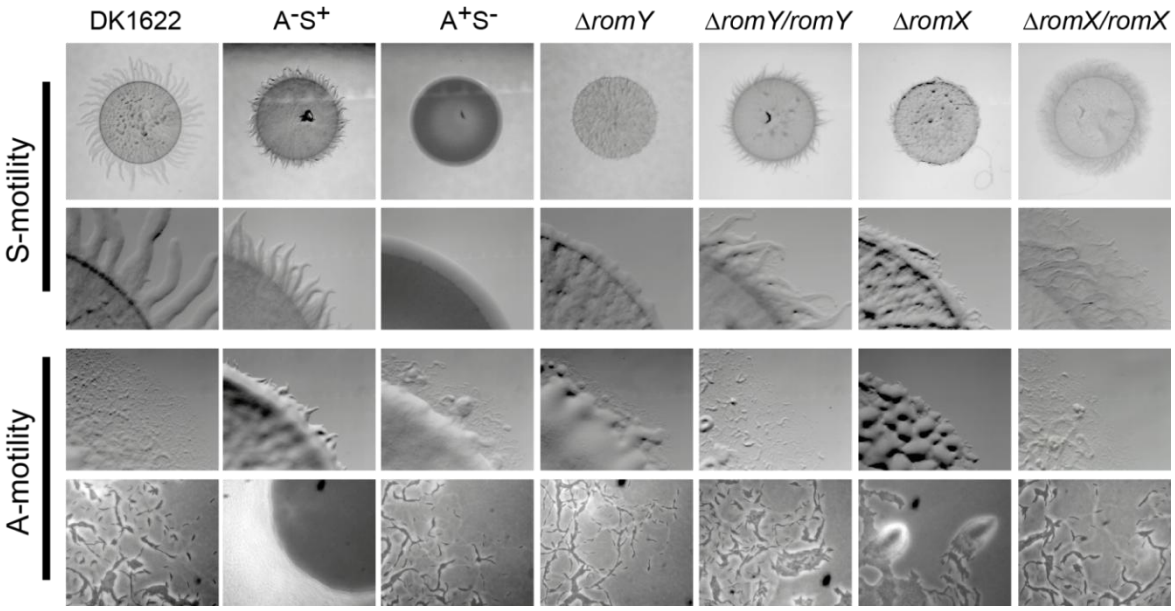

Figure 37: RomX and RomY are involved in motility. Indicated strains were incubated at 32°C for 24 h on 0.5% agar/0.5% CTT medium to score S-motility and 1.5% agar/0.5% CTT medium to score A-motility. Assay as described previously.

As expected, WT cells were able to move with both of the motility systems, forming flares on S-motility agar and displaying single cells for A-motility agar.

Strikingly, both the Δ*romX* mutant and the Δ*romY* mutant displayed defects in motility when compared to WT. A Δ*romY* mutant did not form a completely smooth edge on soft agar as the A^+S^- control, but instead was strongly reduced in S-motility, not showing any flares. However, the Δ*romY* mutant was still able to perform single cell motility, but the cells were not able to spread as far as WT cells. To exclude polar effects, the Δ*romY* mutant was complemented by an integration of P*pilA-romY* at the Mx8 attachment site. The complementation strain *ΔromY/ PpilA-romY* was able to produce flares only slightly shorter than WT. Moreover, this strain was able to move by single cell motility and to spread to a similar extend as WT cells. A Δ*romX* mutant displayed defects in both A- and S- motility. While S-motility was strongly reduced, A-motility was completely abolished, similarly to the A^-S^+ control. In line with that, no single cells were observed under high magnification for the Δ*romX* mutant. Importantly, these phenotypes could be rescued by an integration of P*pilA-romX* at the Mx8 attachment site. The resulting strain was able to make long flares, and move by single cell motility, similar to WT. Both constructs, P*pilA-romY* and P*pilA-romX* were able to complement the defect caused by the respective in-frame deletion.

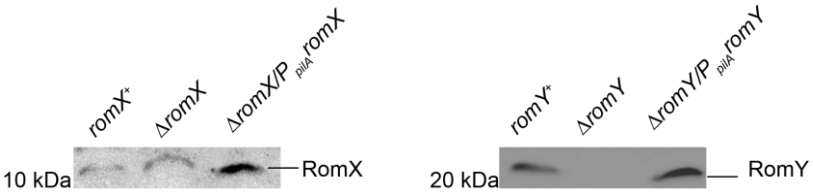

Figure 38: Immunoblots RomX/RomY proteins. Cells were grown as in liquid culture, harvested, and total protein (1 mg per lane) was separated by SDS–PAGE and analyzed by immunoblotting using α-RomX-antibodies, RomX 11 kDa (left) and α-RomY antibodies, RomY 21 kDa (right). The migration of molecular size markers is indicated on the left. Strains as indicated. Details in the text.

To compare protein levels between WT and the complementation strains, immunoblots with antibodies raised against His_6-RomX and His_6-RomY were perfomed, analyzing WT, the in-frame deletion strain and the complementation strains of *romX* and *romY* (Fig. 38). Immunoblot analysis showed that RomY expressed under the *pilA*-promotor is slightly overexpressed compared to WT levels (Fig. 38). Additionally, for RomX a band at the size of RomX was detected in the Δ*romX* strain, but the correct deletion was verified by PCR. This

suggests that RomX antibodies might bind an unspecific protein at this size and require additional purification for future experiments. Regardless, A- and S-motility defects of the in-frame deletions could be successfully complemented indicating that the proteins expressed under the *pilA* promotor were functional. This supports that RomX and RomY are involved in motility. Interestingly, the phenotype of a Δ*romX* mutant shows similarity to the phenotype of a Δ*romR* mutant, which is consistent with the strong co-occurrence relationship identified by bioinformatics analyses. Therefore, we hypothesized that RomX and RomR function in the same pathway. In contrast, RomY shows a stronger phenotype in S-motility and bioinformatics indicate a stronger correlation with MglA. The identification of these novel proteins and their subsequent experimental validation in motility regulation suggests that there are many remaining avenues of exploration in this intriguing system.

2.5.3 Localization of RomX and RomY

To investigate whether RomX and RomY are part of the MglA/MglB/RomR signaling network, the two proteins were localized using C-terminal YFP fusions (Fig. 39). As previously described, MglB and RomR localize asymmetric bipolar with predominant localization to the lagging cell pole, whereas MglA localizes to the leading cell pole (Leonardy et al. 2007; Leonardy et al. 2010; Zhang et al. 2010). We hypothesized that if RomX and RomY directly interact with RomR, MglA or MglB to regulate motility, they would display characteristic patterns of motility proteins in localization.

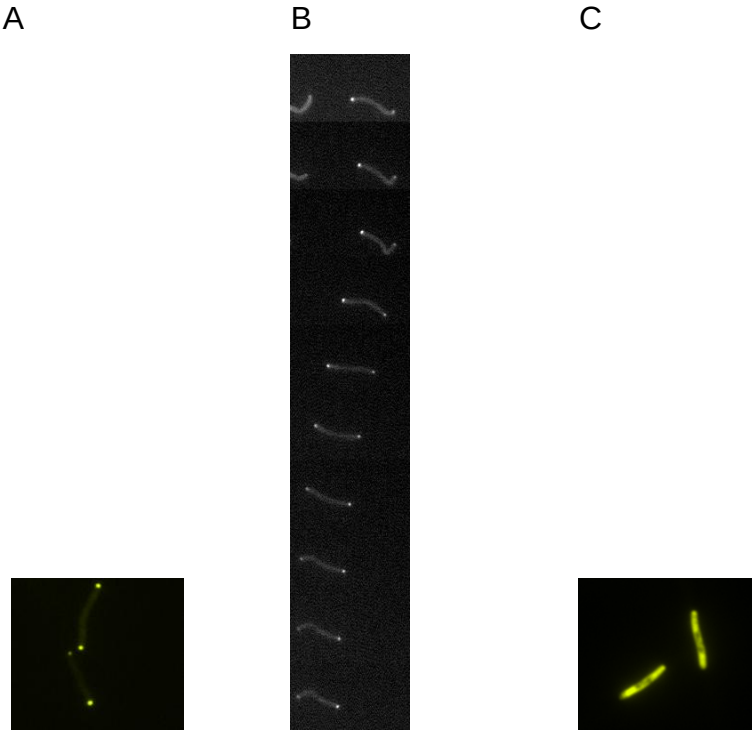

Figure 36: Localization of RomX-YFP and RomY-YFP. For the experiments cells expressing YFP fusions were transferred from liquid cultures to an agar-pad on a slide and imaged by fluorescence microscopy. (A) Cells expressing RomX-YFP (B) Time lapse movie of RomX-YFP: pictures taken every 30 sec. (C) Cells expressing RomY-YFP

Strikingly, RomX-YFP displayed an asymmetric bipolar localization, as seen for RomR and MglB. In contrast, RomY-YFP showed a mainly diffuse localization. Furthermore, time-lapse microscopy with the strain expressing RomX-YFP revealed that the larger cluster localizes at the lagging cell pole and displays the same dynamic reversals observed for RomR and MglB (Fig. 39B). This close correlation between the localization of RomX and RomR provides further support for a functional connection between the two proteins. In contrast, the diffuse localization of RomY does not indicate a function at the cell pole, but could be due to the overexpression under the *pilA* promoter as observed for the proteins expressed without the YFP fusion or to a not fully functional fusion. To examine the localization dependency of RomX and RomY, we conducted localization studies in presence and absence of the other motility factors.

2.5.4 Interactions between RomX, RomY and the RomR/MglA/MglB network

Based on the phylogenetic distribution of RomX and RomY, as well as the phenotypes of their in-frame deletion strains, we concluded that the two proteins are involved in motility. Localization studies revealed that RomX localizes to the cell poles while RomY displayed a mainly diffuse localization. Previously we revealed that RomR, MglA and MglB are mutually dependent for their correct localizations. Therefore, we hypothesized that RomX and RomY may also be dependent on MglA, MglB or RomR for their localizations. To test this hypothesis, we localized RomY and RomX in the absence of RomR, MglA and MglB (Fig. 40A). Additionally, we hypothesized that MglA, MglB or RomR could depend on RomX and RomY, and accordingly, RomR, MglA and MglB were localized in the absence of RomX and RomY (Fig. 40B).

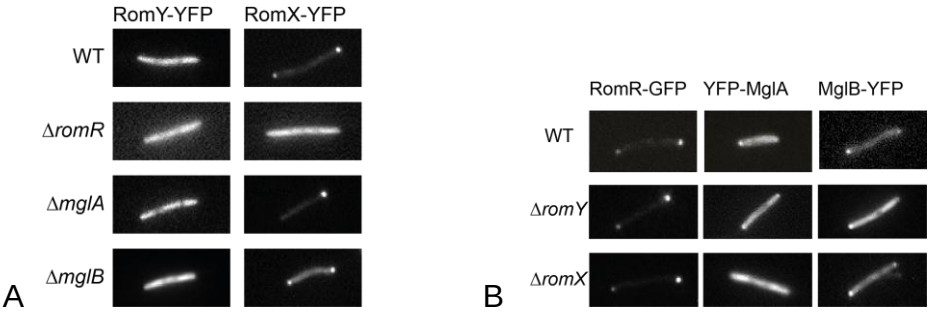

Figure 40: RomX localization studies. For the experiments cells expressing the indicated fusions were transferred from liquid cultures to an agar-pad on a slide and imaged by fluorescence microscopy (A) Localizations of RomY-YFP and RomX-YFP in the indicated strains (B) Localizations of RomR-GFP, YFP-MglA and MglB-YFP in the indicated strains.

RomY-YFP showed a diffuse localization independently of RomR, MglA and MglB (Fig. 40A). Similarly, the absence of RomY did not affect the localization of RomR, MglA, or MglB (Fig. 40B). In contrast, the RomX-YFP localization was affected noticeably by the lack of RomR. RomX-YFP localization changed from asymmetric bipolar in the WT to predominantly diffuse in the absence of RomR, indicating a direct requirement of RomR for RomX localization (Fig. 40A). This hypothesis was further supported by the similar changes observed in RomX-YFP and RomR-GFP localization when each was expressed in the absence of

MglA or MglB (Fig. 40 and 27). Specifically, in a mutant lacking MglA, RomX-YFP and RomR-GFP become unipolar, while in a mutant lacking MglB, RomX-YFP and RomR-GFP become more bipolar. To understand the effects of RomX on RomR, MglA and MglB, these proteins were localized in the absence of RomX. We did not detect strong effects on RomR or MglB localization; however, YFP-MglA was diffuse in the absence of RomX, as previously observed in the absence of RomR. Importantly, the dependency of RomX on RomR and not vice versa indicates that RomX acts downstream of RomR. Furthermore, RomX is required for correct MglA localization, indicating that it acts upstream of MglA. The mechanistic details of how RomR acts on MglA are still unclear. Our data suggest that RomR targets MglA to the pole, and that RomR might have a secondary function in regulating the nucleotide-bound state of MglA. If RomX acts between RomR and MglA, RomX could be involved in one or both of these two functions.

To further determine the function of RomX, biochemical assays with MglA, RomR and RomX are essential. Strikingly, *ΔromR* and *ΔromX* mutants phenocopied each other, and RomR and RomX proteins exhibited the same localization patterns in a variety of mutant backgrounds. Notably, RomX shows a strong correlation with RomR, and its localization depends on RomR. Thus we investigated whether the localization dependency is due to the direct interactions between RomR and RomX by using BACTH assays with RomR and RomX (Fig. 41). As described in chapter 2.4.2., RomR was shown to interact with itself, and therefore it was used as a positive control. In contrast, co-expression of RomR with the empty vector did not show any positive signs of interactions. Notably, this assay revealed a strong interaction between RomR and RomX, which further supports that RomR and RomX function in the same pathway to regulate motility.

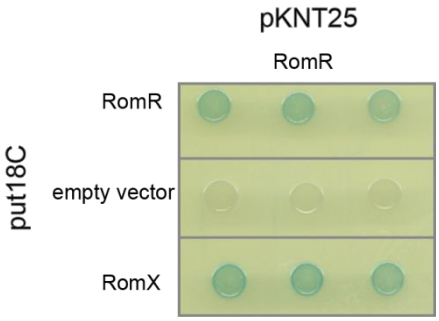

Figure 41: RomX interacts with RomR. Bacterial two hybrid assay performed as described in Materials & Methods. Blue colonies indicate interaction, while white colonies indicate no interaction. For each strain containing the two plasmids (fusion in pKNT25, and fusion in pUT18C) representative colonies are shown.

In summary, we could verify that RomX and RomY are involved in motility. We suggest that the five proteins, RomX, RomY, MglA, MglB and RomR are part of a conserved signaling network. While only four proteins were analyzed in more detail (MglA, MglB, RomR and RomX) all five proteins are predicted to regulate motility and reversals in *M. xanthus*. Furthermore, this network is maintained in genomes lacking the synchronized A- and S-motility systems of *M. xanthus* (Fig. 35), which suggests that it may comprise a universal polarity system with functions beyond motility.

3 Discussion

M. xanthus possesses two genetically independent motility systems: S-motility, cells moving collectively, and A-motility, individual cell movement (Hodgkin and Kaiser 1979). While both systems are genetically independent, they act synchronously during motility and reversals. It was shown previously that the response regulator RomR is an important regulator of A-motility (Leonardy et al. 2007); however, we found that it plays a role in regulating both motility systems. Furthermore, the localization of RomR was suggested to be essential for the regulation of motility because RomR is polarly located as seen with other motility components. Specifically, RomR is targeted to the cell pole in a bipolar asymmetric pattern, with a larger cluster at the lagging cell pole (Leonardy et al. 2007). As with other classic response regulators, RomR is defined by a receiver domain and an output domain. Typically, the phosphorylation state of the receiver domain regulates the activity of the output domain that is often involved in DNA binding or has an enzymatic function; however, the RomR output domain mediates its correct localization (Leonardy et al. 2007). Here we addressed the factors mediating RomR localization by studying the output domain and interaction partners. We were able to show that the output domain contains two independent subdomains, each of which are sufficient to target RomR to the cell pole. Furthermore, we show that MglA and MglB are required for the correct localization of RomR, whereas A-motility proteins only play a minor role. Direct interaction studies support that RomR forms independent complexes with MglA and MglB. Additionally, the three proteins are dependent on each other for their correct localization, which, in turn, is important for motility regulation. It was shown previously that cellular reversals are correlated with an inversion of polarity demonstrated by the relocation of dynamic motility proteins, which switch between poles upon reversal (Mignot et al. 2005; Leonardy et al. 2007; Bulyha et al. 2009). The Frz-system induces reversals (Blackhart and Zusman 1985b), and therefore polarity inversion of these dynamic proteins. Notably, RomR, MglA and MglB exhibit this dynamic behavior (Leonardy et al. 2007; Leonardy et al. 2010; Zhang et al. 2010). The foundation of this study was the detailed characterization of RomR

in order to establish its function in motility and reversals. Here we propose that RomR acts between the Frz chemosensory system and MglA/MglB, in order to link reversals and polarity. The Frz system receives the signal for switching the direction of movement, and this information is transmitted to RomR. Then RomR passes this information to MglA and MglB via direct interactions, leading to a switch in localization of polarly localized proteins. Furthermore, we identified two new players involved in regulation of motility, which are part of a five protein signaling network that includes MglA, MglB, and RomR.

3.1 RomR regulates both motility systems

In this study we show that RomR is involved in both A- and S-motility and reversals by performing qualitative and quantitative motility assays in addition to reversal frequency analyses. These results provide a new understanding about the function of RomR. Originally RomR was thought to be part of the A-motility machinery. However, RomR displays an asymmetric bipolar localization unlike all other localized A-motility proteins, which are distributed along the cell body in putative FACs (Yang et al. 2004; Leonardy et al. 2007; Sun et al. 2011). Previous deletion studies showed A-motility proteins are dependent on each other for proper localization (Nan et al. 2010); however, RomR and its polar targeting subdomains localize to the pole independent of the A-motility machinery. Moreover, a Δ*romR* mutant displayed an intermediate phenotype for S-motility in addition to the abolishment of A-motility, which supports that RomR has a function beyond A-motility regulation. Additionally, bioinformatic analyses revealed that RomR is more widely distributed than A-motility proteins. Interestingly, it was shown that all genomes containing an intact RomR, both its receiver domain and its output domain, also contain an MglA/MglB system. These two proteins have been shown to regulate A- and S-motility in addition to reversals, and we were able to demonstrate that RomR has a role in these processes.

3.2 A-motility machinery is not required for RomR polar targeting

The response regulator RomR localizes with a large cluster at the lagging cell pole, and a small cluster at the leading cell pole (Leonardy et al. 2007). During a cellular reversal, this localization switches, and the new lagging cell pole then contains the larger RomR cluster. It was shown that the protein localization depends on the output domain, but that dynamic relocalizations depend on the phosphorylation state of the receiver domain. To understand how RomR achieves this localization, we first analyzed the output domain in more detail. Bioinformatic analyzes revealed that the output domain can be divided into two subdomains, a Pro-rich linker region and a Glu-rich C-terminal part. We found that both subdomains can localize to the cell pole independently, which indicates the potential existence of two distinct targeting mechanisms. Different possibilities to achieve polar localization have been proposed including: interaction with the septum during cell division (Huitema et al. 2006); interaction with lipid domains in the membrane (Romantsov et al. 2007) or recognition of the different curvature at the cell pole (Lenarcic et al. 2009). To analyze how RomR is targeted to the cell pole, we focused on identifying interaction partners. Although RomR remains polarly localized in the absence of the A-motility machinery, we identified a switch from asymmetric bipolar localization to a symmetric bipolar localization in the absence of certain A-motility proteins. However, when we performed the same analysis with the output domain only, which is not able to switch localization, no difference in RomR localization could be observed between cells containing or lacking these A-motility components. The same was true for the localization of output subdomains. This data supports that the RomR receiver domain plays a role in proper localization in relation to the A-motility machinery. However, it is not clear if this symmetric localization is specific to these A-motility proteins, or if this effect is due to the properties of non-motile cells. One possible model to explain the symmetry of RomR would be that the lack of A-motility proteins interferes with the dynamics indirectly. For a dynamic localization of RomR, activation via phosphorylation in the receiver domain is needed. If cells are not moving, because they lack important parts of the A-motility machinery, but RomR still gets signals to induce reversals, the protein dynamics could become

erratic, leading to a more symmetric localization. While RomR is still able to switch between the two poles, cells are not moving, and therefore the two poles are not defined as leading and lagging cell pole. In line with that, the control strain carrying RomR-GFP, has been observed to display a more symmetric localization before the cells started moving on the agar surface (data not shown).

Interestingly, some of the A-motility proteins showed a stronger effect on RomR localization compared to the others, particularly AglZ, AgmX and AgmK. Therefore these three A-motility components might be connected to the regulation components. Interestingly, AglZ has been shown to directly interact with MglA, an essential regulatory protein required for both motility systems (Yang et al. 2004). Further studies in our lab show effects from A-motility proteins on MglA localization (Hot, unpublished). Therefore it is also possible, that effects on RomR localization by A-motility proteins are indirect through changes in localization of MglA. However, it is not clear why these changes would not be observed for the output domain. In this study, we also found that RomR and MglA can directly interact, but the specific regions mediating this interaction remain an ongoing subject of investigation. It is possible that the receiver domain of RomR is required for direct interaction with MglA. This could explain why only full length RomR is altered in localization in the absence of A-motility proteins. Therefore I propose a model in which the A-motility machinery is required for correct MglA localization, and that the correct MglA localization is required for the correct asymmetric localization of RomR, by interaction with the RomR receiver domain. However, the polar targeting of RomR does not depend on the A-motility machinery or MglA.

3.3 RomR is part of a polarity module together with MglA and MglB

The small GTPase MglA has been shown to regulate motility and reversals depending on its nucleotide-bound state (Leonardy et al. 2010; Zhang et al. 2010; Miertzschke et al. 2011). Furthermore, direct interaction studies, GTPase assays, as well as structural analysis strongly suggest that MglB acts

as a GAP that induces the conversion between MglA-GTP to MglA-GDP. Interestingly, we found that the response regulator RomR co-occurs with MglA and MglB in phylogenetic studies. Strikingly, genomes that encode only a truncated version of RomR, either the receiver domain or the conserved C-terminal region, also lack a complete MglA/MglB pair, which suggests that RomR is functionally connected to the MglA/MglB system. RomR can directly interact with MglA and MglB independently, further supporting that the three proteins regulate motility and reversals together as part of a signaling network. Additionally, all three proteins are mutually dependent on each other for their correct localizations, indicating that these direct interactions also play an important role in complex formation *in vivo*. Consequently, we addressed how the three proteins interact with each other *in vitro* and *in vivo*. Reversal frequency studies as well as localization analyses revealed that MglA-GTP acts as the output of the MglA/MglB system (Leonardy et al. 2010; Zhang et al. 2010). While MglA-GTP can stimulate motility and reversals in the absence of MglB, the opposite is not the case. To analyze the role of RomR in this three protein network, we performed epistasis analysis using motility assays with single and double mutants of *romR*, *mglB*, *mglA* and *mglA-GTP*. Interestingly, an increase in MglA-GTP created by either locking MglA in the GTP-bound form by substitution within the protein or deleting *mglB*, bypasses the *romR* deletion and restores motility and reversals. Thus, MglA-GTP as well as MglB act downstream of RomR, indicating that MglA-GTP is the final output of the three protein network to regulate motility. We confirmed these observations by epistasis analyses using reversal frequencies as readouts, additionally including the two different forms of RomR, which mimic a constituitively active phosphorylated state or a constituitively inactive unphosphorylated state. While these different substitutions did affect reversal frequencies in an $mglA^{+}mglB^{+}$ strain, they could not bypass the lack of MglB, which resulted in a hyperreversing phenotype similar to a single *mglB* deletion mutant. Similarly, MglA locked in the GTP-bound form acts downstream of RomR, leading to a hyperreversing phenotype independent of the phosphorylation state of RomR. In conclusion we suggest that RomR provides a signaling input to the MglA/MglB system, while MglB as well as MglA are the output of this module, with MglA-GTP acting most downstream.

To further understand, how these proteins affect each other *in vivo* we determined their localizations. Interestingly, MglA-GTP, MglB and RomR are all polarly localized, while MglA-GDP is diffused. While MglA-GTP localizes at the leading cell pole, RomR and MglB localize mainly to the lagging cell pole. It has been proposed, that the MglB localization at the lagging cell pole is responsible for the lack of MglA-GTP at that pole (Leonardy et al. 2010; Zhang et al. 2010; Miertzschke et al. 2011). It was hypothesized, that MglA-GTP is not able to form a cluster at the lagging cell pole, because it gets directly converted into MglA-GDP, which is diffused within the cell. We found that the three proteins are mutually dependent on each other for their correct localizations. Strikingly, MglA becomes diffuse in the absence of RomR. To understand why that is the case, we tested the following hypotheses: (1) MglA becomes diffuse, because it is mainly in its inactive GDP-bound state, if RomR is absent or (2) RomR targets MglA to the pole, which results in lack of polar localization in the absence of RomR. We could rule out that this change in localization is exclusively due to the conversion of MglA-GTP to MglA-GDP based on the observation that neither wildtype MglA nor the GTP-locked form of MglA form polar clusters in absence of RomR. Therefore, we suggest that RomR is a direct polar targeting determinant of MglA and has a function in bringing MglA to the pole. Furthermore, we found that the asymmetric localization of MglB and RomR are interdependent, indicating that they need to interact for defining the lagging cell pole. Taken together we propose the following model of polarity in *M. xanthus*. First, RomR targets MglA-GTP to both cell poles. However, we know that in WT cells which are moving, MglA-GTP is found exclusively at the leading cell pole. Therefore, MglB GAP activity is required to convert the MglA-GTP cluster at the lagging cell pole into MglA-GDP, which is diffuse. The direct interactions of the proteins and the interdependency in localization indicate a mutually dependent circuit for the asymmetric localization of the three proteins. After RomR targets MglA-GTP to both poles, forming an MglA/RomR complex, MglB interacts with RomR, forming the RomR/MglB complex at the lagging cell pole, setting up the unipolar localization of MglA-GTP at the leading cell pole. Additionally the MglA-GTP/RomR complex at the leading cell pole is required to maintain the asymmetry, with MglB and RomR mainly localizing at the lagging cell pole. This asymmetry defines the leading pole as the pole where the highest accumulation

of MglA-GTP is present and the lagging pole as the pole where the highest accumulaton of RomR and MglB is present.

To further address, if RomR also plays a role in activation of MglA acting either as a GEF protein, or by inhibiting MglB GAP activity, we analyzed MglA localization in a Δ*romR*Δ*mglB* double mutant. We hypothesized that if RomR acts on the nucleotide-bound state of MglA through MglB, the double mutant would phenocopy the single Δ*mglB* mutant. Interestingly our data show that a Δ*romR* mutant is strongly impaired in motility, while an additional deletion in *mglB* can rescue motility and reversals. The difference between these two strains, a Δ*romR* mutant and a double deletion mutant Δ*romR*Δ*mglB,* is the presence or absence of MglB GAP activity. MglB localizes to both cell poles in a Δ*romR* mutant and therefore converts MglA-GTP effectively into MglA-GDP, which results in the loss of motility. However, in a Δ*romR*Δ*mglB* mutant no GAP activity is present. Therefore, MglA remains in the GTP-bound form and is able to induce motility and reversals. In line with that we observed motility and cluster formation of YFP-MglA in the Δ*romR*Δ*mglB* mutant. Therefore we suggest that RomR might have an additional function in regulating the GTP-bound state of MglA. Remarkably, no polar MglA-GTP clusters have been observed in this strain. Taken together, we propose that RomR is required for polar localization of MglA and increases the levels of MglA-GTP in the cell, directly or indirectly. However, while polar localization of MglA has been suggested to be essential for motility, we created strains that lack polar localization of MglA, but were still able to move and reverse. Therefore we suggest that polar localization of MglA-GTP is not a strict requirement for motility. However, sufficient MglA-GTP levels have to be present in the cell to achieve motility and reversals.

While RomR was shown to be important for polar localization of MglA, it is not fully understood whether RomR shows any additional function in converting MglA-GDP to MglA-GTP by acting as a GEF or indirectly by inhibiting MglB. Future biochemistry analyses, including GTPase assays and GEF assays will be required to address this question. However, the studies presented here showed, that RomR, MglA and MglB interact directly and act in a genetic circuit and furthermore depend on each other to regulate motility and reversals.

Furthermore, we were able to demonstrate that MglA can be locked in the GTP-bound form by two independent approaches. On the one hand, MglA can be locked in the GTP-bound form directly, by substituting important residues in the active site, on the other hand, MglA can be indirectly locked in the GTP-bound form by the loss of MglB or substitutions in MglB which inhibit MglA/MglB interaction. Specifically we were able to demonstrate that strains with mutations in *mglB*, expressing $MglB^{A64/G68R}$, were impaired in MglA/MglB interaction and likely led to an accumulation of MglA-GTP within the cell scored by increase of reversal frequencies. Taken together, this study showed, that MglA-GTP acts most downstream of the RomR-MglA-MglB system, and needs to interact with downstream effectors to induce reversals and motility. Moreover, we found, that cells only expressing MglA-GTP, lacking the conversion to MglA-GDP reverse more frequently with a small variation in reversal periods, while WT cells reverse rather random. It has been shown, that WT cells reversing randomly are able to spread out much more compared to cells which hyperreverse. Therefore the RomR/MglA/MglB system seems to be required, to enable the cells to spread out sufficiently by regulating the reversal period by regulating the localization of MglA-GTP and the ratio between MglA-GTP and MglA-GDP.

3.4 Frz system signals upstream of the MglA/MglB/RomR system

Motile bacteria respond to environmental cues in order to move towards more favorable conditions. The components of the chemotaxis signal transduction systems that mediate these responses are highly conserved among prokaryotes including both eubacterial and archael species. The best-studied system is that found in *Escherichia coli*. Attractant and repellant chemicals are sensed through their interactions with transmembrane chemoreceptor proteins that are localized at one or both cell poles (Baker et al. 2006). The chemoreceptors interact with a histidine protein kinase, CheA and an adaptor protein, CheW, forming a highly ordered lattice. These multimeric protein assemblies act to control the level of phosphorylation of a response regulator, CheY, which dictates flagellar motion.

The Frz chemosensory system is homologous to the chemosensory system found in *E. coli* (McBride et al. 1989; Trudeau et al. 1996). While the input of the system has not been found so far, it has been shown that the phosphorylation state of the response regulator FrzZ controls cellular reversal frequency (Inclan et al. 2007). During a cellular reversal the cell changes direction, which is accompanied by the switch of motility proteins and disassembly of T4P at the old leading pole and reassembly at the new leading pole. Here we propose that the Frz chemosensory system acts as a regulatory module that stimulates cellular reversals by the inversion of the RomR/MglA/MglB polarity module. To understand how the output of the Frz-chemosensory system can serve as an input for the polarity module, FrzZ was included in epistasis analyses that were evaluated by motility assays and reversal frequencies. We showed that RomR acts downstream of FrzZ because a deletion of *frzZ* can be bypassed by substitutions in RomR, but not vice versa. Interestingly, a *romR*^{D53E} mutant, which mimics the activated phosphorylated form, cannot induce reversals to a level of an Δ*mglB* mutant or a GTP-locked *mglA* mutant. We hypothesize that either *romR*^{D53E} leads to a protein, which cannot fully mimic the active form of RomR, or that RomR works in parallel with FrzZ with both proteins being phosphorylated by FrzE. Given that the *romR*^{D53N} mutant has the same low reversal frequency as the Δ*frzZ* mutant, we favor a model in which RomR acts downstream of FrzZ. In this scenario, RomR acts between FrzZ and MglA/MglB, linking the two systems and thereby connecting the input to switch polarity with the module that establishs polarity.

3.5 Signaling between Frz system and RomR is rather indirect

Phosphorelays are common in bacteria, including activation of response regulators after multiple phosphotransfer reactions (Appleby et al. 1996). In Bacillus subtilis phorphorelays play an important role in the initiation of sporulation (Strauch and Hoch 1993) In *M. xanthus* phosphorelays are required for correct development of fruiting bodies (Schramm et al, 2011) In the case of *Caulobacter crescentus* the PleC phosphatase and the DivJ kinase are localized at opposite cell poles. This way they control the phosphorylation state

and subcellular localization of the response regulator DivK (Paul et al. 2008). Furthermore, this study showed that single domain response regulators can facilitate crosstalk, feedback control, and long-range communication among members of the two-component network.

While FrzZ possesses two response regulator receiver domains, FrzE is a CheA-like kinase that has a fused C-terminal receiver domain. Therefore we hypothesized, that RomR could be directly phosphorylated by FrzE. In order to identify any connections between RomR and the Frz system we performed direct interaction studies and phosphotransfer analyses. Bacterial two hybrid-studies did not show interaction for FrzE and RomR or FrzZ and RomR, although they did verify the interaction between FrzE and FrzZ. While phosphotransfer assays could confirm the direct phosphotransfer from FrzE to both receiver domains of FrzZ, no transfer to the RomR receiver domain could be observed. The widespread distribution of organisms with a conserved MglA/MglB/RomR module lacking the Frz-system suggests that there might be a different mechanism for RomR phosphorylation. Possibly, a histidine-protein kinase that has yet to be identified could activate RomR. Alternatively, FrzZ and RomR could be part of a phosphorelay, in which phosphorylated FrzZ can transfer its phosphate group to RomR directly or via an additional phosphotransfer protein.

3.6 RomR connects the inversion module with the polarity module

In this study we showed that RomR functions between the Frz-chemosensory system and the MglA/MglB module. In our current model we explain motility and reversals in *M. xanthus* as follows (Fig. 42): First, cells are moving in one direction, localizing MglA-GTP at the leading cell pole, and MglB and RomR mainly at the lagging cell pole. MglA-GTP is the final output of the RomR/MglA/MglB module and interacts with effector proteins of the A-motility and the S-motility system. While the cell is moving, T4P are localized at the leading cell pole, pulling the cell forward by extension and retraction of the ATP driven T4P. In parallel, the A-motility system generates force towards the same direction via FACs driven by proton motive force.

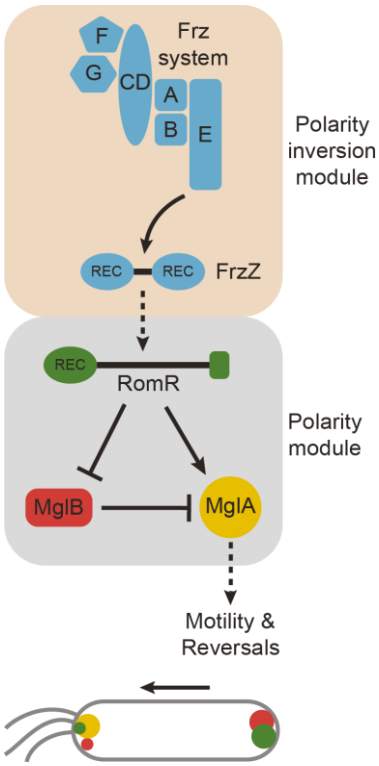

Figure 42: Model: RomR functions to connect inversion module and polarity module. The Frz chemosensory system signals to induce cellular reversals which imply an inversion of polarity. The polarity module consists out of RomR, MglA and MglB, while RomR passes information between the two modules. All three proteins are polarly localized as shown in the cell below.

After 5-15 minutes on average, a signal activates the Frz chemosensory system. The Frz system acts as a polarity inversion module, and consists of at least 7 proteins, including the cytoplasmic MCP, FrzCD; two CheW homologs, FrzA and FrzB; FrzE, possessing both a CheA histidine kinase domain and a CheY-like receiver domain; a methyltransferase FrzF, which methylates FrzCD; a methylesterase FrzG, which demethylates FrzCD; and, FrzZ, composed of two CheY receiver domains acting as the output of this module. FrzE activates FrzZ by phosphorylation. After FrzZ activation, the signal is transferred to the response regulator RomR, leading to phosphorylation of its receiver domain. However, current data suggest that additional proteins are required between FrzZ and RomR, for RomR activation. After RomR activation, the signal is transmitted to the MglA/MglB system, leading to an increase in MglA-GTP. We showed that RomR is required for targeting MglA to the pole. Additionally, MglA activation by RomR could occur directly by either acting on the nucleotide-

bound state of MglA, or indirectly by inhibiting GAP activity of MglB. Negative regulation of MglB by RomR would inhibit the conversion of GTP to GDP by MglA, and therefore indirectly increase the levels of MglA-GTP. In both cases, the signal received by the Frz chemosensory system would lead to an increase of MglA-GTP in the cell, which then leads to a cellular reversal. Therefore motility and reversals depend on the MglA-GTP levels in the cell. Interestingly, many genomes contain genes coding for the RomR/MglA/MglB polarity module, but not for the Frz chemosensory system polarity inversion module. Therefore we suggest that activation of RomR is stimulated by a different mechanism in these organisms, for example by another chemosensory system or a histidine protein kinase.

3.7 RomX and RomY – Two new factors expand the polarity module

To find the potential activator proteins of RomR, we conducted a bioinformatic screen of 1611 genomes, seeking genes with a similar phylogenetic distribution as for RomR. This analysis identified two uncharacterized proteins that we have named RomX and RomY, neither of which contain any conserved domains that could aid function prediction. To date, neither of the respective genes has been identified in any screen searching for genes involved in A-motility, S-motility or reversals. We suggest that the small size of *romX*, with only 264 bp and *romY* with 651 bp decreases the chance of a random insertion as found in transposon mutagenesis screens. Therefore bioinformatic analyses serve as an interesting tool, to find small factors, which might act as accessory proteins. Many genome projects employ an artificial length threshold of 100 amino acids (Frith et al. 2006). Hence, short proteins are underrepresented in protein catalogues; although they are known to play important roles in immunity, cell signalling, and metabolism. While *romX* and *romY* are both encoded in gene clusters predicted not to be involved in motility, these clusters are not conserved and the phylogenetic distributions of the flanking genes do not support a functional connection. Therefore, we hypothesized that they could play a role in regulation of motility and in the

activation of RomR. We created in-frame deletion mutants for each gene, which were then evaluated by motility assays. Interestingly, the Δ*romX* mutant showed a similar phenotype to the Δ*romR* mutant, displaying less S-motility and no A-motility. In contrast the Δ*romY* mutant was still able to perform single cell movements, but was strongly defective in S-motility. Thus, we conclude that both proteins, RomX and RomY play a role in motility.

Interestingly, the RomY amino acid sequence does contain two conserved histidine residues, which could play a role in a phosphotransfer reaction. However, neither one of the new factors contain the domains typical for a histidine kinase or phosphotransfer proteins. Therefore we hypothesize, that RomY could play a role in activation of RomR by a new mechanism, which still remains to be uncovered.

In this work, we found a very strong connection between RomX and RomR. The phenotype of the Δ*romX* mutant indicates a function in the regulation of motility that is similar to the function found for RomR. Furthermore, both proteins display the same localization pattern in WT as well as in deletions of *mglA* or *mglB*. Additionally, we showed that RomX localization depends on RomR. Therefore, RomX cannot localize in the absence of RomR, while RomR can localize to the pole without RomX. Furthermore, both proteins directly interact in a bacterial two-hybrid assay. In addition, some Geobacter genomes encode RomX homologs that are fused to a receiver domain indicating that RomX is strongly connected to a response regulator. Therefore we hypothesize, that RomX may be the functional output of RomR. In this model RomR contains an output domain that mediates localization, while RomX is required for full function of RomR. If RomX is required for RomR activity, RomX might also be important for activity assays *in vitro*. To date, no phosphotransfer has been shown between FrzE and RomR. However, if RomR is non-functional in the absence of RomX, this could explain these results. While activity of FrzE and FrzZ could be demonstrated by phosphotransfer between these two proteins, transfer to RomR could not be shown. Future experiments will go in this direction, to resolve the question of RomR activation. These recent findings indicate that RomX and RomY might play a crucial role in this process. To analyze the function of these proteins in detail, epistasis analysis with RomR, MglA, MglB and FrzZ will be conducted, as well a biochemical studies.

Importantly, direct interaction studies and phosphotransfer studies have to be performed, for final conclusions.

4 Material and Methods

4.1 Chemicals and equipment

Reagents, antibiotics, enzymes and kits which were used in this study are listed in table 2, including the respective supplier. Technical equipment and software to analyse the data is listed in table 2.

Table 2: Chemicals and kits

Reagents	**Supplier**
Pure chemicals	Roth (Karlsruhe), Merck (Darmstadt), Sigma-Aldrich (Taufkirchen)
Media components, agar	Roth (Karlsruhe), Merck (Darmstadt), Difco (Heidelberg), Invitrogen (Darmstadt)
SDS-PAGE size standards	MBI Fermentas (St. Leon-Rot)
Agarose gel electrophoresis size standards	Bioline (Luckenwalde)
Oligonucleotides	Thermo Scientific (Dreieich)
Rabbit antisera	Eurogentec (Belgium)
Anti-GFP monoclonal antibody	Roche (Mannheim)
Rabbit anti-mouse IgG	Roche (Mannheim)
SuperSignal chemiluminescence detection	Pierce/Thermo Scientific (Dreieich)
Antibiotics	
Kanamycin sulfate	Roth (Karlsruhe)
Chloramphenicol	Roth (Karlsruhe)
Ampicillin sodiumsulfate	Roth (Karlsruhe)
Gentamycin sulfate	Roth (Karlsruhe)
Oxytetracycline dehydrate	Roth (Karlsruhe)
Tetracycline hydrochloride	Roth (Karlsruhe)
Enzymes	
PfuUltra™II DNA-Polymerase	Stratagene (Amsterdam)
Restriction endonucleases	New England Biolabs (Frankfurt a. M.)
Antarctic phosphatase	New England Biolabs (Frankfurt a. M.)
T4-DNA-Ligase	MBI Fermentas (St. Leon-Rot)
5 PRIME MasterMix	5 PRIME GmbH (Hamburg)
Kits	
DNA purification (chromosomal DNA)	Epicentre Biotechnologies (Wisconsin,USA)
DNA purification (Plasmid DNA), PCR purification, Gel purification	Zymo Research (Freiburg), Qiagen (Hilden)

Table 3: Equipment and software

Application	Device	Manufacturer
Cell disruption	Branson sonifier	Heinemann (Schwäbisch Gmünd)
Centrifugation	RC 5B plus, Ultra Pro 80, Multifuge 1 S-R, Biofuge frasco, Biofuge pico	Sorvall/Thermo Scientific (Dreieich), Heraeus/Thermo Scientific (Dreieich),
PCR	MasteCycler personal MasteCycler epgradient	Eppendorf (Hamburg)
Electroporation	GenePulser Xcell	Bio-Rad (Munchen)
Protein electrophoresis	Mini-PROTEAN® 3 cell	Bio-Rad (Munchen)
Western blotting	TE77 semi-dry transfer unit	Amersham Biosciences (Munchen)
Chemiluminescence detection	Fuji Photo Film FPM 100A Luminescent image analyzer LAS-4000	Fujifilm (Düsseldorf)
Immunofluorescence microscopy	Diagnostic microscope slides 12 well	Thermo Scientific (Dreieich)
Imaging	Leica DM6000B and DM IRE2 light microscopes MZ75 stereomicroscope Nikon Eclipse TE 2000-E light microscope	Leica Microsystems (Wetzlar) Nikon (Düsseldorf)
Determination of optical densities	Ultrospec 2100 pro spectrophotometer	Amersham Biosciences (Munchen)
Determination of nucleic acids absorption	Nanodrop ND-1000 UV-Vis spectrophotometer	Nanodrop (Wilmington)
DNA illumination and documentation	UVT 20 LE UV table	Herolac (Wiesloch)
Fluorescence microscopy data analysis	Metamorph® v 7.5 Image-Pro® 6.2	Molecular Devices (Union city, CA) MediaCybernetics (Bethesda, MD)
Checking sequences, sequence alignments	Vector NTI advance software, suite 11	Invitrogen (Darmstadt)
Stereomicroscopy	IM50	Leica Microsystems (Wetzlar)

4.2 Media

E. coli cells were cultivated in LB media or on LB-agar plates and *M. xanthus* cells were cultivated in 1% CTT media or on CTT agar plates. Composition of media is described in table 4.

Table 4: Media

Medium	**Composition**
E. coli	
Luria-Bertani (LB)	1% (w/v) tryptone, 0.5% (w/v) yeast extract, 1% (w/v) NaCl
LB agar plates	LB medium, 1% (w/v) agar
M. xanthus	
1% CTT	1% (w/v) BactoTM casitone, 10 mM Tris-HCl pH 8.0, 1 mM potassium phosphate buffer pH 7.6, 8 mM MgSO4
1% CTT agar plates	1% CTT medium, 1.5% agar
CTT soft agar	1% CTT medium, 0.5% agar
Motility assays	
A-motility plates (Hodgkin and Kaiser, 1977)	0.5% CTT, 1.5% agar
S-motility plates (Hodgkin and Kaiser, 1977)	0.5% CTT, 0.5% agar
Microscopy	
A50 microscopy agar	10 mM MOPS pH 7.2, 10 mM CaCl2, 10 mM MgCl2, 50 mM NaCl, 1.5% or 0.7% (w/v) agar

For selection antibiotics and Galactose have been added if needed (Table 5), for protein induction IPTG was added and for selection Xgal was added.

Table 5: Additives

Additive	**Stock solution (dissolved in)**	**Final concentration**
E. coli		
Ampicillin sodium sulfate	100 mg/ml in H_2O	100 µg/ml
Kanamycin sulfate	50 mg/ml in H_2O	50 µg/ml

Tetracyclin	15 mg/ml in 99.99% ethanol	15 µg/ml
IPTG	1 M in H_2O	0.5 mM
Xgal	20 mg/ml in DMF	40 µg/ml
M. xanthus		
Kanamycin sulfate	50 mg/ml in H_2O	50 µg/ml
Oxytetracycline	1 mg/ml in 99.99% methanol	10 µg/ml
Galactose	30 % in H2O	2%

4.3 Strains of *M. xanthus* and *E. coli*

Table 6: *E. coli* strains

Strain	**Genotype**	**Reference**
Top10	F- *mcrA Δ*(*mrr-hsdRMS-mcrBC*), *80lacZΔM15ΔlacX74, deoR*, *recA1*, *arsD139 Δ*(*ara-leu*)*7697*, *galU*, *galK*, *rpsL* (Str^R) *endA1*, *nupG*	Invitrogen (Karlsruhe)
Rosetta 2(DE3)	F^- *ompT hsdS*$_B$(r_B-m_B) *gal dcm*(DE3) pRARE2(Cm^R)	Novagen/Merck (Darmstadt)
BTH101	F-, cya-99, araD139, galE15, galK16, rpsL1 (Str^r), hsdR2, mcrA1, mcrB1	Euromedex (Strasbourg/France)

Table 7: *M. xanthus* strains

Strain	**Genotype**	**Reference**
DK1622	Wild type	(Kaiser 1979)
DK1300	*ΔsglG*	(Hodgkin and Kaiser 1979)
DK1217	*ΔaglB*	(Hodgkin and Kaiser 1979)
DK6204	*ΔmglBA*	(Hartzell and Kaiser 1991b)
MxH2265	*ΔaglZ*	(Yang et al. 2004)
SA3300	*ΔromR*	(Leonardy PhD thesis,

		2009)
SA5923	*ΔaglQ*	(Edina Hot)
SA3387	*ΔmglB*	(Leonardy et al. 2010)
SA4420	*ΔmglA*	(Leonardy et al. 2010)
SA3388	*ΔmglB/mglB-yfp* (pSL69)	(Leonardy et al. 2010)
SA3903	*ΔromR/ romR369-420-gfp* (pDK3)	(Keilberg diploma thesis, 2009)
SA3904	*ΔromR/ -romR116-368-gfp* (pDK4)	(Keilberg diploma thesis, 2009)
SA3905	*ΔromR/ romR332-420-gfp* (pDK5)	(Keilberg diploma thesis, 2009)
SA3906	*ΔromR/ romR116-420-gfp* (pDK6)	(Keilberg diploma thesis, 2009)
SA3916	*ΔromR/ romR-gfp* (pSH1208)	(Keilberg diploma thesis, 2009)
SA3918	Δ*agmK*	this study
SA3919	Δ*agmX*	this study
SA3921	Δ*agmO*	this study
SA3968	Δ*agmU*	this study
SA3969	Δ*aglT*	this study
SA3922	Δ*MXAN_2539*	this study
SA3923	Δ*MXAN_2540*	this study
SA3924	Δ*MXAN_2541*	this study
SA3926	Δ*agmK*Δ*romR*	this study
SA3927	Δ*agmX*Δ*romR*	this study
SA3928	Δ*agmO*Δ*romR*	this study
SA3939	Δ*romR*Δ*aglZ*	this study
SA3932	Δ*romR*Δ*agmU*	this study
SA3933	Δ*romR*Δ*aglT*	this study
SA3934	Δ*romR*Δ*aglQ*	this study
SA3929	Δ*MXAN_2539*Δ*romR*	this study

SA3930	Δ*MXAN_2540*Δ*romR*	this study
SA3931	Δ*MXAN_2541*Δ*romR*	this study
SA3935	Δ*agmO/ pilA-agmO* (pDK110)	this study
SA5911	Δ*MXAN2539/pilA- 2539* (pDK111)	this study
SA5912	Δ*MXAN2540/pilA-2540* (pDK112)	this study
SA3938	Δ*MXAN2541/pilA-2541* (pDK113)	this study
SA5358	Δ*romR*Δ*aglZ /romR-gfp* (pSH1208)	this study
SA5359	Δ*romR*Δ*aglZ/romR369-420-gfp* (pDK3)	this study
SA5360	Δ*romR*Δ*aglZ/ romR332-420-gfp* (pDK5*)*	this study
SA5361	Δ*romR*Δ*aglZ/ romR116-368-gfp* (pDK4*)*	this study
SA5362	Δ*romR*Δ*aglZ/ romR116-420-gfp* (pDK6)	this study
SA5363	Δ*romR*Δ*MXAN_2539/romR-gfp* (pSH1208)	this study
SA5364	Δ*romR*Δ*MXAN_2539/ romR116-420-gfp* (pDK6)	this study
SA5365	Δ*romR*Δ*MXAN_2539/romR332-420-gfp* (pDK5*)*	this study
SA5366	Δ*romR*Δ*MXAN_2539/ romR116-368-gfp* (pDK4*)*	this study
SA5367	Δ*romR*Δ*agmO/romR-gfp* (pSH1208)	this study
SA5368	Δ*romR*Δ*agmO/ romR116-420-gfp* (pDK6)	this study
SA5369	Δ*romR*Δ*agmO/romR332-420-gfp* (pDK5*)*	this study
SA5370	Δ*romR*Δ*agmO/ romR369-420-gfp* (pDK3)	this study
SA5371	Δ*romR*Δ*agmO/ romR116-368-gfp* (pDK4*)*	this study

SA5372	Δ*romR*Δ*agmK/romR-gfp* (pSH1208)	this study
SA5373	Δ*romR*Δ*agmK/ romR116-420-gfp* (pDK6)	this study
SA5374	Δ*romR*Δ*agmK/romR332-420-gfp* (pDK5*)*	this study
SA5375	Δ*romR*Δ*agmK/ romR369-420-gfp* (pDK3)	this study
SA5376	Δ*romR*Δ*agmK/ romR116-368-gfp* (pDK4*)*	this study
SA5377	Δ*romR*Δ*agmX/romR-gfp* (pSH1208)	this study
SA5378	Δ*romR*Δ*agmX/ romR116-420-gfp* (pDK6)	this study
SA5379	Δ*romR*Δ*agmX/romR332-420-gfp* (pDK5*)*	this study
SA5380	Δ*romR*Δ*agmX/ romR369-420-gfp* (pDK3)	this study
SA5381	Δ*romR*Δ*agmX/ romR116-368-gfp* (pDK4*)*	this study
SA5382	Δ*romR*Δ*MXAN_2540/romR-gfp* (pSH1208)	this study
SA5383	Δ*romR*Δ*MXAN_2540/ romR116-420-gfp* (pDK6)	this study
SA5384	Δ*romR*Δ*MXAN_2540/romR332-420-gfp* (pDK5*)*	this study
SA5385	Δ*romR*Δ*MXAN_2540 romR369-420-gfp* (pDK3)	this study
SA5386	Δ*romR*Δ*MXAN_2540/ romR116-368-gfp* (pDK4*)*	this study
SA5387	Δ*romR*Δ*MXAN_2541/romR-gfp* (pSH1208)	this study
SA5388	Δ*romR*Δ*MXAN_2541/ romR116-420-gfp* (pDK6)	this study
SA5389	Δ*romR*Δ*MXAN_2541/romR332-420-gfp* (pDK5*)*	this study
SA5390	Δ*romR*Δ*MXAN_2541/ romR369-420-gfp* (pDK3)	this study
SA5391	Δ*romR*Δ*MXAN_2541/ romR116-*	this study

	368-gfp (pDK4*)*	
SA5939	Δ*romR*Δ*agmU/romR-gfp* (pSH1208)	this study
SA5935	Δ*romR*Δ*agmU/romR116-420-gfp* (pDK6)	this study
SA5931	Δ*romR*Δ*agmU/romR116-368-gfp* (pDK4*)*	this study
SA5930	Δ*romR*Δ*agmU/ romR369-420-gfp* (pDK3)	this study
SA5927	Δ*romR*Δ*agmU/romR332-420-gfp* (pDK5*)*	this study
SA5942	Δ*romR*Δ*aglT/romR-gfp* (pSH1208)	this study
SA5928	Δ*romR*Δ*aglT/ romR116-368-gfp* (pDK4*)*	this study
SA5929	Δ*romR*Δ*aglT/romR116-420-gfp* (pDK6)	this study
SA5925	Δ*romR*Δ*aglT/romR332-420-gfp* (pDK5*)*	this study
SA5933	Δ*romR*Δ*aglT/ romR369-420-gfp* (pDK3)	this study
SA5946	Δ*romR*Δ*aglQ/romR-gfp* (pSH1208)	this study
SA5945	Δ*romR*Δ*aglQ/romR116-420-gfp* (pDK6)	this study
SA5937	Δ*romR*Δ*aglQ/ romR116-368-gfp* (pDK4*)*	this study
SA5934	Δ*romR*Δ*aglQ/romR332-420-gfp* (pDK5*)*	this study
SA5938	Δ*romR*Δ*aglQ/ romR369-420-gfp* (pDK3)	this study
SA3946	*ΔmglB/ mglB*^{G68R}*-yfp* (pDK30)	this study
SA3947	*ΔmglB/ mglB*^{A64R}*-yfp* (pDK29)	this study
SA3950	*ΔmglB/ mglB*$^{A64/G68R}$*-yfp* (pDK31)	this study
SA3951	*ΔmglB/mglB*$^{T13/K14/K120/D123/K127A}$ *–yfp* (pDK32)	this study
SA3948	*ΔmglBA /mglB*^{G68R}*-yfp* (pDK30)	this study

SA3949	*ΔmglBA/ mglB*^{A64R}*-yfp* (pDK29)	this study
SA3952	*ΔmglBA/ mglB*$^{A64/G68R}$*-yfp* (pDK31)	this study
SA3953	*ΔmglBA/mglB*$^{T13/K14/K120/D123/K127A}$ – *yfp* (pDK32)	this study
SA3954	*mglB*$^{A64/G68R}$	this study
SA3955	*mglB*$^{T13/K14/K120/D123/K127A}$	this study
SA3956	*mglB*^{A64R}	this study
SA3957	*mglB*^{G68R}	this study
SA3958	*yfp-mglA* (pSL60)	this study
SA3959	*mglB*$^{T13/K14/K120/D123/K127A}$*/yfp-mglA* (pSL60)	this study
SA3960	*mglB*$^{A64/G68R}$*/yfp-mglA* (pSL60)	this study
SA3833	*mglA*^{Q82A}	This study
SA3995	*mglA*^{Q82A} Δ*romR*	This study
SA4440	Δ*mglA/ yfp-mglA* (pSL60)	(Leonardy et al. 2010)
SA3831	*ΔmglB*Δ*mglA/yfp-mglA*^{Q82A} (pTS10)	(Leonardy et al. 2010)
SA3385	Δ*mglB*Δ*mglA/ yfp-mglA* (pSL60)	(Leonardy et al. 2010)
SA3300	Δ*romR*	This study
SA3916	Δ*romR/ romR-gfp* (pGFy177)	This study
SA3980	Δ*romR/ romR*^{D53N}*-gfp* (pGFy178)	This study
SA3981	Δ*romR/ romR*^{D53E}*-gfp* (pGFy166)	This study
SA3903	Δ*romR/ romR*$^{369-420}$*-gfp* (pDK3)	This study
SA3904	Δ*romR/ romR*$^{116-368}$*-gfp* (pDK4)	This study
SA3905	Δ*romR/ romR*$^{332-420}$*-gfp* (pDK5)	This study
SA3906	Δ*romR/ romR*$^{116-420}$*-gfp* (pDK6)	This study
SA3937	Δ*romR/yfp-mglA*^{Q82A} (pTS10)	This study
SA3982	*mglA*^{Q82A},Δ*romR/romR*^{D53N}*-gfp* (pGFy178)	This study
SA3983	*mglA*^{Q82A},Δ*romR/romR*^{D53E}*-gfp* (pGFy166)	This study

SA3936	Δ*mglB*Δ*romR*	This study
SA3984	Δ*mglA*Δ*romR*	This study
SA3985	Δ*frzZ*	This study
SA3986	Δ*frzZ* Δ*romR*	This study
SA3987	Δ*frzZ*Δ*romR/romR*^{D53N}*-gfp* (pGFy178)	This study
SA3988	Δ*frzZ*,Δ*romR/romR*^{D53E}*-gfp* (pGFy166)	This study
SA3989	Δ*mglB*,Δ*romR/romR*^{D53N}*-gfp* (pGFy178)	This study
SA3990	Δ*mglB*,Δ*romR/romR*^{D53E}*-GFP* (pGFy166)	This study
SA3991	Δ*frzZ/ YFP-mglA*^{Q82A} (pTS10)	This study
SA3963	*mglB-mCherry*	This study
SA3971	Δ*mglA/mglB-mCherry*	This study
SA3966	Δ*romR/mglB-mCherry*	This study
SA3992	Δ*mglB*Δ*romR/romR-gfp* (pGFy177)	This study
SA3993	Δ*mglA*Δ*romR/yfp-mglA* (pSL60)	This study
SA3994	Δ*mglA*Δ*romR/romR-gfp* (pGFy177)	This study
SA3978	Δ*romR, mglB-mcherry/PpilA-romR-gfp* (pGFy177)	This study
SA3979	Δ*romR*Δ*mglA/mglB-mcherry/romR-gfp* (pGFy177)	This study
SA3829	*ΔmglA/yfp-mglA*^{Q82A} (pTS10)	(Leonardy et al. 2010)
SA3996	Δ*romR*Δ*mglA/yfp-mglA*^{Q82A} (pTS10)	This study
SA3997	Δ*romR*Δ*mglB*Δ*mglA/yfp-mglA*^{Q82A} (pTS10)	This study
SA3998	Δ*romR*Δ*mglB*Δ*mglA/yfp-mglA* (pSL60)	This study
SA5958	*ΔromY (MXAN5749)*	this study
SA5972	*ΔromX (MXAN3350)*	this study
SA5974	*ΔromX /romR-gfp* (pSH1208)	this study
SA5975	*ΔromY /romR-gfp* (pSH1208)	this study

SA5976	*ΔromX/mglB-yfp* (pSL69)	this study
SA5977	*ΔromY/mglB-yfp* (pSL69)	this study
SA5978	*ΔromX/yfp-mglA* (pSL60)	this study
SA5979	*ΔromY/yfp-mglA* (pSL60)	this study
SA5980	*ΔmglB/romX-yfp* (pDK96)	this study
SA5981	*ΔmglB/romY-yfp* (pDK97)	this study
SA5969	*ΔmglA/romY-yfp* (pDK97)	this study
SA5971	*ΔmglA/romX-yfp* (pDK96)	this study
SA5960	*ΔromR/romX-yfp* (pDK96)	this study
SA5961	*ΔromR/romY-yfp* (pDK97)	this study
SA5982	*ΔromX/romX-yfp* (pDK96)	this study
SA5983	*ΔromY/romY-yfp* (pDK97)	this study
SA5984	*ΔromX/pilA-romX* (pDK100)	this study
SA5985	*ΔromY/pilA-romY* (pDK101)	this study

4.3.1 Cultivation of *M. xanthus* and *E. coli*

E. coli cells were grown in LB or on plates containing LB supplemented with 1.5% agar at 37 °C with added antibiotics if appropriate (Sambrook and Russell 2001). Liquid cultures were incubated shaking with 220 rpm at 37 °C. DK1622 was used as WT *M. xanthus* strain throughout and all *M. xanthus* strains used are derivatives of DK1622. *M. xanthus* strains were grown at 32 °C in 1% CTT broth (Hodgkin and Kaiser 1977) or on CTT agar plates supplemented with 1.5% agar. Antibiotics were added when appropriate. Liquid cultures were incubated shaking with 220 rpm at 32 °C.

4.3.2 Storage of *M. xanthus* and *E. coli* strains

M. xanthus and *E. coli* strains were kept on plates for short time storage at 18°C and 4°C respectively. For long time storage strains were grown to an OD550 > 1, and after adding 50% Glycerol (*M.xanthus*: 80µl Glycerol + 980µl culture/ *E.coli*: 200µl Gylcerol + 800µl culture) the cells were quickly frozen in liquid nitrogen and then stored at -80°C.

4.4 Molecular biological methods

4.4.1 Primers and plasmids

Table 8: List of primers used in this study

Name	Sequence (5'-3')
M13 forward	CTGGCCGTCGTTTTAC
M13 revers	CAGGAAACAGCTATGAC
oMglA-EcoRI	ATCCGGAATTCATGTCCTTCATCAATTAC
oMglAstop-NotI	ATCGCGGCGGCCGCCTCAAGAAGGGTGGTTGA
oDromR-1	ATCGGTCTAGACATCGCGGAGGCGCTGCC
oDromR-2	GAGCTCCTCGCGGATGGTGAGCGAGTC
oDromR-3	ACCATCCGCGAGGAGCTCGAGCGGCTC
oDromR-4	ATCGGAAGCTTCTCGCGCACCGCGGCGGA
oMglAQ82Aforw	ACGGTGCCCGGTGCAGTCTTCTACGAC
oMglAQ82Arev	GTCGTAGAAGACTGCACCGGGCACCGT
omglB3	ATCCGGATCCGATGGGCACGCAACTGGTG
omglB4	ATCGGGAATTCCCTTGAGCGTGTCGAAGA
HisRomRPstI	ATCGGCTGCAGATGCCCAAGAATCTGCTGGTCGC
HisRomRrv	ATCGGAAGCTTTCAGTGCTGGGTCTCTCGGTCCTTGA
MalE-RomRfw	ATCGGGAATTCATGCCCAAGAATCTGCTGGTCGC
MalE-RomRrv	ATCGGAAGCTTTCAGTGCTGGGTCTCTCGGTCC
MglBfwsur	ATCGGAAGCTTGCGTGAAGCCCTCATAGGTGAGC
MglBrvmcherry	GCTCACCATCTCGCTGAAGAGGTTGTCGATATCG
MglBA-Rfw	GGTAACGTGCGCGCGATGGGTGGCCTGGCCAAGCTGA
MglBA-Rrv	GCCACCCATCGCGCGCACGTTACCGGCCGTCAGCG
MglBG-Rfw	GGTAACGTGGCCGCGATGGGTCGCCTGGCCAAGCTGA
MglBG-Rrv	GCGACCCATCGCGGCCACGTTACCGGCCGTCAGCG
MglBAG/Rfw	GGTAACGTGCGCGCGATGGGTCGCCTGGCCAAGCTGA
MglBAG/Rrv	GCGACCCATCGCGCGCACGTTACCGGCCGTCAGCG
MglB5mutfw1	TTCGCGGCGATCAACGCCGTT
MglB5mutrv1	GATCGCCGCGAACTCCTCTTC
MglB5mutfw2	AAGGCGGCCAGCGCGGAGCTCACGGCGATCTTCGAG
MglB5mutrv2	GATCGCCGTGAGCTCCGCGCTGGCCGCCTTGATGC
Mcherryfw	TTCAGCGAGATGGTGAGCAAGGGCGAGGAGGAT
Mcherryrv	CTTCCCGGGTTACTTGTACAGCTCGTCCATGCCG
MglAfw	TACAAGTAACCCGGGAAGCCATGTCCTTC
MglAsurrv	ATCGGGAATTCACGGGTGACGGGCGGCGGGG
FrzZA	ATCGGGAATTCAGCTGCCCGTGACGCCGACGAA

FrzZB	CAGCTCCTTGGCGCTGTCATCAATGACCAGTA
FrzZC	TTGATGACAGCGCCAAGGAGCTGATGCCCACC
FrzZD	ATCGGAAGCTTCCCTCTTCGACGCGGGGCTG
DA1	ATCGGTCTAGAATGAAGGCGCTGGTCGGC
DA2	ATCGGGATATCAGGCGCACGGGCGCTCGC
DA3	ATCGGTCTAGAATGGCCGCGGATGGGGGC
DA4	ATCGGGATATCGTGCTGGGTCTCTCGGTC
DA5	ATCGGTCTAGAATGTCCATCAGCATCGAGGA
oCrGFP-3	ATCGGGATATCATGGCCAAGGGCGAGGAG
oCrGFP-2	ATCGGAAGCTTTTACTTGTACAGCTCGTCCATGCC
agmXA	ATCGGAAGCTTAAGCGCAGCACCTGGTGG
agmXB	GATGGGCTCCGCGCGGCAGCTGTCGCA
agmXC	TGCCGCGCGGAGCCCATCGACTTCCCG
agmXD	ATCGGGAATTCAGATGCTCGTGGTCGACG
agmXE	GTGCACTCAGTGTCGGACGT
agmXF	TATTACCTCCTGGGCCGCAC
agmXG	AGACCCGCCCTTCAGGAAGA
agmXH	GAAGAGAACGACGCGCTGTC
agmKA	ATCGGAAGCTTGAGCGGTTGGGCGGCGTC
agmKB	CACGTGCGTCGGGTCGTACCAGGCGAA
agmKC	TACGACCCGACGCACGTGGAGGTACAG
agmKD	ATCGGGAATTCTTCGCGGCCTCGGTGGGA
agmKE	GTCTCCGACAACGGAATCCAATCAC
agmKF	TTTCCATTCCAAGGCCCGCC
agmKG	GTCATAGCTGGCGGACGCAT
agmKH	AGGGCAAGCCTACGGAGCTG
agmOA	ATCGGAAGCTTCACCCGGTCTTCCTGGGTGAT
agmOB	GGCGCAGAATCTGACCTCTACAAAGGG
agmOC	GAGGTCAGATTCTGCGCCGGCGCGCTC
agmOD	ATCGGGAATTCGGTCATTCAGCAGCCCGATGA
agmOE	AACCTTCCGCTGGACGCTCTTC
agmOF	CGTCCACGTACTGGAACATTCGCTC
agmOG	CAGGTCCGGATTGACGTCGT
agmOH	AGCGAGATTGGCAAGCCGTG
2539A	ATCGGAAGCTTGTTGTTGTTGGCCGCCGA
2539B	CGACTTGAACTGCGACTCGTCGGTGAG
2539C	GAGTCGCAGTTCAAGTCGACGGGGAGG
2539D	ATCGGGAATTCGCAGCGACACCTTGCCGT

2539E	GGTAGTCCTGGTCCCGAACGCAAA
2539F	AAGGTCTCAGCCAGCAGCGACA
2539G	GCGTCCAGCGGAAGGTTTAC
2539H	TGGAGTTGAGGAACGCCACC
2540A	ATCGGAAGCTTGCTGTCGGTCCGGGGCGC
2540B	GAAGGAGACGGCGAGGAGCACACGGAA
2540C	CTCCTCGCCGTCTCCTTCTTCTTCGGG
2540D	ATCGGGAATTCGCAGCTCGTGCGCCGCCA
2540E	GTGAAGAGCGTCCAGCGGAAGG
2540F	AGCAGCTCGTGCGCCGCCAT
2540G	TCTCCGGCCACGTCTTCCTCAA
2540H	TCAGCCAGCAGCGACACCTT
2541A	ATCGGAAGCTTGCGCGTGGGCTACGCCAT
2541B	GACTTTCCGGGCGACGCGGATGAGCCG
2541C	CGCGTCGCCCGGAAAGTCCAGTCCGCC
2541D	ATCGGGAATTCGCGCCCTGTCCTTCGGCGTGG
2541E	GCGCGACGCGTTCTACAGCAAGTA
2541F	CCGCGCCAATGACTCCCATA
2541G	TTCTTCCGTAACGGCAGCCG
2541H	ACGACAGGGTGATGAGGCTG
agmUA	ATCGGAAGCTTTCCCGGTACTTCTTGATCTCC
agmUB	CTCGTCATTAAGTGTCCGGGAATCTTCGG
agmUC	CGGACACTTAATGACGAGGAGCCGGAGGACTT
agmUD	ATCGGGAATTCGGTAGCGCTGGAGCACCTCC
agmUE	GTGCTCGGAGCACGCGCAGA
agmUF	CGAACTGGCCCATGCCCTTG
agmUG	GCCGCATCGTCGACCTGTACAA
agmUH	CGGTCGGCGAAGTGGTCATA
aglTA	ATCGGAAGCTTGCCGCGCGGCCTGGATGAGGAG
aglTB	CTCCCCGGGCAGGCGCATGGTGCGGGTGG
aglTC	ATGCGCCTGCCCGGGGAGCCGGAAGACGACCT
aglTD	ATCGGGAATTCGGGCTCCAACGTAAAGTGGGTA
aglTE	TGTCGGTGGACCTGGACTGGAAC
aglTF	TGCCCTCGACGCTGCCCATG
aglTG	ACCTGCGCCGCATCCTCCAG
aglTH	TTCGCGTTGACGACGACCTC
agmOfw	ATCGGTCTAGAGTGCCCCATCCCCCCTTTGT
agmOrv	ATCGGAAGCTTTCAATCCGGGATGAGCGCGC

2539fw	ATCGGTCTAGATTGAACCGCCCCAAGTTGCT
2539rv	ATCGGAAGCTTTCATTCCGAGTCCCTCCCCGT
2540fw	ATCGGTCTAGAATGAAGCGTTTCTTCCGTGTGC
2540rv	ATCGGAAGCTTTCATGACTCGGACCCGAAGAA
2541fw	ATCGGTCTAGAATGCGCTCCTTCCGGCTCAT
2541rv	ATCGGAAGCTTTTACATCGCCTCGGCGGACT
romXA	ATCGGAAGCTTAGATCGCCCAGGACTCCGCC
romXB	ATCGGTCTAGACATCGCCTTGACCTTTTCCTCGT
romXC	ATCGGTCTAGAAAGGCGCATGTGAAGTCGAAGATC
romXD	ATCGGGAATTCCAGCCGGTGGTGTCCTTGTCG
romXE	GAGGCTCCGTCCGAGCCGGG
romXF	CTTCTGGAGCGCCACCAGCGC
romYA	ATCGGAAGCTTCCGGAGACGAAGTCCGCGGC
romYB	ATCGGTCTAGAGGTGACGGCTTTTTCGAAGGTTTTC
romYC	ATCGGTCTAGAAGTTACCTGGCGGGTGAGGGCG
romYD	ATCGGGAATTCCCACCGTCCGGTGCGGCAGCA
romYE	GGGCGGATGAGCGCCTTGCCCAGC
romYF	TCTCGCGCGCCTCCGCGCGG
romXfw	ATCGGTCTAGAATGACGGACGAGGAAAAGGTCAAGG
romXyfprv	ATCGGGGATCCCCAGATCTTCGACTTCACATGCGC
romYfw	ATCGGTCTAGAATGACGAAAACCTTCGAAAAAGCCG
romYyfprv	ATCGGGGATCCCTGCTCGCCCTCACCCGCCAGGTAA
romXrvstop	ATCGGAAGCTTTCACCAGATCTTCGACTTCACATGCGC
romYrvstop	ATCGGAAGCTTTCACTGCTCGCCCTCACCCGCCAGGTAA
HisRomRfw	ATCGGGGATCCCATGCCCAAGAATCTGCTGGTCGC
HisRomRrv	ATCGGAAGCTTTCAGTGCTGGGTCTCTCGGTCCTTGA
his-frzEfw	ATCGGGGATCCCATGGACACCGAGGCTCTCAAG
HisfrzEdcheYrv	ATCGGAAGCTTTCAGCGCTTGGCGGCGGGGGCCT
HisFrzZfw	ATCGGGGATCCCATGTCGCGCGTACTGGTCATTGA
HisFrzZrv	ATCGGAAGCTTCTACTCGTTACCGGTGGGCATCAGC
HisFrzCDfw	ATCGGGGATCCCATGTCCCTGGACACCCCCAACG
HisFrzCDrv	ATCGGAAGCTTCTAGTCGGCCTTGAACCGCTTGA
HisFrzAfw	ATCGGGGATCCCATGGCTCCGGACCGCGCCTTG
HisFrzArv	ATCGGAAGCTTTCACCGCGCCACCGCCCGCT
His-romXfw	ATCGGGGATCCCATGACGGACGAGGAAAAGGTCAAGG
His-romXrv	ATCGGAAGCTTTCACCAGATCTTCGACTTCACATGCGC
His-romYfw	ATCGGGGATCCCATGACGAAAACCTTCGAAAAAGCCG
His-romYrv	ATCGGAAGCTTTCACTGCTCGCCCTCACCCGCCAGGTAA

FrzZD52rv	GTTGACGTTCATGAGGATGAGCGA
FrzZD52fw	CATCCTCATGAACGTCAACATGC
FrzZD220rv	CATGCGCACGTTCAGCAGCAC
FrzZD220fw	GCTGCTGAACGTGCGCATGC
MalERecFrzZ1fw	ATCGGGAATTCTCGCGCGTACTGGTCATTGATGA
MalERecFrzZ1rv	ATCGGAAGCTTTCAGGCGGGGGGGCCAATGAGAC
MalERecFrzZ2fw	ATCGGGAATTCCCGCGCATCCTCATCGTGGA
MalERecFrzZ2rv	ATCGGAAGCTTTCAGTTACCGGTGGGCATCAGCTCC
MalERecRomRfw	ATCGGGAATTCATGCCCAAGAATCTGCTGGTCGC
MalERecRomRrv	ATCGGAAGCTTTCAGGACTTCTGGCCGACCAGCG
MalE-RomRfw	ATCGGGAATTCATGCCCAAGAATCTGCTGGTCGC
MalE-RomRrv	ATCGGAAGCTTTCAGTGCTGGGTCTCTCGGTCC
MalEOutputfw	ATCGGGAATTCGCGCTGGTCGGCCAGAAGTC
BACTHRomRfw	ATCGGTCTAGAGATGCCCAAGAATCTGCTGGTCGC
BACTHRomRrv	ATCGGGAATTCGAGTGCTGGGTCTCTCGGTCCTTGA
BACTHMglAfw	ATCGGTCTAGAGATGTCCTTCATCAATTACTCATCC
BACTHMglArv	ATCGGGAATTCGAACCACCCTTCTTGAGCTCGG
BACTHMglBfw	ATCGGTCTAGAGATGGGCACGCAACTGGTGATG
BACTHMglBrv	ATCGGGAATTCGACTCGCTGAAGAGGTTGTCGATATCG
BACTHFrzZfw	ATCGGTCTAGAGATGTCGCGCGTACTGGTCATTGA
BACTHFrzZrv	ATCGGGAATTCGACTCGTTACCGGTGGGCATCAGCT
BACTHFrzEfw	ATCGGTCTAGAGATGGACACCGAGGCTCTCAAGAAA
BACTHFrzErv	ATCGGGAATTCGAGGTCAGCCGGTCGATGGCCT
BACTHRomRrvstop	ATCGGGAATTCGATCAGTGCTGGGTCTCTCGGTCCTTGA
BACTHMglArvstop	ATCGGGAATTCGATCAACCACCCTTCTTGAGCTCGG
BACTHMglBrvstop	ATCGGGAATTCGATTACTCGCTGAAGAGGTTGTCGATATCG
BACTHFrzZrvstop	ATCGGGAATTCGACTACTCGTTACCGGTGGGCATCAGCT
BACTHFrzErvstop	ATCGGGAATTCGATCAGGTCAGCCGGTCGATGGCCT
BACTH3350fw	ATCGGTCTAGAGATGACGGACGAGGAAAAGGTCAAGG
BACTH3350rv	ATCGGGAATTCGACCAGATCTTCGACTTCACATGCGC
BACTH5749fw	ATCGGTCTAGAGATGACGAAAACCTTCGAAAAAGCCG
BACTH5749rv	ATCGGGAATTCGACTGCTCGCCCTCACCCGCCAGGTAA

Table 9: List of plasmids used in this study

Plasmid	Description	Source
pGFy177	*PpilA-romR-GFP* in pSWU30	(Leonardy et al. 2007)
pGFy178	*PpilA-romR*^{D53N}*-gfp* (pSWU30)	(Leonardy et al. 2007)

pGFy166	*PpilA-romR*^{D53E}*-gfp* (pSWU30)	(Leonardy et al. 2007)
pSH1202	*PpilA-romR*$^{116-420}$*-gfp* (pSWU30)	(Leonardy et al. 2007)
pDK3	*PpilA-romR*$^{369-420}$*-gfp* (pSWU30)	(Keilberg/diploma thesis, 2009)
pDK4	*PpilA-romR*$^{116-368}$*-gfp* (pSWU30)	(Keilberg/diploma thesis, 2009)
pDK5	*PpilA-romR*$^{332-420}$*-gfp* (pSWU30)	(Keilberg/diploma thesis, 2009)
pDK6	*PpilA-romR*$^{116-420}$*-gfp* (pSWU30)	(Keilberg/diploma thesis, 2009)
pSL60	*PpilA-yfp-mglA* (pSW105)	(Leonardy et al. 2010)
pTS10	*PpilA-yfp-mglA*^{Q82A} (pSW105)	(Miertzschke et al. 2011)
pBJ114	Vector for generation of in-frame deletions and for gene replacements at native site	(Julien et al. 2000)
pSL37	pBJ114 with in-frame deletion cassette for *romR*	(Leonardy PhD thesis, 2009)
pFD1	pBJ114 with in-frame deletion cassette for *frzZ*	(Drescher/Bachelor thesis 2012)
pTS08	pBJ114 for construction of *mglA*^{Q82A} at native site	(Schöner/Bachelor thesis 2010)
pGEX4T	Vector for GST overexpression	GE-Healthcare
pSL54	For GST-MglA overexpression in pGEX4T	(Leonardy PhD thesis, 2009)
pMal-c2	Vector for MalE overexpression	New England Biolabs
pET45	For overexpression of His_6-tagged protein	Novagen/Merck (Darmstadt)
pES1	For His_6-MglB overexpression in pET45	(Sperling/Bachelor thesis 2010)
MglA-His_6	For MglA-His_6 overexpression	(Zhang et al. 2010)
pBlueskript II SK-	cloning vector	Fermentas
	in-frame deletion/endogenous mutation	
pDK20	pBJ114 with in-frame deletion cassette for *agmK*	This study
pDK21	pBJ114 with in-frame deletion cassette for *2541*	This study
pDK22	pBJ114 with in-frame deletion cassette for *2540*	This study
pDK23	pBJ114 with in-frame deletion cassette for *agmO*	This study
pDK24	pBJ114 with in-frame deletion cassette for *agmX*	This study
pDK25	pBJ114 with in-frame deletion cassette for *2539*	This study

pDK108	pBJ114 with in-frame deletion cassette for *aglT*	This study
pDK109	pBJ114 with in-frame deletion cassette for *agmU*	This study
pDK94	pBJ114 with in-frame deletion cassette for *romX (MXAN3350)*	This study
pDK95	pBJ114 with in-frame deletion cassette for *romY (MXAN5749)*	This study
pDK78	pBJ114 for integration of *mglB-mCherry* at native site	This study
pDK79	pBJ114 for integration of *mglB-mCherry* at native site and deletion cassette for *mglA*	This study
pDK33	pBJ114 for construction of $mglB^{A64R}$ at native site	This study
pDK34	pBJ114 for construction of $mglB^{G68R}$ at native site	This study
pDK35	pBJ114 for construction of $mglB^{A64/G68R}$ at native site	This study
pDK36	pBJ114 for construction of $mglB^{T13/K14/K120/D123/K127A}$ at native site	This study
	attachment site integration	
pDK110	*PpilA-agmO* (pSW105)	This study
pDK111	*PpilA-MXAN2539* (pSW105)	This study
pDK112	*PpilA-MXAN2540* (pSW105)	This study
pDK113	*PpilA-MXAN2541* (pSW105)	This study
pDK29	*PpilA-*$mglB^{A64R}$ *-yfp*(pSW105)	This study
pDK30	*PpilA-*$mglB^{G68R}$ *-yfp* (pSW105)	This study
pDK31	*PpilA-*$mglB^{A64/G68R}$ *-yfp* (pSW105)	This study
pDK32	*PpilA-*$mglB^{T13/K14/K120/D123/K127A}$ *-yfp* (pSW105)	This study
pDK96	*PpilA-romX-yfp (MXAN3350)* (pSW105)	This study
pDK97	*PpilA-romY-yfp (MXAN5749)* (pSW105)	This study
pDK100	*PpilA-romX (MXAN3350)* (pSW105)	This study
pDK101	*PpilA-romY (MXAN5749)* (pSW105)	This study
	Overexpression	
pDK47	For His_6-RomR overexpression in pET45	This study
pDK43	For His_6-FrzZ overexpression in pET45	This study
pDK44	For His_6-$FrzE^{CheA}$ overexpression in pET45	This study
pDK45	For His_6-FrzA overexpression in pET45	This study
pDK46	For His_6-FrzCD overexpression in pET45	This study
pDK48	For His_6-$RomR^{D53N}$ overexpression in pET45	This study
pDK49	For His_6-$RomR^{D53E}$ overexpression in pET45	This study
pDK50	For His_6-$FrzZ^{D52/220N}$ overexpression in pET45	This study
pDK83	For MalE-RomR overexpression in pMal-c2	This study
pDK84	For MalE-$RomR^{D53N}$ overexpression in pMal-c2	This study

pDK85	For MalE-RomR^{D53E} overexpression in pMal-c2	This study
pDK86	For MalE-RomR$^{116-420}$ overexpression in pMal-c2	This study
pDK87	For MalE-FrzZ^{RecD220N} overexpression in pMal-c2	This study
pDK88	For MalR-RomR^{Rec} overexpression in pMal-c2	This study
pDK89	For MalE-FrzZ^{RecD220} overexpression in pMal-c2	This study
pDK90	For MalE-FrzZ^{RecD52N} overexpression in pMal-c2	This study
pDK92	For MalE-FrzZ ^{RecD52} overexpression in pMal-c2	This study
pDK98	For His_6-RomY(MXAN5749) overexpression in pET45	This study
pDK99	For His_6-RomX (MXAN3350) overexpression in pET45	This study
	BACTH	
pDK51	*romR*^{D53E} (pKNT25) N-terminal fusion to T25 fragment	This study
pDK52	*romR*^{D53N}(pKNT25) N-terminal fusion to T25 fragment	This study
pDK53	*frzZ* (pKNT25) N-terminal fusion to T25 fragment	This study
pDK54	*frzE* (pKNT25) N-terminal fusion to T25 fragment	This study
pDK69	*frzZ* (pKNT25) N-terminal fusion to T25 fragment	This study
pDK70	*mglA* (pKNT25) N-terminal fusion to T25 fragment	This study
pDK71	*mglB* (pKNT25) N-terminal fusion to T25 fragment	This study
pDK55	*mglB*(pKT25) C-terminal fusion to T25 fragment	This study
pDK56	*mglA*(pKT25) C-terminal fusion to T25 fragment	This study
pDK57	*mglA*^{G21V} (pKT25) C-terminal fusion to T25 fragment	This study
pDK58	*frzE* (pKT25) C-terminal fusion to T25 fragment	This study
pDK59	*romR*^{D53N}(put18C) C-terminal fusion to T18 fragment	This study
pDK60	*romR*^{D53E}(put18C) C-terminal fusion to T18 fragment	This study
pDK61	*frzZ*(put18C) C-terminal fusion to T18 fragment	This study
pDK62	*frzE*(put18C) C-terminal fusion to T18 fragment	This study
pDK63	*romR* (put18) N-terminal fusion to T18 fragment	This study
pDK64	*romR*^{D53N} (put18) N-terminal fusion to T18 fragment	This study
pDK65	*frzZ* (put18) N-terminal fusion to T18 fragment	This study
pDK66	*frzE* (put18) N-terminal fusion to T18 fragment	This study
pDK72	*romR* (put18C) C-terminal fusion to T18 fragment	This study
pDK73	*mglA*^{Q82A}(put18C) C-terminal fusion to T18 fragment	This study
pDK74	*mglB* (put18C) C-terminal fusion to T18 fragment	This study
pDK75	*mglA* (put18C) C-terminal fusion to T18 fragment	This study
pDK76	*mglA* (put18) N-terminal fusion to T18 fragment	This study
pDK77	*mglB* (put18) N-terminal fusion to T18 fragment	This study
pDK106	*romY* (pKNT25) N-terminal fusion to T25 fragment	This study

pDK107	*romX* (put18C) C-terminal fusion to T18 fragment	This study

4.4.2 Plasmid construction

Genomic DNA of *M. xanthus* DK1622 was used as a template for chromosomal regions, while Plasmid DNA containing the *yfp*, *gfp* or *mcherry* was used, to amplify the gene for fluorescence fusions. Resulting PCR fragments were cloned into the described vectors, and transformed into *E. coli* Top10 cells. After sequencing the Plasmids were transformed into *M. xanthus* cells, *E. coli Rosetta 2* cells (for overexpression) or into *E. coli BTH101* (for BACTH-system).

Plasmids for construction of in-frame deletion mutants of *M. xanthus DK1622:*

The construction of in frame deletion mutants is explained in detail in 4.5.3. In this study the following plasmids have been generated for gene deletion in *M. xanthus DK1622*: pDK20 (*agmK*), pDK21(*MXAN2541*), pDK22(*MXAN2540*), pDK23(*agmO*), pDK24 (*agmX*), pDK25(*MXAN2539*), pDK108(*aglT*), pDK109(*agmU*), pDK94(*romX*), pDK95(*romY*). Briefly, plasmids have been generated fusing the upstream region (amplified by Primer A and Primer B) and the downstream region (amplified by Primer C and Primer D) of the gene of interest leaving only 30 bp on each end of the gene. Primers used are listed in 4.5.1. and were named as the gene of interest, fused to the A, B. C or D, respectively. The fusion construct (fragment fused by PCR using Primer A and Primer D) was cloned into pBJ114 using the restriction sites *EcoR*I and *Hind*III.

Plasmids for mutations at the native site of *M. xanthus DK1622:*

1. Fusion of fluorescent proteins at the native site

pDK78: Plasmid to generate *mglB-mcherry* fusion expressed from the native site. To construct the plasmid pDK78, three PCR fragments were amplified, the AB fragment, containing the upstream region of *mglB* and *mglB* (MglBfwsur/ MglBrvmcherry), the CD fragment, containing *mcherry* (Mcherryfw/Mcherryrv) and the EF fragment containing the downstream region of *mglB* (MglAfw/ MglAsurrv) using chromosomal DNA of *M. xanthus* as a template and a plasmid containing *mcherry,* respectively. The primer MglBrvmcherry contains a homologous region to Mcherryfw and the primer Mcherryrv contains a homologous region to MglAfw. Therefore overlap PCRs could be performed to create a fragment AF. This fragment was cloned into pBJ114 using the restriction sites *Hind*III and *EcoR*I.

pDK79: The plasmid pDK79 was constructed analogous to pDK78, using chromosomal DNA of *ΔmglA* instead of WT DNA as a template for the EF fragment as a template.

2. Introducing mutations into the gene of interest

pDK33: pDK33 contains *mglB*^{A64R} and 489 bp upstream and 442 bp downstream of *mglB* cloned into pBJ114 (*Hind*III, *EcoR*I). For pDK33 MglBsurrfw and MglBAG/Rrv were used to create the first PCR product and MglBAG/Rfw and MglBsurrrv to create the second PCR product. A third PCR was done to fuse the two products together. For this MglBAG/Rrv and MglBAG/Rfw have a homologous region. Then this product was cloned in pBJ114 (*Hind*III, *EcoR*I). pDK36 contains *mglB*^{A5} and 489 bp upstream and 442 bp downstream of *mglB* cloned into pBJ114 (*Hind*III, *EcoR*I). For pDK36 first three PCR products were amplified by using MglBsurrfw / MglB5mutrv1, MglB5mutfw1/ MglB5mutrv2 and MglB5mutfw2/ MglBsurrrv. Another PCR amplified a product to fuse the three products together. For this the primers containing the mutations have homologous regions. Then this product was cloned in pBJ114 (*Hind*III, EcoRI). pDK36 contains mutations in *mglB* to create the substitutions T13/K14/K120/D123/K127A in MglB. pDK34, pDK35 were generated analogous using the primers, using MglBG-Rfw/MglBG-Rrv to introduce the mutation *G68R* and using MglBAG/Rfw/ MglBAG/Rrv introducing the mutation *A64/G68*R into *mglB*.

<u>Plasmids for integration at Mx8 attachment site of *M. xanthus DK1622 :*</u>

To integrate a plasmid into the Mx8 attachment site, the plasmid pSW105 was used, containing a site for integration, a Km resistence cassette, the PpilA promoter and a multiple cloning site. For all the plasmids, pDK110, pDK111, pDK112, pDK113, pDK29, pDK30, pDK31, pDK32, pDK96, pDK97, pDK100, pDK101, the gene of interest was amplified from chromosomal DNA, and cloned into pSW105.

pDK110,pDK111, pDK112 and pDK113 were generated by first amplifying the gene *agmO*, *MXAN2539*, *MXAN2540* and *MXAN2541* respectively, using the following primer pairs: agmOfw/agmOrv; 2539fw/2539rv; 2540fw/2540rv;2541fw/2541rv. Then the PCR fragment was cloned into pSW105 using XbaI and HindIII restriction sites.

pDK29 was constructed by first amplifying *yfp* from pSL69 (Leonardy et al. 2010) using oYFP-9 and YFP. This PCR product was cloned into pSK-Bluescript (*BamH*I/*Hind*III). *mglB* was amplified with primers containing desired substitutions. For pDK29, MglBfw and MglBA/Rrv was used to create the first PCR product and MglBA/Rfw and omglB2 to create the second PCR product. A third PCR was done to fuse the two products. For this MglBA/Rrv and MglBA/Rfw have a homologous region. This product was then

cloned into pSK-Bluescript+ *yfp* (*Xba*I,*Bam*HI). Then *mglB*^{A64R}-yfp was cloned into pSW105 to create pDK29 (*Xba*I, *Hind*III). For pDK32 first three PCR products were amplified using MglBfw/ MglB5mutrv1, MglB5mutfw1/ MglB5mutrv2 and MglB5mutfw2/ omglB2. Another PCR amplified a product to fuse the three products together. For this the primers containing the mutations have homologous regions. This product was then cloned into pSK-Bluescript+ *yfp* (*Xba*I,*BamH*I). Then *mglB* $^{T13/K14/K120/D123/K127A}$ -yfp was cloned into pSW105 to create pDK32 (*Xba*I, *Hind*III). pDK30 and pDK31 were generated analogous using the primers, using MglBG-Rfw/MglBG-Rrv to introduce the mutation *G68R* and using MglBAG/Rfw/ MglBAG/Rrv introducing the mutation *A64/G68*R into *mglB*.

pDK96 and pDK97 were generated by amplifying *romX* using romXfw/romXyfprv and amplifying *romY* using romYfw/ romYyfprv from chromosomal DNA, and cloned into pSW105 using XbaI and BamHI restriction sites. Additionally *yfp* was amplified, using

oYFP-9 and YFP, and cloned the resulting plasmid using BamHI and HindIII restriction sites.

pDK100 and pDK101were generated by ampyfing *romX* using romXfw/ romXrvstop, and *romY* was amplified using romYfw/ romYrvstop. The resulting PCR fragments were cloned into pSW105.

Plasmids for overexpression in *E. coli Rosetta 2* :

For overexpression the gene of interest was amplified using chromosomal DNA of *M. xanthus* and cloned into either pET45 for expression with the His_6-tag or pMal-c2 for expression with the MalE-tag and transformed in *E. coli Rosetta 2* cells.

To generate pDK43 (*frzZ*), pDK44 (*frzEcheA*), pDK45 (*frzA*), pDK46 (*frzCD*) and pDK47 (*romR*) PCR fragments were amplified from genomic DNA of *M. xanthus* using the following primer pairs: HisFrzZfw/HisFrzZrv; his-frzEfw/HisfrzEdcheYrv; HisFrzAfw/ HisFrzArv; HisFrzCDfw/ HisFrzCDrv; HisRomRfw/ HisRomRrv. The PCR fragments were cloned into pET45 using the restriction sites *BamH*I and *Hind*III.

pDK48 and pDK49 were constructed as pDK47, using genomic DNA of SA3980 (*ΔromR/ romR*^{D53N}*-gfp*) and SA3981 (*ΔromR/ romR*^{D53E}*-gfp*) as the respective templates for the PCR reaction.

To generate pDK50, three PCR fragments have been amplified, (1) using HisFrzZfw/ FrzZD52rv; (2) FrzZD52fw/ FrzZD220rv and (3) FrzZD220fw/ HisFrzZrv where mutations have been introduced into the primers to generate substitution in amino acid D52 and D220.The three fragments have been fused by overlap PCR reactions. The

resulting PCR fragment was cloned into pET45 using the restriction sites *BamH*I and *Hind*III.

To generate pDK84, pDK86 and pDK88 fragments of *romR* were amplified from genomic DNA using the following primer pairs: MalE-RomRfw/ MalE-RomRrv (*romR*); MalEOutputfw/ MalE-RomRrv ($romR^{116-420}$) and MalE-RomRfw/ MalERecRomRrv ($romR^{1-115}$). Then the fragments were cloned into pMal-c2 using *EcoR*I and *Hind*III restriction sites. pDK84 and pDK85 were generated as pDK84, using genomic DNA of SA3980 (*ΔromR/ romR*^{D53N}*-gfp*) and SA3981 (*ΔromR/ romR*^{D53E}*-gfp*) as the respective templates for the PCR reaction.

pDK92 and pDK89 were generated by amplifying fragments of *frzZ* using the following primer pairs: MalERecFrzZ1fw/MalERecFrzZ1rv and MalERecFrzZ2fw/ MalERecFrzZ2rv. Then the fragments were cloned into pMal-c2 using *EcoR*I and *Hind*III restriction sites. Analogous pDK87 and pDK90 were generated, using pDK50 as a template, instead of genomic DNA.

pDK98 and pDK99 were generated using primer pairs His-romXfw/His-romXrv to amplify *romX* and His-romYfw/ His-romYrv to amplify *romY* from genomic DNA respectively. The PCR fragments were cloned into pET45 using *BamH*I and *Hind*III restriction sites.

BACTH plasmids for transformation into *E. coli BTH101:*

Plasmids for cotransformation in the bacterial-two-hybrid system were generated by introducing the gene of interest into the plasmids pKT25, pKNT25, put18 and/or put18C provided by Euromedex (France). All primers used to generate these plasmids, were named BACTH plus the name of the gene of interest. Resulting PCR fragments were cloned using *Ecor*I and *Xba*I restriction sites, present in all four plasmids. Only for cloning into pKT25 different revers primers were required, named BACTH plus name of gene of interest plus stop.

Plasmids used in this study constructed in (Keilberg, diploma thesis 2009); integration at Mx8 attachment site:

pDK3: Plasmid for generation of *PpilA-romR*$^{369-420}$*-GFP* fusion expressed from the *attB* site. Primers DA3 and DA4 were used, to amplify the fragment for *romR*$^{369-420}$*.* A second PCR was performed using oCrGFP-3 and oCrGFP-2 to amplify *gfp* from a plasmid containing *gfp*. First the two fragments were cloned into pBluescript II SK- using *Xba*I and *EcoR*V for the *romR* fragment, and *EcoR*V and *Hind*III for gfp, creating a C-terminal *gfp* fusion of the fragment. This fusion fragment was then cloned into pSW105 using *Xba*I and *Hind*III.

pDK4: Plasmid for generation of *PpilA-romR*$^{116-368}$*-GFP* fusion expressed from the *attB* site. Primers DA1 and DA2 were used, to amplify the fragment of *romR*$^{116-368}$*.* A second PCR was performed using oCrGFP-3 and oCrGFP-2 to amplify *gfp* from a plasmid containing *gfp*. First the two fragments were cloned into pBluescript II SK- using *Xba*I and *EcoR*V for the *romR* fragment, and *EcoR*V and *Hind*III for *gfp*, creating a C-terminal *gfp* fusion of the fragment. This fusion fragment was then cloned into pSW105 using *Xba*I and *Hind*III.

pDK5 Plasmid for generation of *PpilA-romR*$^{332-420}$*-GFP* fusion expressed from the *attB* site. Primers DA5 and DA4 were used, to amplify the fragment of *romR*$^{332-420}$*.* A second PCR was performed using oCrGFP-3 and oCrGFP-2 to amplify *gfp* from a plasmid containing *gfp*. First the two fragments were cloned into pBluescript II SK- using *Xba*I and *EcoR*V for the *romR* fragment, and *EcoR*V and *Hind*III for *gfp*, creating a C-terminal *gfp* fusion of the fragment. This fusion fragment was then cloned into pSW105 using *Xba*I and *Hind*III.

pDK6 Plasmid for generation of *PpilA-romR*$^{116-420}$*-GFP* fusion expressed from the *attB* site. Primers DA1 and DA4 were used, to amplify the fragment of *romR*$^{116-420}$*.* A second PCR was performed using oCrGFP-3 and oCrGFP-2 to amplify *gfp* from a plasmid containing *gfp*. First the two fragments were cloned into pBluescript II SK- using *Xba*I and *EcoR*V for the *romR* fragment, and *EcoR*V and *Hind*III for *gfp*, creating a C-terminal *gfp* fusion of the fragment. This fusion fragment was then cloned into pSW105 using *Xba*I and *Hind*III.

4.4.3 Constuction of in frame deletions

In-frame deletion mutants in *M. xanthus* were constructed by a two-step homologous recombination. Approximately, 1060 bp PCR products containing 500 bp of the upstream region of the gene of interest, 500 bp of the downstream region of the gene of interest, and 30 bp from the start end the end of the gene of interest were cloned in the plasmid pBJ114 (Julien *et al.,* 2000), which contains the *galK* gene for counter selection (Fig. 43). Primers used for the constructions are listed in Table 8. Four primers named A, B, C and D were designed to amplify the 1060 bp fragment carrying an in-frame deletion by PCR with *M. xanthus* chromosomal DNA as template. Shortly, primers A and B were used to amplify the upstream flanking region of the gene and Primers C and D were used to amplify the downstream flanking fragment of the gene. While Primer A and Primer D were binding outside the gene of interest, Primer B and Primer C were binding inside the gene of interest, and had to be designed, to leave

exactly 30 bp on each site of the gene to keep the frame after the deletion. Primer A and Primer D contained restriction sites for cloning into pBJ114 and primer B and Primer C contained a region complementary to each other. After the AB fragment and the CD fragment were amplified, a fusion PCR was performed, using both PCR fragments as a template, for a PCR reaction with Primer A and Primer D. This PCR resulted in an AD PCR fragment, containing the restriction sites *Ecor*I and *Hind*III for cloning into pBJ114. After transformation into *E. coli* Top10, the Plasmid was checked by sequencing.

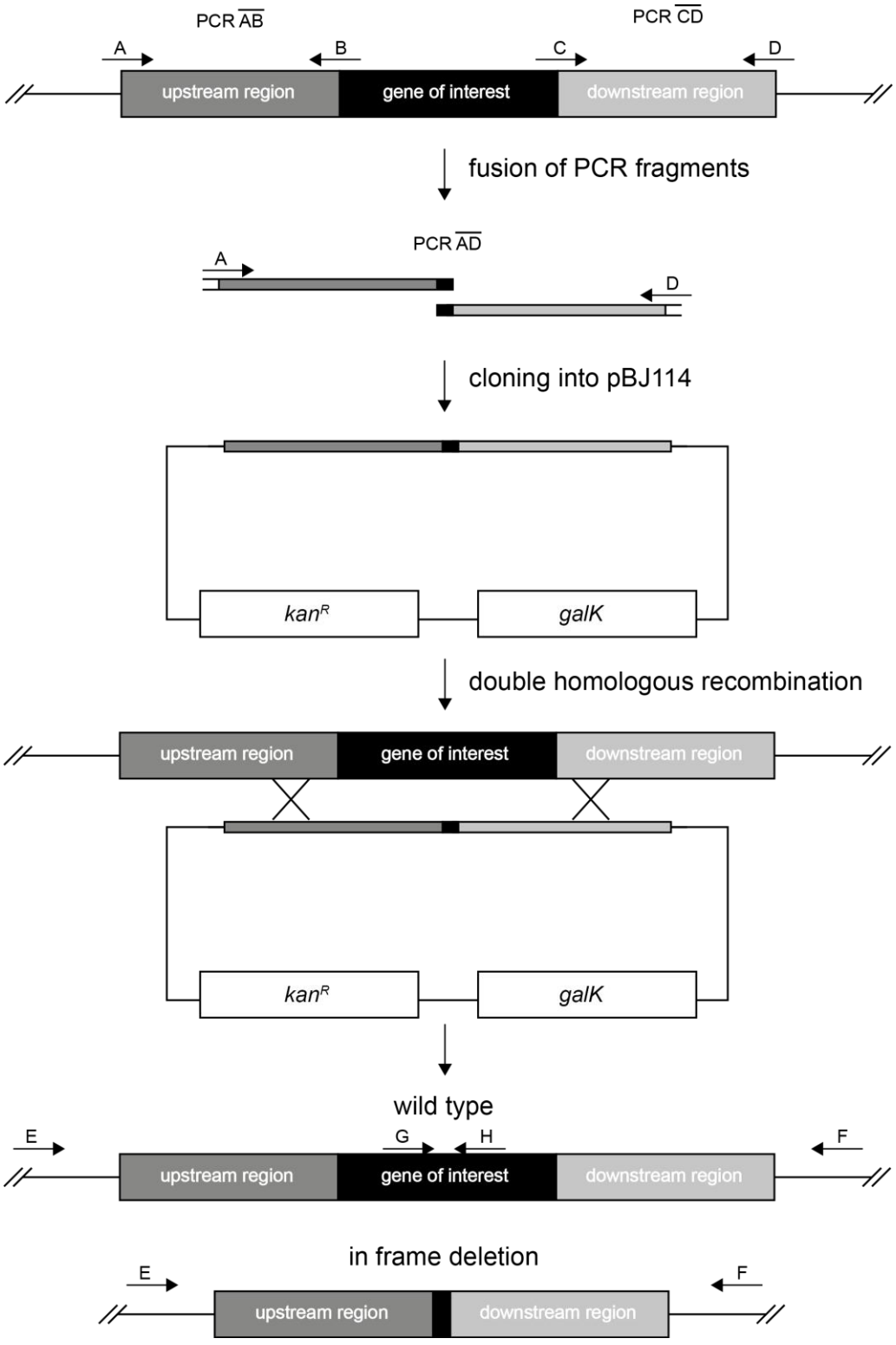

Figure 43: Strategy to generate in frame deletion mutants in *M. xanthus*. Details in the text.

Correct plasmids were introduced into the *M. xanthus* wild type strain DK1622 or derivatives by electroporation. The insertion of plasmids after the first homologous recombination was confirmed by three PCR reactions with three primer pair

combinations: Primers E (binds upstream of primer A) and F (binds downstream of primer D), and primers E and M13-forward (hybridizes to pBJ114), and primers F and M13-reverse (hybridizes to pBJ114). For each in-frame construct, at least one clone with the insertion of the plasmid in upstream flanking region of the gene of interest and one clone with the insertion in the downstream flanking region of the gene of interest were chosen for the second homologous recombination. To isolate clones containing the in-frame deletion, cells were grown in liquid 1.0% CTT medium to mid-log phase, diluted and plated on CTT plate with 2% galactose (Sigma/Roth) for counter-selection. Galactose resistant and kanamycin sensitive colonies were screened out and checked by two PCR reactions with the primers E and F and the primers G and H as displayed in figure 43. Primer E binds upstream of Primer A, while Primer F binds downstream of Primer D. PCR reactions with Primers E and F were performed to distinguish between WT and the deletion mutant after the second homologous recombination. The PCR product of the EF fragment in WT was bigger compared to the in-frame deletion mutant by the size of the gene of interest – 60 bp. Additionally, Primers G and H amplify a fragment within the deleted part of the gene of interst, which is therefore only amplified in WT.

4.4.4 DNA preparation from *E. coli* und *M. xanthus*

Plasmid DNA from *E. coli* was isolated using QIAprep Spin Miniprep Kit (Qiagen) or Zyppy™ Plasmid Miniprep Kit (Zymo) according to the instructions by the manufacturer. *M. xanthus* genomic DNA was prepared using MasterPure DNA preparation Kit (Epicentre) according to the instructions of the manufacturer. Concentration and purity of DNA was determined with the Nanodrop ND-1000 spectrophotometer (Nanodrop, Wilmington). Crude genomic DNA preparations of *M. xanthus* genomic DNA for verification of insertions or deletions by PCR were prepared by boiling cell samples for 5 min in 50 µl H_2O followed by brief sedimantetion of cell debris.

4.4.5 Polymerase chain reaction (PCR)

Amplification of specific DNA fragments was performed in 50 µl reaction volume using *PfuUltra*II-polymerase (Strategene, Amsterdam) with either the provided buffer or Buffer J (Epicentre). The PCR reaction mix was prepared as follows:

PCR reaction mix	
Genomic DNA or Plasmid DNA	1 µl
10 µM Primer (each)	1 µl
10 mM dNTPs (each)	1 µl
10x PfuII Ultra buffer	5 µl
DMSO	5 µl
PfuUltraII Polymerase	0.5 µl
H_2O (HPLC)	36.5 µl

Alternatively, 2xBuffer J (Epicentre) was used instead of 10x PfuII Ultra buffer, already containing 10 mM dNTPs (each).

For Check PCRs to test plasmid integration or in-frame deletions, colony PCRs were conducted in 20 µl reaction volume using Eppendorf® MasterMix (Eppendorf), containing *Taq* polymerase. The PCR reaction mix was prepared follows:

Check PCR reaction mix	
Crude Genomic DNA	3 µl
10 µM Primer (each)	1 µl
2.5x Master Mix	8 µl
DMSO	2 µl
H_2O (HPLC)	6 µl

The PCR programs used in this study are represented in Table 10 and 11. PCR conditions were modified based on the predicted primer annealing temperature (Tm) and expected product sizes.

Table 10: PCR programme check PCR

Standard/Check PCR			
Step	**Temperature**	**Time**	
Initial denaturation	94 °C	3 min	
Denaturation	94 °C	30 sec	30 cycles
Primer annealing	dependend on Primer Tm (Check PCR: 55 °C)	30 sec	
Elongation	72 °C	dependend on the gene length (Check PCR 3 min)	
Final elongation	72 °C	3 min	
Hold	4 °C		

Table 11: PCR programme touch down PCR

Touch down PCR			
Step	**Temperature**	**Time**	
Initial denaturation	94 °C	3 min	
Denaturation	94 °C	30 sec	9 cycles
Primer annealing	70 °C	30 sec	
Elongation	72 °C	dependend on the gene length	
Denaturation	94 °C	30 sec	9 cycles
Primer annealing	60 °C	30 sec	
Elongation	72 °C	dependend on the gene length	
Denaturation	94 °C	30 sec	9 cycles
Primer annealing	55 °C	30 sec	
Elongation	72 °C	dependend on the gene length	
Final elongation	72 °C	3 min	
Hold	4 °C		

PCR product size was verified by agarose gel electrophoresis. Correct PCR products were either directly purified using DNA Clean&Concentrator-5 kit or extracted from the agarose gel and purified with Gel Recovery Kit (ZymoResearch Hiss Diagnostics).

4.4.6 Agarose gel electrophoresis

Nucleic acid fragments were separated by size using agarose gel electrophoresis at 120 V in TAE buffer (Invitrogen). Ethidium bromide was added to agarose in the final concentration of 0.01% (v/v). DNA samples were mixed with 5x sample loading buffer (Bioline). Agarose gels were imaged using 2UV transilluminator (UVP-Bio-Doc-It-System, UniEquip) at 365 nm.

4.4.7 Restriction and ligation of DNA fragments

For restriction, Plasmid DNA or PCR products were incubated with restriction endonucleases for 1h up to 3h at 37°C, according to the specific requirements for the enzyme used. Restricted DNA was purified with DNA Clean&Concentrator kit or Gelpurification kit according to the instructions (ZymoResearch Hiss Diagnostics).

Ligation reactions were performed with T4 DNA ligase. DNA fragments were ligated into vectors applying 3-5-fold molar excess of insert DNA. The ligation reaction was ligated for 2 h at room temperature or at 18°C over night, followed by the inactivation of the enzyme at 65°C for 10 min.

4.4.8 DNA sequencing

For sequencing purified plasmids or PCR products were sent to Eurofins MWG Operon as recommended by the company; Sequencing Primer were either sent additionally or provided by Eurofins MWG Operon. Received DNA sequences were analyzed using Vector NTI Advance suite 11 (Invitrogen).

4.4.9 Preparation of chemical- and electrocompetent *E. coli* cells

Chemicalcompetent *E. coli cells*

To prepare chemicalcompetent *E. coli* cells, overnight cultures were diluted 1:200 to inoculate 1 L of LB medium. Cells were grown at 37°C on horizontal shakers at 230 rpm. At OD600=0.5 cells were harvested by centrifugation at 4700 rpm for 20 min at 4°C. Cells were resuspended in 200 ml 50mM $CaCl_2$. Then cells were centrifuged

again at 4700 rpm for 20 min at 4°C. Final pellet was resuspended in 20 ml 50 mM $CaCl_2$/10% Glycerol and 300 µl aliquots were fast frozen in liquid nitrogen and stored at -80°C for later use.

Electrocomentent *E. coli cells*

To prepare electrocompetent *E. coli* cells, overnight cultures were diluted 1:200 to inoculate 1 L of LB medium. Cells were grown at 37°C on horizontal shakers at 230 rpm. At OD600=0.5 cells were harvested by centrifugation at 4700 rpm for 20 min at 4°C. The cell pellet was resuspended in 500 ml ice-cold sterile 10% glycerol and centrifuged again. The washing steps were carried out with10% glycerol and repeated with 100 ml, 50 ml and 10 ml volumes. Final cell pellet was resuspended in 2 ml sterile 10% glycerol, 50 µl aliquots were fast frozen in liquid nitrogen and stored at -80°C for later use.

4.4.10 Preparation of eletrocompetent *M. xanthus* cells

M. xanthus cells were grown in 5 ml CTT medium to an OD550=0.5-0.8, 2 ml of this culture were centrifuged at 13,000 rpm for 2 min at room temperature. The cell pellet was resuspended in 1 ml of sterile deionized water and centrifuged as above. Washing step was repeated twice. The final cell pellet was resuspended in 50 µl of sterile deionized water. Cells were kept on ice for direct transformation.

4.4.11 Transformation of E. coli cells

Chemicalcompetent *E. coli cells*

For transformation into chemicalcompetent cells, 7 µl of heat-inactivated ligation reaction or plasmid DNA were first dialysed against sterile water (VSWP membrane from Millipore) for 30 min and then added to 200 µl chemicalcompetent *E. coli* cells on ice. Cells were incubated on ice for 25 min, and then transferred to 42°C for 2 min for heat shock. Next, the cells were incubated for 5 min on ice. Then 1 ml LB media was added, and the cells were incubated shaking at 230 rmp for 1h at 37°C. . After 1 h incubation cells were harvested by centrifugation at 5000 rpm for 2 min, resuspended in 100 µl of LB medium and plated on LB agar plates containing appropriate antibiotics. The plates were incubated at 37°C overnight; grown colonies were transferred onto fresh agar plates and screened for the presence of the plasmid containing the insert by restriction digestion with subsequent agarose gel electrophoresis. For sequencing obtained constructs were sent to Microfins MWG Operon; received DNA sequences were analyzed using Vector NTI Advance suite 11 (Invitrogen).

Electrocomentent *E. coli cells*

For electroporation, 7 µl of heat-inactivated ligation reaction plasmid DNA were first dialysed against sterile water (VSWP membrane from Millipore) for 30 min and then added to 50 µl electrocompetent *E. coli* cells on ice. The mixture was transferred into an electroporation cuvette (Bio-Rad, Munchen) and pulsed with 1.8 kV, 25 µF and 200 Ω. 1 ml LB medium was added; the suspension was transferred into a sterile plastic tube and incubated for 1 h at 37°C shaking at 230 rpm. After 1 h incubation cells were harvested by centrifugation at 5000 rpm for 2 min, resuspended in 100 µl of LB medium and plated on LB agar plates containing appropriate antibiotics. The plates were incubated at 37°C overnight; grown colonies were transferred onto fresh agar plates and screened for the presence of the plasmid containing the insert by restriction digestion with subsequent agarose gel electrophoresis. For sequencing obtained constructs were sent to Microfins MWG Operon; received DNA sequences were analyzed using Vector NTI Advance suite 11 (Invitrogen).

4.4.12 Transformation of *M. xanthus* cells

For electroporation, 100 ng of plasmid DNA for integration at the chromosomal Mx8 attachment site, or 1 µg of plasmid DNA for integration at the endogenous site were dialysed against sterile deionized water (VSWP membrane from Millipore). Next, dialysed DNA was added to 50 µl suspension of electrocompetent *M. xanthus* cells, the mixture was transferred into an 0.1 cm electroporation cuvette (Bio-Rad, Munchen) and pulsed with 0.65 kV, 25 µF and 400 Ω. 1 ml CTT medium was added immediately; the suspension was transferred into a sterile Erlenmeyer flask and incubated for 6-8 h (for integration at Mx8 attachment site) or over night (for integration at the endogenous site) at 32°C and 230 rpm in the dark. Then the suspension was mixed with 4 ml of CTT soft agar (only for integration at the endogenous site) and plated on CTT agar plates containing appropriate antibiotics. The plates were incubated at 32°C for 5 to 10 days; grown colonies transferred onto fresh agar plates. The integration of the plasmids was verified by PCR.

4.4.13 Cotransformation for BACTH system

For cotransformtaion, required for the BACTH system, first chemicalcompetent cells of BTH101 were prepared and transformed as described in 4.4.9. and 4.4.11. For

each transformation, 50 ng plasmid DNA of the two plasmids were added to the competent cells, one containing the T25 fragment (derivatives of pKT25 or pKNT25) and one containing the T18 fragment (derivatives of put18 or pu18C). After transformation, cells were incubated for 1h at 37°C shaking at 230 rpm. Next, 50µl of the suspension was plated on selection plates containing 100 µg/ml ampicillin, 50 µg/ml kanamycin, 0.5 M IPTG and 40 µg/ml Xgal.

4.5 Microbiological methods

4.5.1 BACTH system

The bacterial two hybrid system was used to detect direct interactions of proteins. Therefore, the reporter strain, BH101 lacking the gene *cyaA* (catalytic domain of adenylate cyclise) has been used for transformations as described by Euromedex. (CyaA) Plasmids containing T25 and T18 fragments of CyaA were provided by Euromedex. When these two fragments are fused to interacting polypeptides, X and Y, heterodimerization of these hybrid proteins results in functional complementation between T25 and T18 fragments and, therefore, cAMP synthesis. Detection of *in vivo* interactions between two proteins of interest with the BACTH system requires the co-expression of these proteins as fusions with the T25 and T18 fragments in. BH101 cells were co-transformed with the two recombinant plasmids and plated on indicator media (LB, Xgal, IPTG, Km, Amp) to reveal the resulting Cya+ phenotype. After transformation cells were incubated at 30°C over night. From each transformation plate 3 representative clones were picked, incubated in LB media containing approbriate concentrations of Kanamycin and Ampicillin, and then spotted on indicator plates again. After 24 hours of incubation at 30°C, pictures of the plates were taken and evaluated. While blue colonies demonstrated a positive interaction between the two tested proteins, white colonies demonstrated no interaction. For comparison, for each transformation, a positive control using the plasmid (pKNT25-Zip/put18C-Zip) and a negative control using empty plasmids (pKNT25/put18C) provided by the company were transformed in parallel.

4.5.2 Motility assays

Cells were grown to a cell density of 7×10^8 cells/ml, harvested and resuspended in 1% CTT to a calculated density of 7×10^9 cells/ml. 5 µl aliquots of cells were placed on 0.5% and 1.5% agar supplemented with 0.5% CTT and incubated at 32 °C. After 24 h, colony edges were observed using a Leica MZ8 stereomicroscope or a Leica IMB/E

inverted microscope and visualized using Leica DFC280 and DFC350FX CCD cameras, respectively. To quantify differences in motility, the increase in colony diameter after 24 h was determined. Briefly, the diameter of each colony was measured at two positions at 0 and 24 h. The increase in colony diameter was calculated by subtraction of the size at 0 h from the size at 24 h. Colony diameters were measured for three colonies per strain.

4.6 Microscopy and determination of reversal frequency

For microscopy, *M. xanthus* cells were placed on a thin 1% agar-pad buffered with A50 buffer (10 mM MOPS pH 7.2, 10 mM $CaCl_2$, 10 mM $MgCl_2$, 50 mM NaCl) on a glass slide and immediately covered with a coverslip, and then imaged. Quantification of fluorescence signals was done as follows. The integrated fluorescence intensity of polar clusters and of a similar cytoplasmic region was measured using the region measurement tool in Metamorph 7.7. The intensity of the cytoplasmic region was subtracted from the intensity of the polar cluster. These corrected intensities of the polar clusters were used to calculate the ratios between the polar signals in individual cells. If the ratio is ≤2.0, the localization is defined as bipolar symmetric, if the ratio is ≥2.1 and ≤10.0 the localization is defined as bipolar asymmetric, and if the ratio was ≥10.1 the localization is defined as unipolar. For each strain 200 cells were analyzed. For time-lapse microscopy, cells were recorded at 30-s intervals for 15 min. Images were recorded and processed with Leica FW4000 V1.2.1 or Image Pro 6.2 (MediaCybernetics) software. Processed images were visualized using Metamorph (Molecular Devices). Reversals were counted for > 50 cells of each strain followed for 15 minutes and displayed in a Box plot.

4.7 Biochemical methods

4.7.1 Overproduction and purification of proteins

Overexpression strains expressing His-tagged proteins (carrying derivatives of pET45) MalE-tagged proteins (carrying derivatives of pMAL-c2) or GST-tagged proteins (carrying derivatives of pGEXT) were grown in LB containing 100 µg/ml ampicillin. At a cell density of 7×10^8 cells/ml, protein production was induced by adding 0.1 mM isopropyl-1-thio-ß-D-galactopyranoside (IPTG) for 20h at 18 °C. Cells were harvested by centrifugation at 4.700 rpm, 20 min, 4 °C and resuspended in lysis buffer. Except for His_6-FrzA all proteins used in this study were purified under native consitions as described below. His_6-FrzA was purified under denaturing conditions, as recommended

by QiaExpressionist (Qiagen) and then renatured by dialysis against dialysis buffer containing 50 mM NaH_2PO_4 pH 8.0, 300 mM NaCl.

For His-tagged proteins the lysis buffer was: 50 mM NaH_2PO_4 pH 8.0, 300 mM NaCl, 10mM imidazole,Protease Inhibitor tablets (Roche), 1mg/ml lysozyme (Merck). For MalE-tagged proteins and GST-tagged proteins the lysis buffer was: 20 mM Tris/HCl pH 7.5, 300 mM NaCl, 10% glycerol, Protease Inhibitor tablets (Roche), 1mg/ml lysozyme (Merck) Protease Inhibitors, lysozyme. Cells were lysed by ultrasonication and debris removed by centrifugation at 4.700 rpm, 20 min, 4 °C. His_6-tagged proteins were purified using Ni^{++}-NTA columns (Macherey-Nagel), GST-tagged proteins were purified using a glutathione-Sepharose column (Novagen), and MalE-tagged proteins were purified using amylose beads (Biolabs) as recommended by the manufacturers. Elutions were performed with elution buffers containing 50 mM NaH_2PO_4 pH 8.0, 300 mM NaCl, 200mM imidazole for His_6-tagged proteins, 20 mM Tris/HCl pH 7.5, 300 mM NaCl, 10% glycerol, 10 mM glutathione for GST-tagged proteins, and 20 mM Tris/HCl pH 7.5, 300 mM NaCl, 10% glycerol, 10 mM maltose for MalE-tagged proteins. After elution, proteins were dialysed against a storage buffer containing 50 mM NaH_2PO_4 pH 8.0, 300 mM NaCl, 10% glycerol for His_6-tagged proteins, or 20 mM Tris/HCl pH 7.5, 300 mM NaCl, 10% glycerol for GST-tagged or MalE-tagged proteins, and stored at -80 °C. The protein concentration and purity was analyzed using the BioRad Protein assay Kit (Bio-Rad) and SDS-page (Sambrook and Russell 2001), respectively.

4.7.2 Concentration determination of proteins

To determine protein concentrations the Bio-Rad protein assay kit was used in accordance to the recommendations of the manufacturer (Bio-Rad). To measure the protein concentration, 20 µl of the sample were added to 980 µl of a 1:5 dilution of the Bio-Rad solution and incubated for 10 min at RT in the dark. In the same way, different dilutions of BSA as shown in table 12 were added, to create a standard curve showing protein concentration (based on the concentration of the added 20µl) versus measured absorbance. Therefore, absorbance was measured at 595 nm with Ultrospec 2100 pro spectrophotometer (Amersham Biosciences, München) for BSA and the sample. Based on the BSA standard curve, protein concentrations could be calculated from the measured absorbance of the sample.

Table 12: protein concentration by Bio-Rad

1. Bio-Rad 1:5	980 µl	980 µl	980 µl	980 µl
2. water	20 µl	10 µl	0 µl	0 µl
3. sample/BSA (2 mg/ml BSA)	0 µl BSA	10 µl	20 µl BSA	20 µl sample
concentration (for standard curve)	0 mg/ml	1 mg/ml	2 mg/ml	?

4.7.3 SDS polyacrylamide gelektrophoresis (SDS-PAGE)

To separate proteins under denaturing conditions SDS-PAGE (Laemmli, 1970) with 14% gels, with components as listed in table 13, was performed. To denature proteins, samples were mixed with 5x loading buffer (50% (v/v) glycerol, 250 mM Tris-HCl pH 6.8, 10 mM EDTA, 10% (w/v) SDS, 0.5 M DTT, 1% (w/v) bromphenol blue) and heated at 96˚C for 5 min prior to loading the gel. Gel electrophoresis was carried out in Bio-Rad electrophoresis chambers (Bio-Rad, München) at 120-150 V in 1x Tris/Glycine SDS (TGS) running buffer from Bio-Rad. To estimate molecular weight of proteins prestained protein markers from Fermentas (St. Leon-Rot) were used. Proteins were visualized by staining for 20 min at room temperature in Coomassie brilliant blue (Sambrooket al., 1989).

Table 13: Composition of 14% gels for SDS-Page (Lämmli).

lower gel 14% (2 gels)	**volume**
1.5 mM Tris-HCl, pH 8.8	2.5 ml
40% Acrylamid/Bisacrylamid (37:1)	3.5 ml
H_2O, ad 10 ml	4 ml
TEMED	7 µl
Ammoniumpersulfate (APS) 10%	60 µl
upper gel (for 10 gels)	
0.5 M Tris-HCl, pH 6.8	2.5 ml
40% Acrylamid/Bisacrylamid (37:1)	1 ml
H_2O, ad 10 ml	6.5 ml
TEMED	6 µl
Ammoniumpersulfate (APS) 10%	12 µl

4.7.4 Immunoblot analysis

Immunoblot analyses were performed using a standard protocol (Sambrook *et al.*,1989). Equal amounts of protein (between 5 and 15 µg protein or protein from approximately $7*10^7$ cells per lane) were loaded onto SDS-PAGE and transferred to a nitrocellulose membrane using semi-dry blotting (Hoefer apparatus: Amersham Biosciences, München) with a constant amperage of 0.8 mA/cm^2 for 2 hours. Buffers used for the transfer are listed in Table 14. After transfer, nitrocellulose membranes were blocked using 1x TTBS buffer (0.05% (v/v) Tween 20, 20 mM TrisHCl, 137 mM NaCl pH 7) supplemented with 5% (w/v) non-fat milk powder shaking 1-20 h at 4˚C. Then membranes were incubated with the proper dilution of primary antibodies in 1xTTBS buffer containing 2% (w/v) non-fat milk powder for 2-20 h at 4°C. After incubation with primary antibodies, membranes were washed 2x5 min with 1xTTBS buffer and finally incubated with 1:15000 dilution of secondary anti-rabbit IgG or 1:2500 dilution of secondary anti-mouse IgG horseradish peroxidase (HPR) coupled antibodies (Pierce/Thermo Scientific, DakoCytomation). After 1 h incubation at 4°C with secondary antibodies, membranes were washed twice with 1xTTBS buffer. Then chemiluminescence substrate (Pierce/Thermo Scientific) was added for 1 min and finally signals were visualized using luminescent image analyzer LAS-4000 (Fujifilm).

Table 14: Buffer for immunoblot transfer reaction

membrane (anode)		**gel (kathode)**	
chemicals per liter H_20	final concentration	chemicals per liter H_20	final concentration
3,03 g Tris	25 mM	6,06 g Tris	50 mM
14,4 g glycine	192 mM	28,8 g glycine	384 mM
0,1 g SDS	0,01%	2,0 g SDS	0,2%
250 ml methanol	25%	100 ml methanol	10%

4.7.5 Antibody production

For Immunoblot analysis the following antibodies were used: α-RomR, α-MalE, α-GST, α-MglB, α-GFP, α-RomX and α-RomY.

α-MalE, α-GST and α-GFP were produced by Biolabs (New England Biolabs /Frankfurt) and used as recommended by the manufacturer. α-RomR and α-MglB were produced and described previously (Leonardy et al. 2007;Leonardy et al. 2010). Antibidies α-RomX and α-RomY were raised against purified His_6-RomX and His_6-RomY. Proteins were purifies as described in 4.7.1. Next, 2 mg of each purified protein

was sent to Eurogentec (Belgien) for antibody production. Antibodies α-RomX and α-RomY were used in a dilution 1:2000 for immunoblots.

4.7.6 Pull down experiments

0.5 mg of purified His_6-MglB or MglA-His_6 in buffer H (50 mM NaH_2PO_4 pH 8.0, 300 mM NaCl, 10mM imidazole) was applied to a Ni^{2+}-NTA-agarose column (Macherey-Nagel). *M. xanthus* cell lysate was prepared as follows: 200 ml of exponentially growing WT cells at a cell density of 7×10^8 cells/ml were harvested, resuspended in buffer H in the presence of proteases inhibitors (Roche) and lysed by sonication. Cell debris was removed by centrifugation at 4700× g for 20 min, 4 °C and the cell-free supernatant applied to the Ni^{2+}-NTA-agarose column with or without bound His_6-MglB or MglA-His_6. After two washing steps with each 10 column volumes of the buffer H, bound proteins were eluted with buffer H supplemented with 250 mM imidazole. Proteins eluted from the columns were analyzed by two methods: SDS-PAGE and gels stained with Coomassie Brilliant Blue R-250 and SDS-PAGE with immunoblot analysis using α-RomR antibodies (Leonardy et al. 2007).

To test for direct protein-protein interactions, 0.2 mg of purified prey protein (His_6-RomR or His_6-MglB or as a negative control His_6-PilP) was mixed with 0.2 mg of purified bait protein (GST-MglA or MalE-RomR) and as a control with 0.2 mg of GST or MalE, respectively. Proteins were incubated with 0.5 ml sepharose beads (for MalE-tagged proteins: amylose beads; for GST-tagged proteins: glutathione beads) in buffer D (50 mM NaH_2PO_4 pH 8.0, 300 mM NaCl) for 5h, 4 °C. After washing the beads with 25 column volumes of buffer D, the elutions were performed with buffer D supplemented with 10 mM glutathione for GST-tagged proteins, and with 10 mM maltose for MalE-tagged proteins. Proteins eluted from the columns were analyzed by immunoblot analysis using α-GST antibodies (Biolabs), α-MalE antibodies (Biolabs), α-His antibodies (Piercenet), α-RomR antibodies (Leonardy et al. 2007) and α-MglB antibodies (Leonardy et al. 2010). Immunoblots were carried out as described (Sambrook and Russell 2001).

4.7.7 Phosphotransfer assays

Autophosphorylation of $FrzE^{CheA}$

The autophosphorylation reaction to phosphorylate $FrzE^{CheA}$ was mixed carefully with following reagents: 50 mM Tris pH 8.0, 150 mM NaCl, 10% glycerol, 10 µM protein, 50 mM KCl and 20 mM $MnCl_2$ (or 20 mM $MgCl_2$). The reaction is started by adding 1/10 volume of the ATP mixture with 1:1 ratio of 10 mM ATP, [γ-32P] -ATP (>220 TBq/mmol, Hartmann analyticGmbH) at defined times and a control reaction without

ATP mixture was started together with the longest incubation time of reaction. The reactions were incubated at 25°C in Thermomixer (Eppendorf) and stopped at the same time point by adding 3x SDS loading buffer (180 mM Tris-HCl, pH 6.8, 6% SDS, 30%glycerol, 0.015% bromo-phenol-blue, 15 mM EDTA and 0.3 M DTT). All of the reactions were loaded into 12% SDS-PAGE followed by electrophoresis at 150V for 50 min in Biorad gel system. The gel tank was dissembled and the dye front of the gel was cut to get rid of the signal interruption from free phosphate and ATP. The gel was covered with plastic bag and exposed to the phosphor screen in cassette overnight. After exposure, the phosphor screen was scanned by phosphorimager.

Phosphotransfer between $FrzE^{CheA}$ and FrzZ/RomR proteins

$FrzE^{CheA}$ (10 µM) was autophosphorylated with [γ-32P] ATP for 30 min. Adequate amount of the autophosphorylated $FrzE^{CheA}$ was mixed with FrzCD, FrzA and the receiver domain protein (FrzZ or RomR). For each phosphotransfer reaction the proteins were diluted to a final concentration of 1µM in buffer containing 50 mM Tris pH 8.0, 150 mM NaCl, 10% glycerol, 10 µM protein, 50 mM KCl and 20 mM $MnCl_2$. The proteins were incubated at 25°C for a defined time. The reactions were stopped by adding 3xSDS loading buffer, separated by SDS-PAGE and detected by phosphoimaging and pageblue staining as described for autophosphorylation.

4.8 Bioinformatics methods

4.8.1 Sequences and domain analysis

All of the protein or gene sequences of *M. xanthus* were retrieved from Tigr database (http://cmr.tigr.org/tigr-scripts/CMR/GenomePage.cgi?org=gmx). The proteins from other organisms are from NCBI database (http://www.ncbi.nlm.nih. gov/sites/gquery). The domain analyses were performed in SMART database (http://smart.embl-heidelberg.de/). Selected sequences were analyzed and aligned using VectorNTI (Invitrogen).

Genomic distributions of RomR, MglA, MglB, the Frz-chemosensory system and the two motility systems, RomX and RomY were analyzed by K. Wuichet (MPI Marburg) comparing complete prokaryotic genomes downloaded from NCBI as explained in detail in material and methods of (Keilberg et al. 2012)

References

Appleby JL, Parkinson JS, Bourret RB (1996) Signal transduction via the multi-step phosphorelay: not necessarily a road less traveled. Cell 86:845-848

Baker MD, Wolanin PM, Stock JB (2006) Signal transduction in bacterial chemotaxis. Bioessays 28:9-22

Blackhart BD, Zusman DR (1985a) Cloning and complementation analysis of the "Frizzy" genes of *Myxococcus xanthus*. Mol. Gen. Genet. 198:243-254

Blackhart BD, Zusman DR (1985b) "Frizzy" genes of *Myxococcus xanthus* are involved in control of frequency of reversal of gliding motility. Proc. Natl. Acad. Sci. U S A 82:8771-8774

Blair DF, Berg HC (1990) The MotA protein of E. coli is a proton-conducting component of the flagellar motor. Cell 60:439-449

Bos JL, Rehmann H, Wittinghofer A (2007) GEFs and GAPs: critical elements in the control of small G proteins. Cell 129:865-877

Bulyha I, Hot E, Huntley S, Sogaard-Andersen L (2011) GTPases in bacterial cell polarity and signalling. Curr Opin Microbiol 14:726-733

Bulyha I et al. (2009) Regulation of the type IV pili molecular machine by dynamic localization of two motor proteins. Mol Microbiol 74:691-706

Bustamante VH, Martinez-Flores I, Vlamakis HC, Zusman DR (2004) Analysis of the Frz signal transduction system of *Myxococcus xanthus* shows the importance of the conserved C-terminal region of the cytoplasmic chemoreceptor FrzCD in sensing signals. Mol. Microbiol. 53:1501-1513

Craig L, Li J (2008) Type IV pili: paradoxes in form and function. Curr Opin Struct Biol 18:267-277

Dubnau D (1999) DNA uptake in bacteria. Annu Rev Microbiol 53:217-244

Galperin M (2005) A census of membrane-bound and intracellular signal transduction proteins in bacteria: Bacterial IQ, extroverts and introverts. BMC Microbiology 5:35

Galperin MY (2010) Diversity of structure and function of response regulator output domains. Curr. Opin. Microbiol. 13:150-159

Gerding MA, Ogata Y, Pecora ND, Niki H, de Boer PA (2007) The trans-envelope Tol-Pal complex is part of the cell division machinery and required for proper outer-membrane invagination during cell constriction in E. coli. Mol Microbiol 63:1008-1025

Goldman BS et al. (2006) Evolution of sensory complexity recorded in a myxobacterial genome. Proc Natl Acad Sci U S A 103:15200-15205

Hartzell P, Kaiser D (1991a) Function of MglA, a 22-kilodalton protein essential for gliding in *Myxococcus xanthus*. J Bacteriol 173:7615-7624

Hartzell P, Kaiser D (1991b) Upstream gene of the mgl operon controls the level of MglA protein in Myxococcus xanthus. J Bacteriol 173:7625-7635

Hodgkin J, Kaiser D (1977) Cell-to-cell stimulation of movement in nonmotile mutants of *Myxococcus*. Proc. Natl. Acad. Sci. USA 74:2938-2942

Hodgkin J, Kaiser D (1979) Genetics of Gliding Motility in *Myxococcus xanthus* (Myxobacterales): Two gene systems control movement. Mol. Gen. Genet. 171:177-191

Huitema E, Pritchard S, Matteson D, Radhakrishnan SK, Viollier PH (2006) Bacterial birth scar proteins mark future flagellum assembly site. Cell 124:1025-1037

Hunter P (2008) Not so simple after all. A renaissance of research into prokaryotic evolution and cell structure. EMBO Rep 9:224-226

Inclan YF, Laurent S, Zusman DR (2008) The receiver domain of FrzE, a CheA-CheY fusion protein, regulates the CheA histidine kinase activity and downstream signalling to the A- and S-motility systems of Myxococcus xanthus. Mol Microbiol 68:1328-1339

Inclan YF, Vlamakis HC, Zusman DR (2007) FrzZ, a dual CheY-like response regulator, functions as an output for the Frz chemosensory pathway of Myxococcus xanthus. Mol Microbiol 65:90-102

Jakovljevic V, Leonardy S, Hoppert M, Sogaard-Andersen L (2008) PilB and PilT are ATPases acting antagonistically in type IV pilus function in Myxococcus xanthus. J Bacteriol 190:2411-2421

Jelsbak L, Søgaard-Andersen L (1999) The cell surface-associated intercellular C-signal induces behavioral changes in individual *Myxococcus xanthus* cells during fruiting body morphogenesis. Proc. Natl. Acad. Sci. USA 96:5031-5036

Jenal U, Galperin MY (2009) Single domain response regulators: molecular switches with emerging roles in cell organization and dynamics. Curr. Opin. Microbiol. 12:152-160

Julien B, Kaiser AD, Garza A (2000) Spatial control of cell differentiation in *Myxococcus xanthus*. Proc. Natl. Acad. Sci. USA 97:9098-9103

Kaiser D (1979) Social gliding is correlated with the presence of pili in *Myxococcus xanthus*. Proc. Natl. Acad. Sci. USA 76:5952-5956

Keilberg D, Wuichet K, Drescher F, Sogaard-Andersen L (2012) A Response Regulator Interfaces between the Frz Chemosensory System and the MglA/MglB GTPase/GAP Module to Regulate Polarity in Myxococcus xanthus. PLoS Genet 8:e1002951

Keilberg D (2009) Cis-and trans-acting determinants of the response regulator RomR in *M. xanthus*, Diploma thesis

Kim SK, Kaiser D (1990) Cell motility is required for the transmission of C-factor, an intercellular signal that coordinates fruiting body morphogenesis of *Myxococcus xanthus*. Genes & Dev. 4:896-904

Kirkpatrick CL, Viollier PH (2011) Poles apart: prokaryotic polar organelles and their spatial regulation. Cold Spring Harb Perspect Biol 3

Kortholt A, van Haastert PJ (2008) Highlighting the role of Ras and Rap during Dictyostelium chemotaxis. Cell Signal 20:1415-1422

Lam H, Schofield WB, Jacobs-Wagner C (2006) A landmark protein essential for establishing and perpetuating the polarity of a bacterial cell. Cell 124:1011-1023

Lenarcic R et al. (2009) Localisation of DivIVA by targeting to negatively curved membranes. EMBO J 28:2272-2282

Leonardy S, Bulyha I, Sogaard-Andersen L (2008) Reversing cells and oscillating motility proteins. Mol Biosyst 4:1009-1014

Leonardy S, Freymark G, Hebener S, Ellehauge E, Sogaard-Andersen L (2007) Coupling of protein localization and cell movements by a dynamically localized response regulator in Myxococcus xanthus. Embo J 26:4433-4444

Leonardy S, Miertzschke M, Bulyha I, Sperling E, Wittinghofer A, Sogaard-Andersen L (2010) Regulation of dynamic polarity switching in bacteria by a Ras-like G-protein and its cognate GAP. EMBO J. 29:2276-2289

Leonardy S (2009) Regulierung der Polarität des A-Bewegungssystems in *M. xanthus*; PhD thesis

Li Y et al. (2003) Extracellular polysaccharides mediate pilus retraction during social motility of *Myxococcus xanthus*. Proc. Natl. Acad. Sci. USA 100:5443-5448

Luciano J et al. (2011) Emergence and modular evolution of a novel motility machinery in bacteria. PLoS Genet 7:e1002268

Maddock JR, Shapiro L (1993) Polar location of the chemoreceptor complex in the Escherichia coli cell. Science 259:1717-1723

Maier B, Potter L, So M, Long CD, Seifert HS, Sheetz MP (2002) Single pilus motor forces exceed 100 pN. Proc Natl Acad Sci U S A 99:16012-16017

Mattick JS (2002) Type IV pili and twitching motility. Ann. Rev. Microbiol. 56:289-314

Mauriello EM et al. (2010) Bacterial motility complexes require the actin-like protein, MreB and the Ras homologue, MglA. EMBO J 29:315-326

Mauriello EM, Nan B, Zusman DR (2009) AglZ regulates adventurous (A-) motility in Myxococcus xanthus through its interaction with the cytoplasmic receptor, FrzCD. Mol Microbiol 72:964-977

McBride MJ, Weinberg RA, Zusman DR (1989) "Frizzy" aggregation genes of the gliding bacterium *Myxococcus xanthus* show sequence similarities to the chemotaxis genes of enteric bacteria. Proc. Natl. Acad. Sci. U S A 86:424-428

Miertzschke M et al. (2011) Structural analysis of the Ras-like G protein MglA and its cognate GAP MglB and implications for bacterial polarity. EMBO J. 30:4185-4197

Mignot T, Merlie JP, Jr., Zusman DR (2005) Regulated pole-to-pole oscillations of a bacterial gliding motility protein. Science 310:855-857

Mignot T, Shaevitz JW, Hartzell PL, Zusman DR (2007) Evidence that focal adhesion complexes power bacterial gliding motility. Science 315:853-856

Morano KA, Thiele DJ (1999) Heat shock factor function and regulation in response to cellular stress, growth, and differentiation signals. Gene Expr 7:271-282

Muller FD, Treuner-Lange A, Heider J, Huntley SM, Higgs PI (2010) Global transcriptome analysis of spore formation in Myxococcus xanthus reveals a locus necessary for cell differentiation. BMC Genomics 11:264

Nan B, Chen J, Neu JC, Berry RM, Oster G, Zusman DR (2011) Myxobacteria gliding motility requires cytoskeleton rotation powered by proton motive force. Proc Natl Acad Sci U S A

Nan B, Mauriello EM, Sun IH, Wong A, Zusman DR (2010) A multi-protein complex from Myxococcus xanthus required for bacterial gliding motility. Mol Microbiol 76:1539-1554

Nudleman E, Wall D, Kaiser D (2006) Polar assembly of the type IV pilus secretin in Myxococcus xanthus. Mol Microbiol 60:16-29

Patryn J, Allen K, Dziewanowska K, Otto R, Hartzell PL (2010) Localization of MglA, an essential gliding motility protein in Myxococcus xanthus. Cytoskeleton (Hoboken) 67:322-337

Paul R et al. (2008) Allosteric regulation of histidine kinases by their cognate response regulator determines cell fate. Cell 133:452-461

Pelicic V (2008) Type IV pili: e pluribus unum? Mol Microbiol 68:827-837

Pelling AE, Li Y, Shi W, Gimzewski JK (2005) Nanoscale visualization and characterization of Myxococcus xanthus cells with atomic force microscopy. Proc Natl Acad Sci U S A 102:6484-6489

Punta M et al. (2012) The Pfam protein families database. Nucleic Acids Res 40:D290-301

Ridley AJ et al. (2003) Cell migration: integrating signals from front to back. Science 302:1704-1709

Rodrigue A, Quentin Y, Lazdunski A, Mejean V, Foglino M (2000) Two-component systems in Pseudomonas aeruginosa: why so many? Trends Microbiol 8:498-504

Romantsov T, Helbig S, Culham DE, Gill C, Stalker L, Wood JM (2007) Cardiolipin promotes polar localization of osmosensory transporter ProP in Escherichia coli. Mol Microbiol 64:1455-1465

Rosenberg E, Keller KH, Dworkin M (1977) Cell density-dependent growth of Myxococcus xanthus on casein. J Bacteriol 129:770-777

Sambrook J, Russell DW (2001) Molecular cloning : a laboratory manual, 3rd edn. Cold Spring Harbor Laboratory Press, Cold Spring Harbor, N.Y.

Scott AE, Simon E, Park SK, Andrews P, Zusman DR (2008) Site-specific receptor methylation of FrzCD in Myxococcus xanthus is controlled by a tetra-trico peptide repeat (TPR) containing regulatory domain of the FrzF methyltransferase. Mol Microbiol 69:724-735

Schramm, A., B. Lee, et al. (2012). "Intra- and interprotein phosphorylation between two-hybrid histidine kinases controls Myxococcus xanthus developmental progression." J Biol Chem 287(30): 25060-72.

Shapiro L, McAdams HH, Losick R (2009) Why and how bacteria localize proteins. Science 326:1225-1228

Shi X, Wegener-Feldbrugge S, Huntley S, Hamann N, Hedderich R, Sogaard-Andersen L (2008) Bioinformatics and experimental analysis of proteins of two-component systems in Myxococcus xanthus. J Bacteriol 190:613-624

Shimkets L, Woese CR (1992) A phylogenetic analysis of the myxobacteria: basis for their classification. Proc Natl Acad Sci U S A 89:9459-9463

Skerker JM, Berg HC (2001) Direct observation of extension and retraction of type IV pili. Proc. Natl. Acad. Sci. USA 98:6901-6904

Spormann AM, Kaiser AD (1995) Gliding movements in *Myxococcus xanthus*. J. Bacteriol. 177:5846-5852

Stock AM, Robinson VL, Goudreau PN (2000) Two-component signal transduction. Annu Rev Biochem 69:183-215

Strauch MA, Hoch JA (1993) Signal transduction in Bacillus subtilis sporulation. Curr Opin Genet Dev 3:203-212

Sun H, Zusman DR, Shi W (2000) Type IV pilus of *Myxococcus xanthus* is a motility apparatus controlled by the *frz* chemosensory system. Current Biology 10:1143-1146

Sun M, Wartel M, Cascales E, Shaevitz JW, Mignot T (2011) From the Cover: Motor-driven intracellular transport powers bacterial gliding motility. Proc Natl Acad Sci U S A 108:7559-7564

Trudeau KG, Ward MJ, Zusman DR (1996) Identification and characterization of FrzZ, a novel response regulator necessary for swarming and fruiting-body formation in *Myxococcus xanthus*. Mol. Microbiol. 20:645-655

Ulrich LE, Koonin EV, Zhulin IB (2005) One-component systems dominate signal transduction in prokaryotes. Trends Microbiol 13:52-56

Vetter IR, Wittinghofer A (2001) The guanine nucleotide-binding switch in three dimensions. Science 294:1299-1304

Wall D, Kaiser D (1999) Type IV pili and cell motility. Mol Microbiol 32:01-10

Wennerberg K, Rossman KL, Der CJ (2005) The Ras superfamily at a glance. J Cell Sci 118:843-846

Wireman JW, Dworkin M (1977) Developmentally induced autolysis during fruiting body formation by Myxococcus xanthus. J Bacteriol 129:798-802

Wu SS, Kaiser D (1995) Genetic and functional evidence that Type IV pili are required for social gliding motility in *Myxococcus xanthus*. Mol Microbiol 18:547-558

Wuichet K, Cantwell BJ, Zhulin IB (2010) Evolution and phyletic distribution of two-component signal transduction systems. Curr. Opin. Microbiol. 13:219-225

Wuichet K, Zhulin IB (2010) Origins and diversification of a complex signal transduction system in prokaryotes. Sci Signal 3:ra50

Yang R et al. (2004) AglZ is a filament-forming coiled-coil protein required for adventurous gliding motility of Myxococcus xanthus. J Bacteriol 186:6168-6178

Youderian P, Burke N, White DJ, Hartzell PL (2003) Identification of genes required for adventurous gliding motility in Myxococcus xanthus with the transposable element mariner. Mol Microbiol 49:555-570

Youderian P, Hartzell PL (2006) Transposon insertions of magellan-4 that impair social gliding motility in Myxococcus xanthus. Genetics 172:1397-1410

Yu R, Kaiser D (2007) Gliding motility and polarized slime secretion. Mol Microbiol 63:454-467

Zhang Y, Franco M, Ducret A, Mignot T (2010) A bacterial Ras-like small GTP-binding protein and its cognate GAP establish a dynamic spatial polarity axis to control directed motility. PLoS Biol 8:e1000430

Zhang Y, Guzzo M, Ducret A, Li YZ, Mignot T (2012) A dynamic response regulator protein modulates G-protein-dependent polarity in the bacterium Myxococcus xanthus. PLoS Genet 8:e1002872

Abbreviations

ADP/ATP	Adenine di- /Adenine triphosphate
bp	Base pairs
BSA	Bovine serum albumin
Cm	Chloramphenicol
CTT	Casitone Tris medium
DMSO	Dimethyl sulfoxide
DTT	Dithiothreitol
ECM	Extracellular matrix
EPS	Exopolysaccharides
GDP/GTP	Guanosine di- /Guanosine triphosphate
GFP	Green fluorescent protein
h	Hours
IPTG	Isopropyl β-D-1-thiogalaktopyranoside
Km	Kanamycin
min	Minutes
s	seconds
SDS-PAGE	Sodium dodecyl sulfate polyacrilamide gel electrophoresis
T4P	Type IV pili
YFP	Yellow fluorescent protein
WT	Wild type

Acknowledgements

Most of all I would like to thank my supervisor, Prof. Lotte Sogaard-Andersen, to always support me during the last four years, first in my diploma thesis and then during my PhD thesis. I got a very interesting project, which was sometimes challenging and competitive. Thankfully, Lotte always helped me with advice and discussions about the research, and tought me how to survive in science. I thank her for constructive criticism regarding my work, presentations and reports.

I would like to thank everybody in the LSA lab, specifically Dr. Iryna Bulyha, who tought me a lot about motility of *M. xanthus*, and for proof-reading my PhD thesis. I also want to thank Edina Hot, for help with many presentations and for many helpful discussions about MglA and MglB. Special thanks also to everybody else who is working in the motility lab, Beata and Dorota, or was working in the motility lab, Simone and Gerald.

I also would like to thank Kristin Wuichet, who was a great help with the RomR paper, and did not only provide important results for the project, but also helped with proofreading the manuscript as well as my PhD thesis.

I would like to thank T. Mignot, for helping me to publish the RomR paper back-to-back.

Furthermore, I would like to thank the IMPRS research school, for improving my skills in scientific writing and presentations and my IMPRS committee and thesis committee, specifically Prof. Lotte Sogaard-Andersen, Prof. Martin Thanbichler, Dr. Sonja Verena-Albers, Prof. Andrea Maisner and Prof. Susanne Önel.

And last but not least I would like to thank my family and friends:

Als erstes danke ich meinem Freund, Michael Brauer, der immer für mich da war, mit nach Marburg gezogen ist, und mich in jeder Zeit meiner Doktorarbeit unterstützt hat. Weiterhin danke ich meinen Eltern die mir immer gesagt haben, dass ich es schaffen kann und ohne die ich nie soweit gekommen wäre. Besonders danke ich meiner Oma, die mein Interesse an der Natur und wie sie funktioniert schon als Kind entfacht hat und mich zu allem ermutigt.

Curriculum Vitae

Personal data

Name	Daniela Keilberg
Geburtsdatum	21.11.1984 in Zwickau, Deutschland
Nationalität	Deutsch
Familienstand	ledig

Education

10/2009 – 12/2012

PhD (Dr.rer.nat.)

Philips University Marburg / Max Planck Institute Marburg, Germany

„Regulation of motility and polarity in *Myxococcus xanthus*"

Supervisor: Prof. Lotte Sogaard-Andersen

10/2008 – 09/2009

Diploma Thesis

University Halle / Max Planck Institute Marburg, Germany

„Cis and Trans-acting determinants of RomR in *M. xanthus*"

Supervisor: Prof. Lotte Sogaard-Andersen

10/2004 – 09/2008

Diploma of Biology

University Halle, Germany
Main subjects: Microbiology, Plant Physiology, Pharmacy and Organic Chemistry

08/1995 – 07/2004

High school with Abitur certificate

J.-Kepler Gymnasium Chemnitz, Germany

List of publications

Herzog A., Voss , **Keilberg D.**, Hot E., Søgaard-Andersen L., Garbe C., Kostina E. (2012) A stategy for identifying fluorescence intensity profiles of single rod-shaped cells. Journal of Bioinformatics and Computational Biology Online Ready 1250024

Keilberg D., Wuichet K., Drescher F. & Søgaard-Andersen L. (2012)
A response regulator interfaces between the Frz chemosensory system and the MglA/MglB GTPase/GAP module to regulate polarity in *Myxococcus xanthus*. PLoS Genetics. 9, e1002951.

Miertzschke M., Koerner C., Vetter I.R., **Keilberg D.**, Hot E., Leonardy S., Søgaard-Andersen L. & Wittinghofer A. (2011)
Mechanistic insights into bacterial polarity from structural analysis of the Ras-like G protein MglA and its cognate GAP MglB. EMBO J. 30, 4185-4197.

Keilberg D., Huntley S. & Søgaard-Andersen L. (2012)
Two-component systems involved in regulation of motility and development in *Myxococcus xanthus.* In "Two component systems in bacteria" ed. Gross, R. & Beier, D.. Horizon Scientific press and Caister Academic Press.

Erklärung

Hiermit versichere ich, dass ich die vorliegende Dissertation mit dem Titel „Regulation of motility and polarity in *Myxococcus xanthus*“ selbstständig verfasst, keine anderen als die im Text angegebenen Hilfsmittel verwendet und sämtliche Stellen, die im Wortlaut oder dem Sinn nach anderen Werken entnommen sind, mit Quellenangaben kenntlich gemacht habe.

Die Dissertation wurde in der jetzigen oder einer ähnlichen Form noch bei keiner anderen Hochschule eingereicht und hat noch keinen sonstigen Prüfungszwecken gedient.

Daniela Keilberg	Ort, Datum

Einverständniserklärung

Ich erkläre mich damit einverstanden, dass die vorliegende Dissertation

Regulation of motility and polarity in *Myxococcus xanthus*

in Bibliotheken allgemein zugänglich gemacht wird. Dazu gehört, dass sie

von der Bibliothek der Einrichtung, in der ich meine Arbeit anfertigt habe, zur Benutzung in ihren Räumen bereitgehalten wird;

in konventionellen und maschinenlesbaren Katalogen, Verzeichnissen und Datenbanken verzeichnet wird;
im Rahmen der urheberrechtlichen Bestimmungen für Kopierzwecke genutzt werden kann.

Marburg, den

(Unterschrift des Autors) (Unterschrift des betreuenden Hochschullehrers)